This is to certify that the
dissertation entitled

GREEN BIOCOMPOSITES FROM POLYHYDROXY-BUTYRATE-CO-VALERATE (PHBV), WOOD FIBER AND TALC

presented by

SANJEEV SINGH

has been accepted towards fulfillment
of the requirements for the

Ph.D. degree in Packaging

Amar Kumar Mohanty
Major Professor's Signature

June 8, 2009
Date

GREEN BIO-COMPOSITES FROM POLYHYDROXY-BUTYRATE-CO-VALERATE (PHBV), WOOD FIBER AND TALC

By

Sanjeev Singh

A DISSERTATION

Submitted to
Michigan State University
in partial fulfillment of the requirements
for the degree of

DOCTOR OF PHILOSOPHY

Packaging

2009

ABSTRACT

GREEN BIO-COMPOSITES FROM POLYHYDROXY-BUTYRATE-CO-VALERATE (PHBV), WOOD FIBER AND TALC

By

Sanjeev Singh

Wood/Natural fiber plastic composites (W/NPCs) have been widely accepted and are an enormously growing segment of the commodity plastics market. These are predominantly being used in decking, household interiors, etc., and more recently have made inroads in automotive interior applications. These are short fiber composites developed by using wood/natural fiber as reinforcement in the plastic matrix. Generally, plastic constitutes from 30 to 70% of the entire product mass of the composite and the most used plastics are conventional petroleum based i.e., polyethylene, polyvinyl chloride, polypropylene and nylon. Polyhydroxyalkanoates (PHAs) are bacterially produced plastics from commonly available biomass, and are projected to be sustainable and viable alternatives to petroleum based plastics. This research focuses on a holistic approach to shift W/NPCs from partially to fully green biocomposites, by replacing the conventional plastic constituent in the W/NPCs with a renewable source based and biodegradable bioplastic i.e., PHAs. This broadly addresses the evolving environmental concerns related to conventional petro-plastics. In this process of transformation from partially to fully green bio-composites, issues coupled to biopolymers based W/NPCs such as, cost, processablity, performance, compatibility of reinforcing agent and matrix, and raw material availability are addressed. These fully green biocomposites can find potential applications in rigid packaging, distribution, household items and automotive interiors.

This dissertation advances in four consecutive syllogistic stages:

1. In the first stage, the development of wood fiber reinforced bio-plastic i.e., polyhydroxybutyrate-co-valerate (PHBV) bio-composites is accomplished on the performance evaluation, and comparison to conventional WPCs is addressed.
2. In the second stage, bio-composites from natural fiber, i.e., bamboo fiber, and PHBV, at 30 & 40 wt% fiber content, were fabricated and their analogy to wood fiber reinforced PHBV bio-composites is determined.
3. In the third stage, a comparative study of anisotropy, static and dynamic mechanical evaluation of biocomposites fabricated using two different molding processes, i.e. injection and compression molding, was accomplished.
4. In the final stage, "green hybrid bioplastic composites" containing synergistic reinforcements of talc and wood fiber were designed and fabricated.

The biocomposites were extrusion processed followed by injection molding and analyzed for static and dynamic mechanical, thermal & morphological aspects. The tensile and flexural modulus of the bio-composites with 40 wt% of the wood fiber was enhanced by ~167%, and the heat deflection temperature by 21%. Statistically, there was no effect of the fiber type (i.e., bamboo and wood fiber) on the mechanical properties, except for notch impact strength and heat deflection temperature. The squeeze flow test revealed the anisotropy in the injection molded short fiber bio-composites. Synergetic reinforcement of the talc platelets and cylindrical wood fibers increased Young's and flexural modulus, by ~200%, at 20 wt% of each in PHBV. The high surface energy of talc platelets allows good talc-PHBV interfacial interactions as shown by the morphological study and no additional crystallization of PHBV was observed.

ACKNOWLEDGMENTS

I would like to express my thanks to my major supervisor Dr. Mohanty for his guidance and support during the course of this study. His perseverance to hard work had been a great source of motivation during the progress of this research.

My special thanks to Dr. Sher Paul Singh, who has always been there for his support during my stay in School of Packaging. His kind and giving attitude would always be indebted.

I express my greatest gratitude to Dr. Pourboghrat, a person of great humility, intelligence and mentorship. I would always carry his wisdom and guidance with me as an example of great teacher and professionalism.

I also express my utmost thanks and best regards to Dr. Harte for all his support, guidance and suggestions during the course of study as a graduate student in School of Packaging.

This research was made possible through the funding from USDA-CSREES under the McIntire-Stennis program of the Michigan Agricultural Experiment Station, Michigan State University. This support is greatly appreciated.

TABLE OF CONTENTS

LIST OF TABLES

LIST OF FIGURES

INTRODUCTION

In the perspectives of the environmental concerns and fluctuating oil prices, consumer markets all across the world have initiated a drive for bio based material as an alternatives for holistically, sustainable economic growth. Automotive industry in Europe and America have, by now, embraced the rationality and feasibility of replacing the plastic components with the biomaterials, and are estimating an opportunity of more than 50 billion US $ by 2015 [1,2,3]. Medical world have also ventured in to exploring the use of biomaterial in medical application, and the projected market is more than 100 billion US $. The forecast to grow in the near future is by 14% [4,5]. Biomaterials for other applications, such as, industrial and structural, are also being explored for the sustainable economic growth, in conjunction with green environment. Biopolymers from the biomass, like polylactic acid, starch based plastic, Polyhydroxyalkanoates, and other bio-oil based resin are being envisaged as a prospective alternate to their counterpart in the olefin plastics. PLA and starch plastic products are already in the consumer market for textile, packaging, foam etc., applications [6,7]. PHAs, bioplastics have yet to meet the challenges based on cost and inherent characteristics, and make inroad as a considerable probable. Polyhydroxybutyrate-co-valerate (PHBV), is an intracellular bacterially produced biodegradable bioplastic from a renewable source, i.e., biomass like corn, switch grass etc. The current challenges it posses for commercialization are cost, brittleness and processing. The objective of this research was to develop an all green biomaterial from PHBV utilizing the conceptual fundamentals of wood plastic composite (WPC) in processing/manufacturing and applications. Besides, this research also takes into the consideration of the trio, cost-

characteristics-processing, co-relationship and optimizing the three, most appropriately, during the development of the biomaterial. These fully green biocomposites from various bio-sources can run the gamut of applications in rigid packaging, distribution, household items and automotive interiors.

WPC are the fastest growing segment in the plastic industry with their ongoing growth of 25% [8]. The current market of wood plastic composites (WPC) is 1.2 billion pounds and is expected to grow with an average annual growth rate of 9.8%, giving a market of 1.9 billion pounds by the year 2009 [9].The wide acceptance of W/NF PC by the global market has been due to their reduced cost, weight, superior properties over wood and plastic alone, recycling ability, adaptation to the existing plastic processing techniques, and the desire for the eco-friendly products.

This thesis is divided in to six chapters, beginning from the literature survey in the first chapter to the development of hybrid all green bio composite from polyhydroxy-co-valerate (PHBV) in the fifth chapter. The subsequent second, third, and fourth chapters proceed in a logical sequence based on the illations drawn from the preceding chapter. The second chapter targets the development and characterization of the biocomposite from wood fiber and PHBV. The third, describes the development and characterization of biocomposites from a natural fiber i.e., bamboo fiber, and PHBV, and comparison of the two, PHBV based, biocomposites from wood fiber and natural fiber. The fourth chapter illustrates on the isotropy of the short wood fiber biocompostes processed with two different processing methods. The final and sixth chapter summarizes the research.

The first chapter gives the description from the literature regarding the conventional short wood and natural fiber plastic composite, biopolymers and the other two components of the hybrid composites, i.e., wood and talc. The literature collected from various sources provides the current and the future scenario of the wood plastic composites in the consumer market, in terms of demand and growth. The economic viability discussion of the WPC is followed by the section on the mechanics of the short fiber reinforced composites that details the understanding of the isotropic characteristic of the short fiber composites. The interfacial shear stress based on the shear lag model is described as well. The interface of wood and plastic plays a vital role in the structure of wood plastic composites, and the literature also focuses on various kinds of interfacial phenomenons. A subsection of the second chapter focuses on the synthesis, manufacturing, structure, properties, limitations and modification of polyhydroxyalkanoates. Wood fiber and talc are the two different kinds of reinforcements that had been used to reinforce the thermoplastic, i.e., polyhydroxybutyrate-co-valerate, therefore it becomes imperative to discuss their fundamental structures and properties. The last two sections of this chapter focus on these.

The second chapter describes the fabrication of a wood fiber reinforced PHBV composites and evaluate the static and dynamic mechanical and thermo-mechanical properties as a function of wood fiber weight content in the PHBV matrix. The experimental findings were correlated with theoretical models presented by Halpi-Tsai and Tsai-Pagano. The morphological aspects such as fiber dispersion and fiber-matrix interface were also investigated using scanning electron microscopy (SEM).

The third chapter illustrates the fabrication and evaluation of the bamboo fiber based PHBV biocomposites, and also describes the rationality of bamboo fiber quid pro quo to wood fiber. Characteristic study of the bamboo based biocomposites using differential scanning calorimetry (DSC), thermogravimetric analysis (TGA), Fourier transform infrared spectroscopy (FTIR), and their morphology is also illustrated. The experimental results of the tensile modulus were compared with the persisting theoretical model and additionally, comparative analysis by performing a two-way ANOVA on the mechanical properties of the bamboo fiber biocomposites and the wood fiber-PHBV biocomposites has been discussed.

The fourth chapter discusses the comparison between the two different processing techniques, i.e., injection molding and compression modeling of the wood fiber composites from PHBV, in terms of the anisotropy associated with them. This chapter also draws a direct comparison of the static and dynamic mechanical properties between the compression molded specimens and injection molded specimens of the same biocomposite.

The fifth chapter elaborates the development of a completely biodegradable hybrid biocomposite consisting of talc and wood fibers in PHBV. It also discusses the experimentally determined dynamic-mechanical and thermo-mechanical properties of the hybrid biocomposites. A theoretical discussion, based on the surface energy parameters, of the interacting components in the composite system is described to explain the reinforcing effect of talc and wood fiber. The Morphological analysis of the hybrid composite was carried out to study the interfacial interactions among the different components in the hybrid biocomposite system.

References

1) Crawford, C. Ontario Bioauto Council, Presentation. 4/11/08. Presentation available at; http://www.sobin.ca/files/BioAuto%20Council%20-%20April%2011,%202008.pdf. Date accessed; 12/8/08.

2) Khalil, H. Woodbridge Foam Corporation, "The use of bio material in automotive parts manufacturing", Presentation to Canadian conference on industrial bioproduct innovation, Montreal. 11/6/08. Available at; http://www.biop.ca/PPT_pdf/KHALIL_Hamdy.pdf. Date accessed; 12/08/08.

3) Cascadden, A. M. "Bio-Materials – Why is the Auto Industry interested?" AUTO21 NCE, Toronto, Ontario, July 12, 2006, available at; http://www.agrifoodforum.com/2006/presentations/AFIF06-05-Cascadden.pdf. Date accessed; 12/08/08.

4) Amsden, B. CHEE 340 course lecture, Queens University. Available at; http://www.chemeng.queensu.ca/courses/CHEE340/lectures/documents/biomaterials12006.ppt#264,1,BIOMATERIALS. Date accessed; 12/08/08.

5) Grammenou, E. Medical Devices Research Analyst, "Technology development drive the market in Europe", published on 5/4/2006, available at; http://www.frost.com/prod/servlet/market-insight-top.pag?docid=68525981, Date accessed; 12/08/08.

6) Available at; http://www.ides.com/generics/PLA/PLA_applications.htm, Date accessed; 12/8/08.

7) Available at; http://www.starch.dk/isi/applic/applic.htm, Date accessed; 12/8/08.

8) Principia partner's presentation in, *7th international conference of wood fiber-plastic composites* 2003. Madison (WI), USA.

9) Available at; *Http://Www.Principiaconsulting.Com/Consulting/News.Cfm*. Date accessed 05/15/2006,

Chapter 1

Literature Review

1.0 Introduction

Wood or natural fiber plastic composites predominantly exist as short fiber composites in most of the applications. Time and again, since their inception in 1990's, these have occupied ever-increasing share of market year by year. In the future prospects, W/NPC's have the potential to grow up to $ 60 billion market, from the existing just over $ one billion US market [1].Their modern-day principal application fields in North America are building structural products such as, decking, fencing, railings, window and door profiles, and shingles, where they constitute over 85% of the total demand. Other application arenas like, infrastructure, automotives and industrial/consumer segment are also catching up with good pace. In Europe, the automotive application have an edge over North America, where the W/NPC's account for over half of the total consumption [2]. A boom in the W/NPC's market has also lead to a growth explosion in the injection molding industry, as the extensively used process for W/NPC's manufacturing has been extrusion, and this is supplemented by injection molding. Anticipated demand for the injection molded wood-plastic composites is 70% average annual growth, which was supposed to reach a market of over $350 million in 2008 [3, 4]. The driving impulse for this industry is that W/NPC's lend a hand in reducing the dependence on the petroleum based plastics by limiting the use of plastics in them. The fiber constitutes from 30 to 70 wt% in the composite, and the major cellulose fiber used in these composites are wood fiber (pine or maple saw dust), recycled newsprint, hemp, sisal, kenaf, jute, flax or rice hulls. The scarce of the natural

or wood fiber, as a long and continuous, but in abundance as a short length and low-price, presented an opportunity to use these as short fiber reinforcement in the matrix, which has been plausible with the available plastic processing technology. The leading thermoplastics used are PE, PVC, PP, and nylon. Unlike, long fiber composites, which are termed as orthotropic, the short fiber composites are assumed to be isotropic in nature, due to their randomly oriented dispersion in the matrix. The mechanics of the isotropic materials can be well appreciated by assuming these to be a simplified case of orthotropic composites, where the stress-strain response of the material can be assumed to equal/similar along the *x, y and z* axis. Figure 1.1 and 1.2 represents the schematic sketches of long and short fiber reinforced thermoplastic composite.

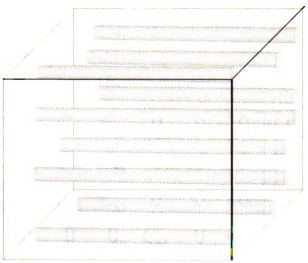

Figure 1.1: Sketch of long and continuous fiber composite

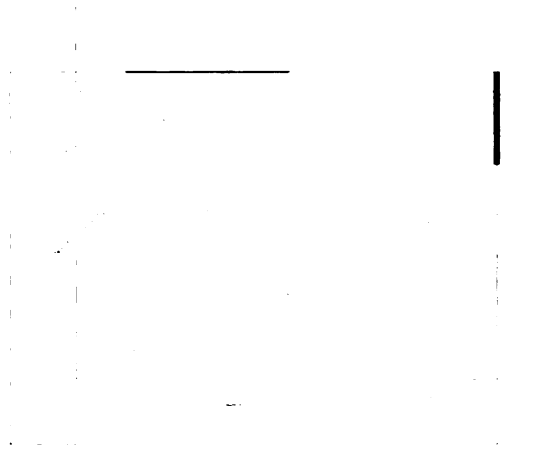

Figure 1.2: Sketch of randomly oriented sort fiber composite

Mechanical properties of an anisotropic material are defined by the following stiffness and compliance matrix.

$$\begin{Bmatrix} \sigma_1 \\ \sigma_2 \\ \sigma_3 \\ \tau_{23} \\ \tau_{13} \\ \tau_{12} \end{Bmatrix} = \begin{bmatrix} C_{11} & C_{12} & C_{13} & 0 & 0 & 0 \\ C_{21} & C_{22} & C_{23} & 0 & 0 & 0 \\ C_{31} & C_{23} & C_{33} & 0 & 0 & 0 \\ 0 & 0 & 0 & C_{44} & 0 & 0 \\ 0 & 0 & 0 & 0 & C_{55} & 0 \\ 0 & 0 & 0 & 0 & 0 & C_{66} \end{bmatrix} \begin{Bmatrix} \varepsilon_1 \\ \varepsilon_2 \\ \varepsilon_3 \\ \gamma_{23} \\ \gamma_{13} \\ \gamma_{12} \end{Bmatrix}$$

$$\begin{Bmatrix} \varepsilon_1 \\ \varepsilon_2 \\ \varepsilon_3 \\ \gamma_{23} \\ \gamma_{13} \\ \gamma_{12} \end{Bmatrix} = \begin{bmatrix} S_{11} & S_{12} & S_{13} & 0 & 0 & 0 \\ S_{21} & S_{22} & S_{23} & 0 & 0 & 0 \\ S_{31} & S_{23} & S_{33} & 0 & 0 & 0 \\ 0 & 0 & 0 & S_{44} & 0 & 0 \\ 0 & 0 & 0 & 0 & S_{55} & 0 \\ 0 & 0 & 0 & 0 & 0 & S_{66} \end{bmatrix} \begin{Bmatrix} \sigma_1 \\ \sigma_2 \\ \sigma_3 \\ \tau_{23} \\ \tau_{13} \\ \tau_{12} \end{Bmatrix}$$

Where $\varepsilon_i, \sigma_i, \tau_{ij}, \gamma_{ij}$, are strain, stress, shear stress and shear strain, respectively, along $i,j=1,2,3$ directions. $[S_{ij}]$ and $[C_{ij}]$ are compliance and stiffness matrices defined as.

$S_{11} = 1/E_1$, $S_{12} = - \acute{\imath}_{12}/E_1$, $S_{13} = - \acute{\imath}_{13}/E_1$

$S_{22} = 1/E_1$, $S_{23} = - \acute{\imath}_{12}/E_2$, $S_{33} = 1/E_1$

$S_{44} = 1/G_{23}$, $S_{55} = 1/G_{13}$, $S_{66} = 1/G_{12}$

E_i *and* G_{ij} are elastic and shear modulus, $\acute{\imath}_{ij}$ is poison's ratio in their respective directions.

$C_{11} = (S_{22}S_{33} - S_{22}S_{33})/S$ $C_{12} = (S_{13}S_{23} - S_{12}S_{33})/S$

$C_{22} = (S_{33}S_{11} - S_{13}S_{13})/S$ $C_{13} = (S_{12}S_{23} - S_{13}S_{22})/S$

$C_{33} = (S_{11}S_{22} - S_{12}S_{12})/S$ $C_{23} = (S_{12}S_{13} - S_{23}S_{11})/S$

$C_{44} = 1/S_{44}$ $C_{55} = 1/S_{55}$ $C_{66} = 1/S_{66}$

For Isotropic material, imposing the condition that it has same properties in all the directions, therefore

$E_1 = E_2 = E_3 = E$, $\acute{\imath}_{13} = \acute{\imath}_{23} = \acute{\imath}_{12} = \acute{\imath}$,

$G_{12} = G_{23} = G_{13} = G = E/2(1+\acute{\imath})$

The compliance matrix become

$$\begin{bmatrix} S_{11} & S_{12} & S_{12} & 0 & 0 & 0 \\ S_{12} & S_{11} & S_{12} & 0 & 0 & 0 \\ S_{12} & S_{12} & S_{11} & 0 & 0 & 0 \\ 0 & 0 & 0 & S_{44} & 0 & 0 \\ 0 & 0 & 0 & 0 & S_{44} & 0 \\ 0 & 0 & 0 & 0 & 0 & S_{44} \end{bmatrix}$$

where $S_{11} = 1/E$, $S_{12} = -\acute{\imath}/E$, $S_{44} = 1/G = 2(1+\acute{\imath})/E$

and the stiffness matrix becomes

$$\begin{bmatrix} C_{11} & C_{12} & C_{12} & 0 & 0 & 0 \\ C_{12} & C_{11} & C_{12} & 0 & 0 & 0 \\ C_{12} & C_{12} & C_{11} & 0 & 0 & 0 \\ 0 & 0 & 0 & C_{44} & 0 & 0 \\ 0 & 0 & 0 & 0 & C_{44} & 0 \\ 0 & 0 & 0 & 0 & 0 & C_{44} \end{bmatrix}$$

where $C_{11} = E/((1+\nu)(1+2\nu))$, $C_{12} = ((1-\nu)E)/((1+\nu)(1+2\nu))$,

$C_{44} = G = E/(2(1+\nu))$

As elaborated by Bhagwan and Lawrence [5], a good estimate of average mechanical properties of short fiber composites can also be obtained by assuming them as a *quasi-isotropic laminate* made from unidirectional laminae. *Quasi-isotropic laminate* has an elastic coefficient that is independent of continuous fiber orientation in the plane. Other models for the prediction of properties are described in the subsequent chapters.

The interface properties between fiber and matrix plays a vital role while describing the micro- structure of the composite and therefore, it becomes necessary to discuss the stress transfer mechanism from matrix to fiber along its length. The shear lag model is the most widely used model, which is based on the transfer of tensile stress from matrix to fiber by means of interfacial shear stress. This model is based on considering the interfacial bonding between the matrix and fiber. According to the shear lag model, the tensile stress experienced by the fiber, aligned along the external axial loading, is given by the following equation, neglecting the stress transfer at the fiber ends.

$$\sigma_f = E_f \varepsilon_l [1 - \cosh(nx/r)\sec h(ns)$$

The modified equation that takes in to account of the stress transferred at the fiber end is as follows.

$$\sigma_f = \varepsilon_l[E_f - (E_f - E_m^{'})\cosh(nx/r)\sec h(ns)]$$

Where, $$E_m^{'} = \frac{[E_f(1-\sec h(ns)+E_m]}{2}$$,

$$n = \left[\frac{2E_m}{E_f(1+\nu_m)\ln(1/f)}\right]^{1/2}$$

'σ_f'is the tensile stress in the fiber along the length 'x', 'r' is the radius of the fiber, 's' is the aspect ratio i.e., L/r, 'L'is the length of the fiber. 'E_f' and 'E_m' are the elastic modulus of fiber and matrix, respectively. 'f' is the fiber volume fraction in matrix and 'ν_m' is the matrix poison ratio. 'ε_l' is the over all composite strain.

The interfacial shear stress, τ_i, along the fiber length is given by

$$\tau_i = \frac{n\varepsilon_l}{2} E_f \sinh(nx/r)\sec h(ns)$$

The tensile stress or the axial stress in the fiber along the fiber length attains maximum in the mid section of the fiber. It decreases gradually towards the fiber ends, as depicted in the figure 1.3 and 1.4. For higher aspect ratio fibers, the tensile stress forms a plateau over a considerable length of the fiber before plummeting to its minimum values at the fiber ends. The interfacial shear stress reaches maxima near the

fiber ends due to the shear deformation of the matrix under an externally applied, axial load, along the fiber length, to the composite. The interfacial shear stress in the mid section of the fiber has minima due to low shear deformation of the matrix in the middle section of the fiber along its length. For higher aspect ratio fibers, the minimum interfacial stress values continuous to a considerable length of the fiber before attaining the maxima at the fiber ends. Therefore, higher aspect ratio fibers are more efficient in stress transfer than the short fibers because these have sufficient length to attain the maximum tensile stress in the fiber or in other words to transfer the stress from matrix to fiber. Stress transfer aspect ratio 's_t' is defined as the minimum aspect ratio of the fiber, when the stress reaches its maximum possible value. It is given as

$$s_t \approx 3/n$$

Stiffer the matrix shorter is the s_t, and stiffer the fiber longer is the s_t.

As the composite strain increases, the stress in the fiber also increases with the increased interfacial shear stress, and subsequently the fiber undergoes fracture. A reduced fiber length does not allow the stress to reach it maximum value. Therefore, a critical aspect ratio 's_c' of a fiber can be defined as the minimum length below which the fiber does not undergo fracture, i.e., the value of tensile stress in fiber when it just reaches its ultimate strength 'σ_f^*'.

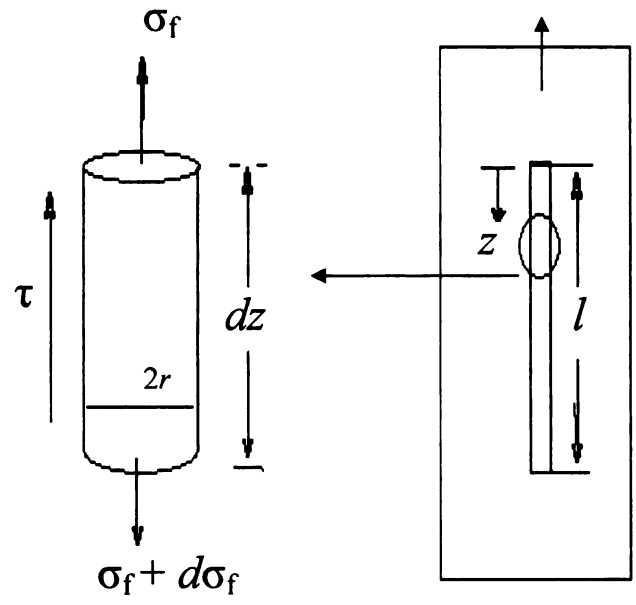

Figure 1.3: Stress Equilibrium on fiber aligned parallel to applied load. σ_f is the tensile stress on fiber, τ is the shear stress, l is the length of fiber, σ_c is the stress acting on composite (Redrawn from reference [6])

$$s_c = \sigma_f^* / 2\,\sigma_i^*$$

σ_i^* is the critical shear stress at which the onset of inelastic strain/behavior occurs in the composite.

Generally, incase of composites having a fibers well above the critical aspect ratio, as the composite load increases, sliding at the interface or yielding phenomena is predominant before the fiber fractures [5, 6].

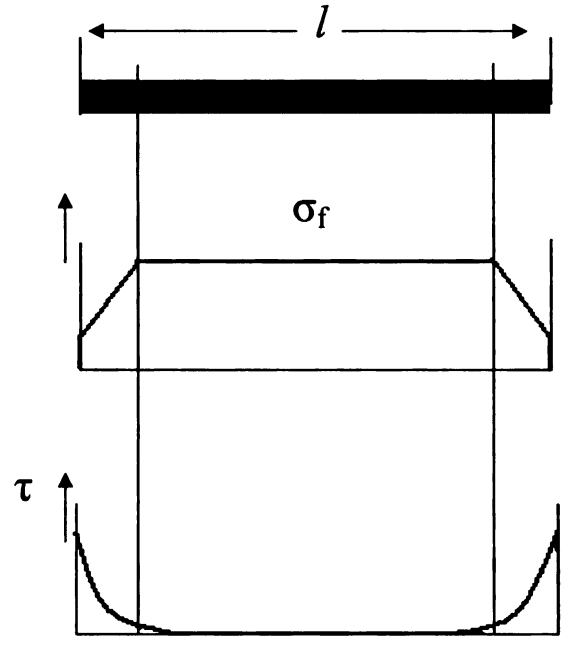

Figure 1.4: Sketch of the tensile stress acting at the fiber length and shear stress acting at the interface (Redrawn from reference [6])

1.1 Polyhydroxyalkanoate (PHA) Biopolymers

1.1.1 Synthesis and Production

These belong to the family of microbial energy reserve materials that are accumulated as granules within the cytoplasm of cells [7-10]. PHA accumulation in microorganism gets triggered when it faces the metabolic stress such as limitation of essential nutrients (e.g. nitrogen, oxygen and phosphorus) in excess of carbon source[11]. PHAs are produced in various species of bacteria as spherical bodies. The diameter of these inclusions in bacteria is roughly 0.5 μm [8]. Under regulated conditions PHAs may constitute up to 90% of the biomass of some bacteria species. The PHB synthesis mechanism in the bacteria *Alcaligenes eutrophus* is carried out as follows. The first step constitutes the enzymatic self condensation of *Acetyl CoA* (available from the fermentation of various feedstocks such as glucose and other simple sugars, methanol, and acetic acid) to form *acetoacetyl-CoA*. Subsequently, in the second step this compound is further enzymatically reduced to *R-Â-hydroxybutyryl-CoA* which is finally added to the growing PHB chain by *PHB synthase* in the third and final step. Other PHAs can be produced by inducing bacteria to the varying growth media. One such other PHA is polyhydroxyvalerate, PHV. The appropriate concentration of propionic acid are added to the glucose feedstock in the fermenter to induce bacteria to make a copolymer of PHB and PHV, polyhydroxybutyrate valerate (PHBV) with a controlled ratio of hydroxyl- butyrate (HB) to hydroxyl valerate (HV) monomers varying from 0 to 47 mole%. Higher HV fractions, up to 90 mole%, in the copolyester can be attained by using pentanoic acid in the feedstock with glucose [9]. Although commercially not available, PHAs can be chemically synthesized.

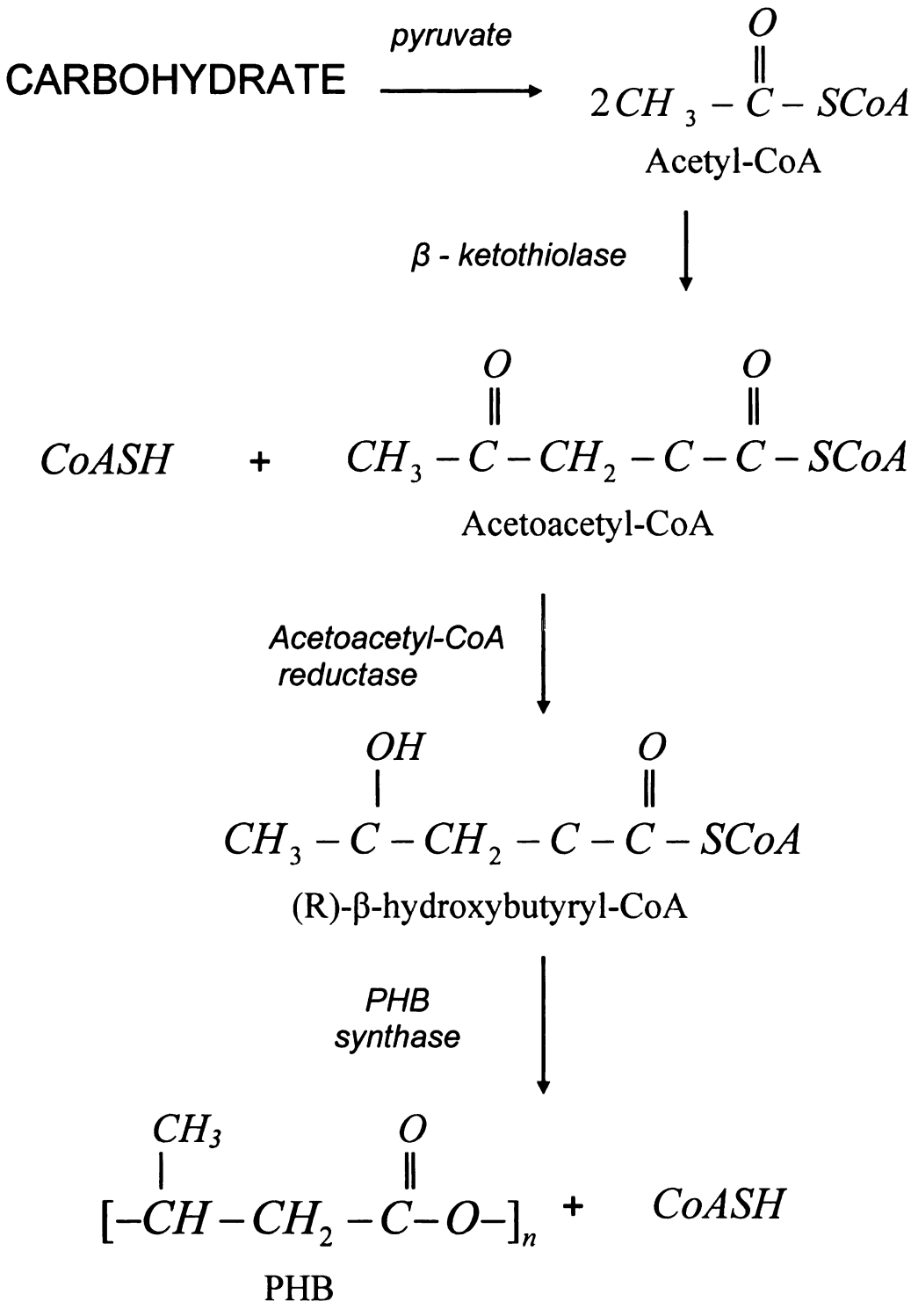

Figure 1.5: Enzymatic Path of PHB synthesis (Redrawn from reference)

This approach provides one to more easily and predictably accommodating variations

in molecular weight, co-monomer type, and co-monomer content with the availability of pure monomers.

PHA copolymerization is a ring-opening polymerization of α-lactones as shown following.

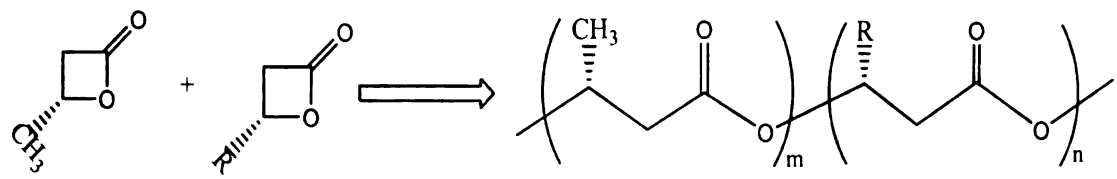

R can be, C_3H_7, C_5H_{11}, $C_{15}H_{31}$

Initiator used to prepare the isotactic PHA copolymers is difunctional zinc compound, ethylzinc isopropoxide (EZDP). Reaction temperature is reported to be at 60-65 °C because the 3-alkyl-α-lactones are unstable at higher temperatures. Lactones become more thermally labile with the longer the alkyl group, thus decomposing to carbon dioxide and terminal alkene. Therefore, there is always a need of balance among the polymerization temperature and reaction time with the thermal stability of the α-lactone monomers. Incorporation of the co-monomers is well accommodated in the molecular chain, and even at lower conversions of 30-50% the co-monomer incorporation is greater than 50% of the feed ratio. Other initiators reported in literature for this type of synthesis are aluminoxanes, distannoxanes and alkylzinc alkoxide. These initiator system give PHA with molecular weights >30 000. The appreciable mechanical properties of isotactic PHA polymers are only realized at the weight-average molecular weights (Mw) of 500 000 or greater. The use of highly purified and highly enantiomerically (enantiomeric excess > 90%) enriched monomers give isotactic PHA

polymers and copolymers with Mw up to several hundred thousand. The differences in the synthetic PHA are because these synthetic copolymers are not perfectly isotactic as the starting monomer 3-alkyl-α-propiolactones had only 92-95% stereo-purity. Stereochemistry plays a vital role in chemical synthesis as low levels of stereoimperfections causes 10 °C drop in melting point for synthetic PHB compared to the melting point of bacterial PHB. As reported in the literature this initiator system performs well in bulk polymerizations as well as in solution polymerization with toluene and tetrahydrofuran (THF) as a reaction media (in case of THF if the copolymer produced is soluble in THF). The polydispersities (PDI) of the polymer can be seen to be around 1.5 [12]. Utilizing the genetic engineering technique, genes in *R. eutropha* responsible for all the three enzymes in synthesis of PHB were transfer to other forms of bacteria *Escherichia coli* that have tenfold larger cell thus producing ten times as much polymer. In another, isolated genes were added to an *E. coli* strain that bursts at 42 °C thereby facilitating separation. Strains containing only the synthase gene can express enzyme in sufficiently large quantities for isolation and purification. The purified enzyme is stable in aqueous solution and was used for in vitro polymerization reactions of a wide variety of 3- and 4-hydroxyalkanoate-CoA monomers. In vitro polymerization reactions forms "living polymers", thus giving a polymerization process with no chain termination reaction therefore, propagating end group remains active indefinitely and very high molecular weight polymers can be prepared in vitro[13].

The genome sequence of the PHA producing bacteria, *Ralstonia eutropha* H16 had been reported by Pohlmann *et al* [14]. This opens new ventures for bioplastic producer improving PHA biosynthesis. The decoding of genome sequence provides an

opportunities for optimizing PHA biosynthesis and for developing metabolic-engineering strategies to generate bioplastics with improved properties[15].

In another the most exciting genetic engineering synthesis involves the transfer of PHA genes in plants so that they will convert acetyl CoA to PHAs as they grow. This accomplishment in the plant *Arabidopsis thaliana* came by a group of scientists from our university (Michigan State University) and James Madison University in 1992. Monsanto in 1994 took initiative to produce PHAs in the leaves and stem of corn. Thus, plastic production could, theoretically, be produced from plants. However, the challenge of efficient energy and cost remains in separating the PHAs from the plant material and purifying it [7-13].

Production

The first prototype of PHAs, polyhydroxybutyrate (PHB), was discovered in 1927 at the Pasteur Institute in Paris and the first commercialization was done by W.R. Grace Co. in the 1950s. Recently, a series of PHA copolymers are being commercially produced under the trade name of BIOPOL by Zeneca Bio Products (formerly ICI Bio Products),[7]. More recently, Metabolix has announced new grades of PHBV under the trade name of *Mirel* Natural Plastics for injection molding and paper coating. General mass production of PHAs is done by fermentation process as illustrated in figure 1.6. Extraction of PHAs from the bacteria is carried out in the final stage. This can be accomplished by the following three techniques 1) Solvent extraction, 2) Sodium hypochlorite digestion, and 3) Enzymatic digestion.

Solvent extraction is expensive and requires large volumes of solvent but produces high purity and high molecular weight PHA. Benefit of sodium hypochlorite

digestion is that it degrades and dissolves all cellular components of biomass except PHAs, but it can also damage the polymer product and is difficult to separate from the final product. The extraction process of enzymatic digestion involves the use of several enzymes to maintain an appropriate temperature to dissolve DNA that is released along with PHAs otherwise it becomes difficult to separate it from the viscous suspension [9].

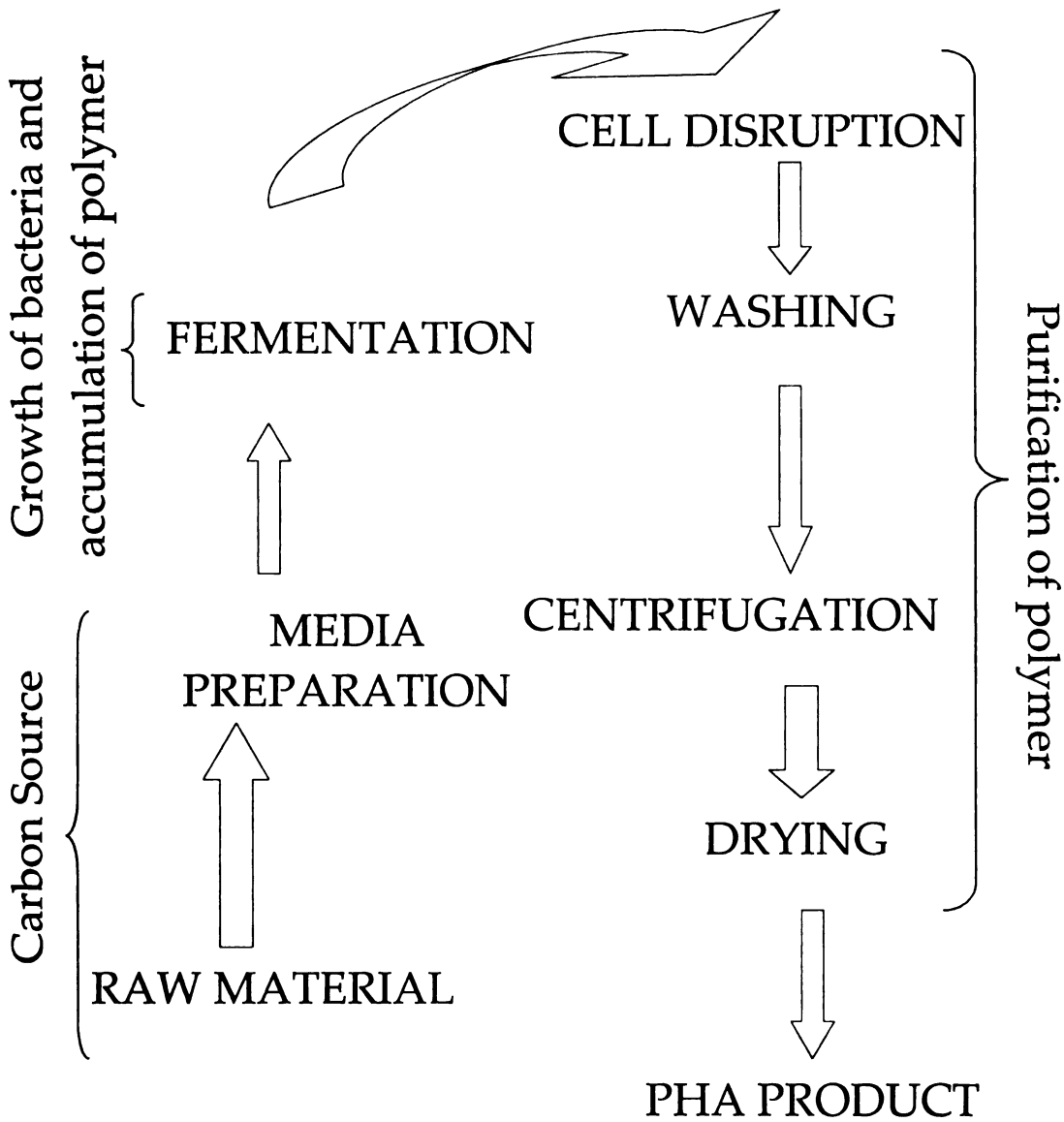

Figure 1.6: PHA production Process (Redrawn from source: Bioinformation Associates, Boston MA)

1.1.2 Structure and Properties

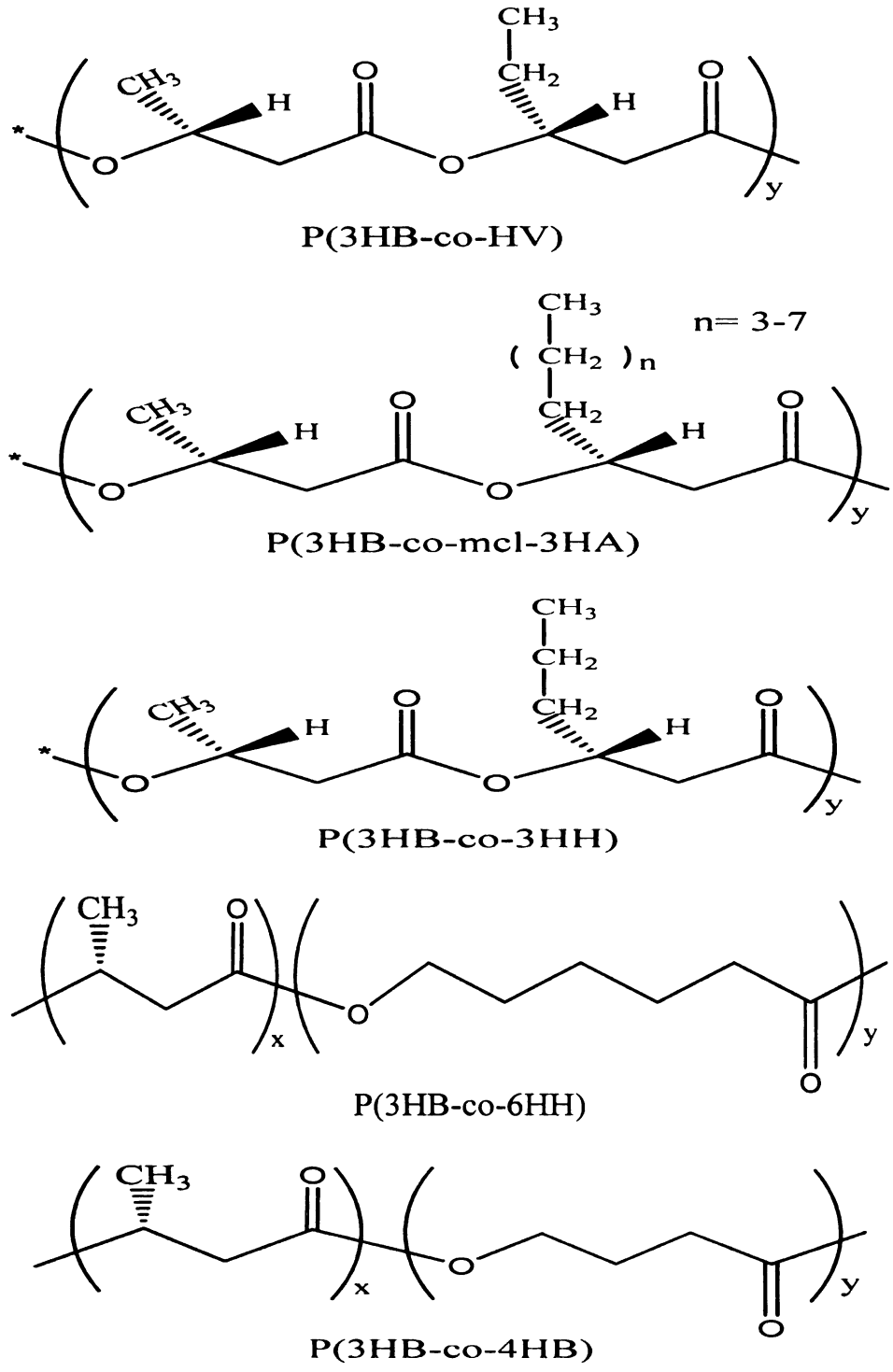

Figure 1.7: Structures of different PHAs, (HB) hydroxy butyrate, (HA) hydroxy valerate, (HH) hydroxy hexanoate.

The general structures of PHAs are shown in figure 1.7. By altering the feedstocks and the microorganisms PHAs copolymers of different compositions can be framed with properties ranging from highly crystalline, rigid plastics to rubbery elastomers. The side chains can be of different functional groups or with different number of methylene groups at â-position (3^{rd} carbon from carbonyl group) or the polymer's main chain itself can have different number of carbon atoms. There are more than hundreds of monomers reported as PHA constituents, but only few have been commercialized. PHA's thus produced by microbial synthesis bear a highly stereoregularity in their molecular structure and all the chiral carbon atoms in the backbone chain are in the R (-) configuration [10, 16]. PHB is isotactic with methyl groups on carbon chain in a single conformation [17].

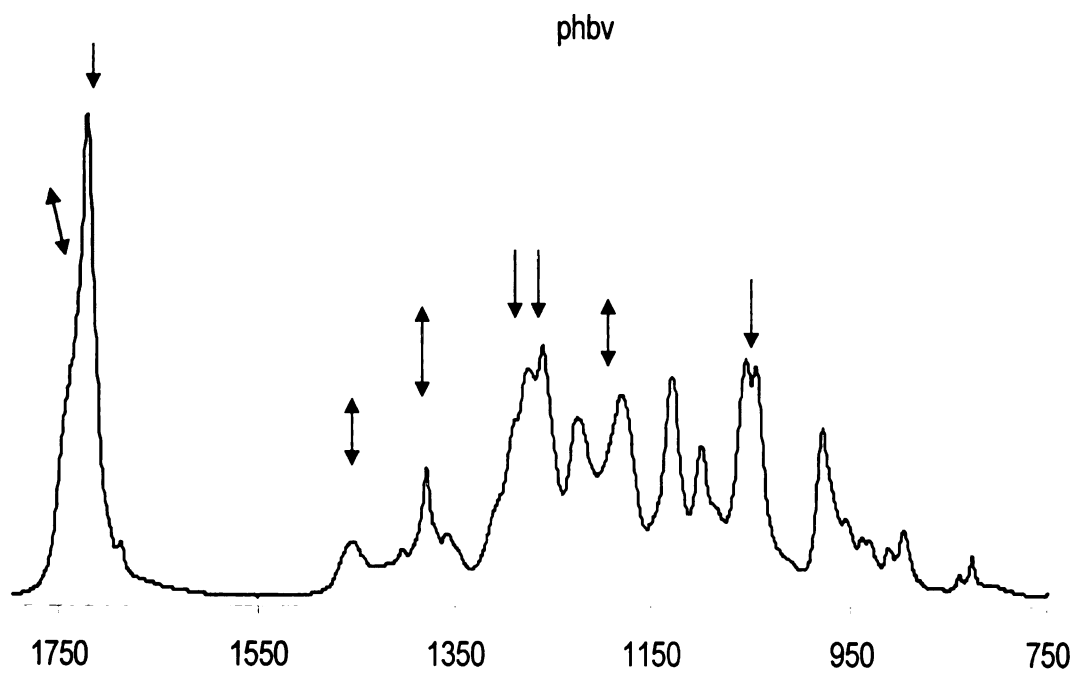

Figure 1.8: FTIR spectra of PHBV

The figure 1.8 above is the FTIR spectrum of PHBV and describes various absorption bands by functional groups of the polymer. In the spectrum, band at 1720 cm^{-1} was the C=O stretch of the ester group present in the molecular chain of highly ordered crystalline structure[18]. A small hump at 1740 cm^{-1} was of C=O stretch in the amorphous region of a semicrystalline PHBV. Characteristic peaks of symmetric –C–O–C– stretching vibration were present from 800 cm^{-1} to 975 cm^{-1} and the antisymmetric –C–O–C– stretching between 1060 cm^{-1} and 1150 cm^{-1}. Band around 1378 cm^{-1} corresponds to the symmetrical wagging of CH_3 groups and at 1453 cm^{-1} was due to asymmetric deformation of methylene groups, the intensity of both the peaks is independent of crystallinity or in other words insensitive to cystallinity. The absorption bands at 1720, 1276, 1228, and 980 cm^{-1} arose from the crystalline regions(designated with arrows) and bands at 1740, 1453, 1176 cm^{-1} from the amorphous regions (designated with double arrows, pointed both ways in opposite directions) of PHBV. Peak at 1228 cm^{-1} was purely of the conformational band of crystalline helical molecular chains and therefore are absent in amorphous region [19]. Crystallinity Index (CI) give the relative measure of degree of crystallinity in PHBV. It is given as

$$CI = \frac{I_{at1378cm^{-1}}}{I_{at1176cm^{-1}}}$$ (*ratio of intensity of the band insensitive to crystallization to the band sensitive to crystallization*), where I is intensity of the peak at a given wave number.

^{13}C and ^{1}H NMR of PHB reveals the details of its structure by elucidating the environment of carbon and hydrogen atoms, respectively in the molecule. The peak at about 69.6 ppm is assigned to the α carbons that are at branching of methyl or ethyl groups. Similarly, the peak at 42.8 ppm is attributed to α carbon neighboring the carbonyl groups and peak of carbonyl carbons is observed at 171 ppm. Branched methyl group carbons of PHB show peak at 21.3 ppm and in case of PHBV branched ethyl has two carbon atoms (CH_3CH_2), carbons corresponding to CH_3 show peak at about 10 ppm and that corresponding to CH_2 shows at about 37 ppm (intensity of peaks very small). Intensity of peaks corresponds to the % of valerate (HV) content in the PHBV copolymer [20]. The sharpness of peaks or signals may arise from the orderliness of the structure therefore, an estimation of the crystalline regions can be made using NMR. For further details reference can be consulted [21]. In ^{1}H NMR spectra, the methine proton attached to the asymmetric carbon or α carbon shows multiplet at 5.25 ppm. Proton or hydrogen atoms on the methylene (CH_2) shows multiplet at 2.53 ppm, which consists of eight peaks due to the conformational inequivalence of the two hydrogens on it. Protons on methyl group (CH_3) have a simple doublet at 1.27 ppm. In case of PHBV methyl protons shows a triplet at around 0.89 ppm. Due to various stereo isomers of PHBV or PHB, different conformations of branched groups on the main chain are possible. Thus the different tacticity of the stereomers may lead to further splitting of multiplets. Further discussions regarding the use of ^{1}H and ^{13}C NMR to study stereoregulation of PHB and PHV can be read in

reference [22]. Using the ^{1}H NMR spectra of PHBV the compositions of copolyester PHBV samples can be determined from the areas of the methyl resonances in the side groups of HB and HV repeating units. In another option, the peak area of the proton from methylene resonance due to the HV (CH_3CH_2) ethyl side group can also be utilized to determine copolymer compositions. However, presence of water in the sample leads to faulty inference of high copolymer due to impurity peak at -1.67 ppm, which overlaps the methylene resonance of HV in $CDCl_3$ therefore this is not a recommended analysis [23].

PHB or PHV molecule forms a left handed 2_1 helix with two molecular chains passing through the unit cell. The unit cells of the lattice system for both PHB and PHV are orthorhombic ($\alpha = \beta = \gamma = 90^0$) with P $2_12_12_1$ ($D_2{}^4$) index and the axis are ***a*** = 0.576 nm, ***b*** = 1.320 nm, and ***c*** = 0.596 nm (fiber repeat) for PHB and ***a*** = 0.952 nm, ***b*** = 1.008 nm, and ***c*** = 0.556 nm (fiber repeat) for PHV). PHBV or P(HB-co-HV) is a copolymer of HB and HV monomer units and is an isodimorphous system (i.e. it can crystallizes with two different structures depending on the HV content in the copolymer). The PHB or P(3HB) crystal lattice (fiber repeat 0.596 nm) is observed when the compositions of HV ranges from 0 to 37 mol % while the PHV or P(3HV) crystal lattice (fiber repeat 0.556) is observed when the compositions of HV ranges from 53 to 95 mol %. Lattice transformation takes place at about 40 mol % of HV content and it is assumed that both crystal structures coexist in an intermediate pseudoeutectic composition ranging from 36 to 56 mol% HV. The d-spacing of PHBV

or P(3HB-co-3HV) are listed in Table 1.1, borrowed from the reference [24]. For the copolyester PHBV with HV content ranging from 0 to 37 mol % which has the P(3HB) lattice pattern. Among the calculated (020), (110), and (002) d spacing, the (001) d spacing was found to be increasing and (020) and (002) d remained unchanged with the increasing HV mol %. The author suggests that the increasing (110) d spacing which is associated with the "***a***" parameter of the unit cell was due to the ethyl group (which is

Table 1.1: Listing 2Θ values corresponding to d-spacing of PHBV lattice

Planes	020	110	111	031	040	002
d-spacing (A)	6.58	5.254	4.048	3.493	3.300	2.988
2 θ (^{o})	13.75	17	22	25.3	27	30

bigger in size than methyl) of HV units which expand the (110) plane of the P(3HB) lattice because of the steric hindrances. Whereas for the compositions of PHBV with HV content ranging from 53 to 95 mol % which have P(3HV) lattice pattern, there was no change in all the observed {(020), (110), and (211)} d spacings, thus leading to the conclusion that the P(3HV) unit cell parameters were not influenced by the methyl side chains of 3HB units (as the methyl units as smaller than ethyl units thus fits well in the units of PHV lattice) [24, 25]. The degree of crystallinity can be obtained from the X-ray diffracted intensity data in the range of 2 Θ = 10-38.5^{o}. The peaks at 2Θ =17^{o} corresponds to (110) diffraction patterns and at 13.7^{o} corresponds to (020) diffractions [26]. The approximate 2Θ values corresponding to the d spacing of the lattice plane are listed in the table 1.1.

PHB produces bacterially has a low nucleation density and thus have a spherulites of very large dimensions which may grow up to several millimeters in diameter at high crystallization temperatures during the crystallization from the melt [27].

As suggested by the author in reference[28] there are some intermolecular interactions between the C= O and CH_3 groups in the lattice, and these interactions decrease along the ***a*** axis of the crystal lattice with temperature. (Ozaki) The author in the same reference discusses the conformational rearrangements of PHB during the melt crystallization using 2D-IR- correlation spectroscopy and infers that there is a cooperative structural change of various functionalities within a polymer chains. During the melt-crystallization of PHB, a different rate of changes was observed for the C-O-C and C-C backbones. The author further suggests that a sequential change of chains occurs during their structural adjustment and these sequential changes occur in the order stated. During the crystallization process, Firstly, the ester groups are the localized and flexible moieties and instantly adjust their conformation. Secondly, long and regular 2_1 helix chain sequences starts developing through annealing and in the final stage these regular 2_1 helix sequences packs themselves into the crystal unit cell, which takes the longest annealing time [28].

Mechanical properties

Generally, the properties of PHAs corresponds to the type, composition, and distribution of co-monomer units in the polymer chains, and also to the weight average molecular weight (M_w) and molecular weight distribution (poly dispersity index) of the

polymer. Their mechanical characteristics can be tailored to resemble elastic rubber or hard crystalline plastic. The minimum M_w required for these polymer to exhibit appreciable mechanical properties is 500,000 Da [12]. Often its properties have been compared to polypropylene thermoplastic as there elastic modulus and strength are of the similar order. PHB and PHBV produced in bulk quantities have elastic modulus of 1.7 and 1.2 GPa, with the strength (or yield stress) of 35 and 25 MPa, respectively. These are brittle materials with low impact strength of the order of 3 kJ/mm and low elongating (> 7-8%)[29]. In fact PHBV copolymer was produced in order to improve upon the brittleness of PHB by inducing the valerate (HV) units in to the PHB molecular chain. It was assumed that the ethyl group may interfere with the ordered unit cell of PHB and disrupt the crystallinity, which was responsible for its brittleness. Because of the bio origin, PHB has a high order of stereo-regularity of the isotactic chain thus leading to high crystallinity and its subsequent brittleness. The primary reason associated with its brittleness is the secondary crystallization. During the aging or the storage time at the room temperature post crystallization phenomena of the amorphous phase occurs, which further constrains it within the crystallites. Due to high purity of bacterial synthesis, PHB has low nucleating density leading to large spherulite size which may run up to several millimeters in size and exhibit interspherulitic cracks. Both these factor leads to rapid decrease of elongation at break or embrittlement, increase in its elastic modulus, strength and density. The elastic modulus increases from ~1.5 GPa of the up to ~3.5 GPa, whereas the impact strength decreases accompanying the reduction in elongation to > 7-10 % [12, 30, 31]. Brittle failure of PHB due to

presence of radial and circumferential cracks in spherulites which grows on straining has also been reported in literature [32].

PHAs have poor thermal stability and thermal degradation begins ~200°C. The melt temperatures is at ~ 170°C and even at this temperature with prolong processing under conventional techniques molecular weight reduction has been observed. Thus, this gives a very narrow processing window of these polymers [12, 30, 31].

The crystals of PHB bears no center of symmetry and therefore change in the direction of average dipole moment occurs if the deformation of crystals are carried in a particular way i.e., the material is a piezoelectric.

PHB has a lower solvent resistance but is more resistance to ultraviolet weathering than polypropylene.

Being a crystalline material its film has an excellent gas barrier properties, five times more effective to CO_2 as a barrier than PET and as strong as polypropylene but not as tough as PET and PP [33].

In an attempt to improve upon mechanical properties of PHB and PHBV copolymer nucleation, plasticization and lubrication have been carried through in processing [29].

PHAs biodegrade in microbial active environments. Since, PHAs function as an intracellular energy and carbon source and use them as reserve materials, bacteria can degrade PHAs. Microorganisms attack PHBV by secreting enzymes (depolymerases) that break down the polymer into its basic hydroxybutyrate (HB) and hydroxyvalerate (HV) constituents. The HB and HV fragments are then consumed by the cells to sustain growth. Under aerobic conditions, the final biodegradation products are water and

carbon dioxide; under anaerobic conditions, methane is produced as well. The degradation of PHBV can be quite rapid in biologically active systems. A range of soil micro-organisms, both bacterial and fungal, can utilize PHAs as a source of carbon and energy [7, 9].

1.1.3 Methods of modification and processing

1.1.3.1 Copolymerization

A special approach to design the copolymer molecular chains was investigated by McChalicher et al., in which the differences in mechanical properties between the random copolymers and block copolymers of the same copolymer were investigated as the properties change over time. It was shown that the block copolymers maintain more elasticity over a period of time than the similar random copolymers of analogous composition [34].

To improve upon the material properties or act as a useful functionalized polymer, a copolymer containing 3-hydroxy butyrate (3HB) and 3-hydroxy-4-pentenoic acid (3HPE) was reported. This was done to obtain a copolymer with low *T*g, low degree of crystallinity, and a functionality that could be cross-linked during processing [35].

With an objective to reduce the melting temperature of the PHB, and assuming this would be an effective method to prevent its thermal degradation, and allow it for lower processing temperatures in the hot-drawing process. Tsuge et al, synthesized a copolymer P(3HB-co-3HA) with a small (3HA)fraction, where 3HA were the medium chain length hydroxy alkanoates with number of carbon atom ranging from 6 to 12 [36]. In an another similar study to improve the flexibility of the PHB by incorporating

medium-chain length monomers (PHAmcl, C6–C12) in the molecular chain, the synthesis of a copolymer, poly(3-hydroxybuty-rate-co-3-hydroxyoctanoate) [P (HB-HO)] was reported [37].

To obtain a set of useful properties not achieved by more traditional PHA polymers, like PHB homopolymer or PHBV copolymers another simplest form of mcl 3-hydroxyhexanoate (3HHx) units were introduced to obtain a copolymer P(3-HB-co-3HHx), which is branded under the name of "Nodax"[38]. The industrial scale production, and economical production of this copolymer from palm oil are also listed[39, 40] .

Glycogen accumulating organisms (GAOs) were used, in a study by Dia e tal, to produce PHA copolymers from a simple and cheap carbon source. The production of poly(3-hydroxybutyrate (3HB)-*co*-3-hydroxyvalerate (3HV)-*co*-3-hydroxy-2-methylvalerate (3HMV)), with 7–35 C-mol% of 3HV fractions from acetate as the only carbon source with the use of GAOs was described [41, 42].

To further widen the scope of PHAs, a unique biosynthesis of the copolymer of 3-hydroxybutyrate and 3-mercaptopropionate, poly(3HB-co-3MP), with a molar fraction of 3MP of up to 43% was described [43]. In addition, PHAs with the side chain substitution of phenyl, cyno and halogens were also reported [44].

PHA was attempted to copolymerize with Polyethylene glycol (PEG), thus producing PHA-PEG terminated copolymers[45, 46]. The introduced PEG group may react with a range of molecules, thus, setting up the opportunity of new conjugates between PHAs and other natural or synthetic polymers. Poly(ester-urethane) (PU) multiblock copolymers from hydroxyl-terminated poly(ethylene glycol) (PEG) and

hydroxylated poly[(*R*)-3-hydroxyalkanoate] (PHA-diol) were synthesized for blood contact applications, using 1,6-hexamethylene diisocyanate as a coupling reagent [47]. For medical and pharmaceutical applications, such as drug delivery systems, an investigation to observe the influence of P(3HB-*co*-4HB) composition ratio and drug loading level on the biocompatibility of P(3HB-*co*-4HB) was reported [48].

In an another attempt to reduce the melting point and crystallization of PHB the biosynthesis and characterization of HB-rich co- polymers containing 2-4mol% of hydroxycaproate (HC) units, as well as a terpolymer containing HC and hydroxyoctanoate (HO) units was reported [49].

To exploit the advantages of natural and synthetic polymers, methyl metha acrylic acid (MMA) was grafted on PHA-soybean to obtain new composite materials [50].

Investigation concerning the optimization of the cost effective production of PHA copolymers had been carried out by many researchers by altering the various parameters like, carbon feed source, bacteria, genetic modification, enzymes [38, 40, 51-58].

Other than copolymerizing different PHA monomers among themselves, a copolymer of PHB and PLA monomeric units was carried out by Dahlia et al.. This was achieved via ring-opening polymerization of L-lactide using PHA as a macroinitiator with stannous octoate as catalyst, thus introducing PHA units, up to 20 wt %, into PLA [59].

1.1.3.2 Plasticization

Plasticization of the PHB was another attempt to overcome its brittleness for commercialization purpose. Plasticizers interfere with the intermolecular interactions

within the polymer molecular chains and therefore, ease their conformational degree of freedom. This alters the glass transition and flexibility/deformability of the polymer. Change in the degree or rate of crystallization can also be observed due to the plasticization effect in a polymer. Preferably, plasticizer used for PHB must be "biodegradable" so that it retains the integrity of biodegradability. Numerous plasticizers irrespective of their biodegradability have been used to improve upon its brittleness. *Citric acid based esters like, triethyl citrate, acetyl triethyl citrate, acetyltributyl citrate, butyryltrihexyl citrate* were reported to be used in PHBV as a biocompatible plasticizers[60]. Another type of plasticizers for biodegradable polymers mentioned are glycerine based esters. Kunze et al. give a description of *salicylic esters, acetyl salicylic esters, aryl propionic esters and phthalic acid esters* as the plasticizers in PHB films [60]. Among these, *salicylic acid decyl ester, acetyl salicylic acid hexyl ester and ketoprofen ethyl ester* were stated to give increased elongation at break of PHB [60].

Biber eta al., used a series of plasticizer, *i.e., dioctyl sebacate, dibutyl sebacate, polyethylene glycol, Lapro1503, and Lapro15003,* These plasticizers were reported to be compatible and forming monophase with the PHB up to 15 – 20 wt% in composition. The relative breaking elongation of PHB with *Laprol 503,* at room temperature was mentioned to increase up to 250-300%[61].

Acylglycerols were used as plasticizers by Iskawawa et al., and among these glycerol triacetate (GTA) was reported to be the best for PHB. At 30 wt% the elongation at break increased from 5% to 130% (as mentioned) [62]. An increase in the

elongation at break of pure PHB by addition poly (ethylene glycol) (PEG) in varying proportions was reported as well [63].

Soya bean oil (SO) and epoxydized Soya bean oil (ESO) were used as the biodegradable plasticizers in PHB and PHBV [64, 65]. Epoxydized Soya bean oil was stated to be more effective as a plasticizer and in increasing the elongation at break and impact strength of the films. The amount of these plasticizer was mentioned to be varied from 5 to 30 % in the blend composition [64, 65]. In a comparative study, plasticization effect of dibutyl phthalate (DBP) and triethyl citrate (TEC) was weighed against the SO and ESO by the same author. It was affirmed that TEC or DBP were better plasticizers than SO and ESO for PHBV [64, 65].

PHB was plasticized with another set of plasticizers dioctyl (o-)phthalate, dioctyl sebacate, and acetyl tributyl citrate (ATBC) by Wang et al.[66]. Among these, ATBC was stated to be a competent one.

1.1.3.3 Blending

Blends can be defined as physical mixtures of structurally different polymers which may exist as a single phase (miscible blends) or distinct phases (immiscible blends). The physical properties of blends are strongly dependent on this miscibility and hence most work on PHB based blends is concentrated in achieving miscibility. Thermodynamically miscible blends of PHB have been reported with poly (vinyl alcohol), [67] poly (ethylene oxide), [68], [69] poly (lactide), [70, 71] poly (butylene succinate-co-butylene adipate), [72] poly (ε-caprolactone-co-lactide), [73] poly (butylene succinate-co-ε-caprolactone), [72] cellulose acetate butyrate, [74] poly (ethylene-co-vinyl acetate, [75] poly (vinylidene chloride-co-acrylonitrile) [76].

Compatible blends of PHB have been obtained with poly (ε-caprolactone), [77, 78] and polysaccharides [79]. Miscible blends of PHB have been formed with non-biodegradable polymers such as poly (epichlorohydrin), [80] and partly miscible blends are formed with poly (methylmethacrylate), [81] ethylene-propylene rubber, [82] and poly (butylacrylate) [83].

The miscibility of the PHB with poly(caprolactone-co-lactide) (P(CL-co-LA)) was studied by Naoyuki Koyama et al [71]. The varying ratios of caprolactone to lactic acid in P(CL-co-LA) describes the miscibility as a function of the ratio of two components in P(CL-co-LA). He further provides the details of the persisting relationship among the number average molecular weight (M_n) and the lactic acid fraction in P(CL-co-LA) on the miscibility of the, PHB/(P(CL-co-LA), blend and discussed it in context of Flory Huggin's theory. The transition of immiscibility to the miscibility of the blends was favorable at low Mn and over 21% LA content in (P(CL-co-LA) copolymer, therefore, depicting the decrease in Flory Huggin parameter for the P[(R)-3HB]/P(CL-co-LA) blend with the increasing LA fraction in the P(CL-co-LA) copolymer component. These blends were, additionally, investigated for their spherullite morphology, further, suggesting that the uncrystallizable P(CL-co-LA) component exists within the spherulites of P[(R)-3HB]. The spherulites of P[(R)-3HB] exhibited banding in the miscible blends, and in case of immiscible blends, phase separation of the P[(R)-3HB] and P(CL-co-18 mol % LA) components in the interfibrillar regions within the P[(R)-3HB] spherulites. In respect of the biodegradability of the blends, the author concludes the decrease in the rates of enzymatic hydrolysis with the increasing P(CL-co-LA)

content, and the biodegradability was independent of the miscibility of the blending components.

Wang et al.[74] discusses the PHB and cellulose acetate butyrate (CAB) blends in different blending ratios. The author states the miscibility of both the components over the entire scale of mixing ratios in a melt state. The decrease in the melting temperature and the crystallinity of the PHB with the increasing CAB percentage in the blends was reported, and the CAB content, more than 50%, lead to an improvement in the PHB toughness with the development of homogeneous amorphous phase. CAB content in the blends was a controlling parameter of the degradation rate of the blends.

In a study by Yoon et al. [75], PHB and poly(ethylene-co-vinyl acetate) (EVA) blends, with the 70% and 85% vinyl acetate(VA) content in EVA, confirms the miscibility of both at a higher VA fraction. The blends were solution casted. The author establishes the miscibility of PHB-EVA (at 85% VA) on the basis of Flory interaction parameter (χ_{12}), which come out to be negative from the depression in melting temperature with increasing EVA fraction in the blends. The growth rate of the PHB spherulite was also shown to be reducing with the increasing EVA content at 85%.

Gonzalez et al.[76] reports the solution precipitated blends of PHB and poly(vinylidene chloride-co-acrylonitrile) copolymer (VDC-co-AN) with the improved CO_2 permeability at 50 wt% of poly(VDC-co-AN). Blends, containing 32 mole % of AN units in poly(VDC-co-AN) copolymer, were miscible over the complete set of blended compositions. The appearance of distinct glass transition temperature, and the depression in melting point of PHB, reflected the miscibility of the blends, and the interaction parameter, obtained from the melting point depression analysis, was

reported to be -0.08. The miscibility of PHB and poly (VDC-co-AN) was contemplated due to the conditioned dipole–dipole interaction between the carbonyl group of PHB and chloride atoms of VDC-co-AN copolymer.

Rosa et al.[84] studied the effects of oxidized polyethylene wax (OPW) on the tensile properties of PHB/LDPE blends. The blends were stated to be immiscible with or without the presence of OPW and no significant deviation in any of the properties were demonstrated.

Binary blends of PHB with poly(-caprolactone) (PCL), poly(1,4-butylene adipate) (PBA) and poly(vinyl acetate) (PVAc) were studied by Kumagai and Doi in respect of their miscibility, morphology and biodegradability [77] PHB/PCL and PHB/PBA blends were stated to be immiscible, and phase separation occurring at macro and micro scale, respectively, whereas, the PHV/PVAc blend was miscible. Enzymatic degradation of PHB was affected by the weight fraction of second component in the blends. In case of PHB/PBA or PHB/PVAc blends the rate of degradation plummeted with the increased weight fraction of PBA and PVAc. Though, PHB and PCL blends were immiscible, Gassner and Owen[85] mentions that these blends formed mechanically compatible films containing phase-separated partially crystalline domains. In order to be temperature-resistant, the blended composition, due to the low melting point of PCL (60°C), was restricted to have the PHB fraction no lees than 0.6 in the entire composition.

Paglia et al [80] details that atactic poly(epichlorohydrin) (PECH), when above the equilibrium melting temperature of the two components, has tendency to form a thermodynamically stable miscible blends with PHB, and this was inferred from the

negative value of the χ_{12}. The miscibility of blends was also confirmed from the appearance of distinct single glass transition temperature depending on the varying composition of the components and their agreement with the Fox equation.

Tertiary blends of PHB with poly(ethylene oxide) (PEO) and poly(methyl methacrylate) (PMMA) were attempted by Yoon et al [81] subsequently, after establishing the miscibility of PEO individually, with PHB and PMMA, but PEO was ineffective to stimulate the compatibility among the two. Miscibility of PHB with PEO and immiscibility of PHB with PMMA was reasserted with their respective negative and positive values of χ_{12}. The substantial effect of compositions on the χ_{12} value was emphasized.

Immiscibility of PHB and (ethylene-propylene rubber (EPR) and its compatibility with poly(vinyl acetate) (PVAc)) was reported by Greco and Martuscelli [82]. Miscibility of PHB and PVAc in perspective of distinct single glass transition temperature of blends and depression of equilibrium melting temperature of PHB was highlighted. Phase segregation of EPR and occlusion in intraspherulitic regions of PHB spherulites during the growth from the melt was elucidated using optical microscopy.

A unique study by Avella et al.[83], with an objective to improve upon the impact strength of PHB, reactively blended polymeric PHB with butyl acrylate monomer to form inclusive poly(butyl acrylate) and PHB blends. The paper discusses the enhanced impact strength with the poly(butyl acrylate) inclusions and details the preparation of the reactive blending of the two. It also discusses the morphology of the prepared blends in different proportion of the two components.

1.2 Wood Plastic Composites

1.2.1 Conventional Wood Plastic Composites

In the past few years wood and natural fiber plastic composite (W/NF PC) are well-known in the consumer market of plastic composites, and there dynamic emergence have made them the fastest growing segment in the plastic industry with their ongoing growth of 25% and projecting a strong market demand in the near future [86]. The current market of wood plastic composites (WPC) is 1.2 billion pounds and is expected to grow with an average annual growth rate of 9.8% thus providing a market of 1.9 billion pounds by the year 2009 [87]. Not only, do they have a proven market in outdoor and indoor applications like decking, railing, fencing, furniture, etc. they also hold a large share of the European market in automotive applications[88]. The wide acceptance of W/NF PC by the global market has been due to their reduced cost, weight, superior properties over wood and plastic alone, recycling ability, adaptation to the existing plastic processing techniques, and above all the motivation of industry to ahead for the eco-friendly products. Most of the thermoplastics being used in W/NF PC are recyclable, and are being looked as a profitable opportunity for these materials. Contemporary W/NF PC are based on conventional thermoplastics and naturally available cellulose fiber, the fiber content varying from 30 to 70 wt.% in the composites. Polypropylene has the major market share of W/NF PC followed by polyethylene, polyvinylchloride and other resins. Various kinds of lignocellulosic natural and wood fiber have been used to achieve improved mechanical properties of W/NF PC. These lignocellulosic filler includes various wood fibers/flour (e.g maple,

pine, birch etc.), flax, jute, bagasse, corncobs, cereal straw, kenaf, jute, sisal, coir, flax, banana, rice hulls, newsprint, pulp, and even waste wood.

The enhancement in the mechanical properties of the W/NF PC are governed by properties of the matrix and the reinforcement, phase state of matrix after reinforcement, interface developed due to the interaction between the matrix and reinforcement. Amount, shape (aspect ratio), distribution/dispersion and alignment/ orientation of the fibers within the composite matrix, and fabrication process also plays a crucial role in governing the properties of the W/NF PC [89].

While, all afore listed factors affect the composite characteristics, among all, the interphase between the matrix and fiber typically, plays an important role. It determines the extent of the stress developed in the matrix that is transferred to the reinforcement. A good interface gives an efficient stress transfer between the two due to the better adhesion, and therefore, gives the best of mechanical properties (Strength and toughness).

The possible adhesion mechanisms occurring between the matrix and the filler reinforcement are adsorption, chemisorptions, electrostatic interactions, mechanical interlocking. Adsorption happens due to the intimate intermolecular interactions between the molecules of substrate (fiber) and resin (thermoplastic), which results from Van derWaals forces or Hydrogen bonding. Chemical bonds created between the substance and the surface of substrate as a result of chemical reactions is called chemisorption. Electrostatic mechanism of adhesion is attributed to the creation of opposite charges on the interacting surfaces of fibers and thermoplastic thus, an interface consisting of two layers of opposite charges is formed, which accounts for the

adhesion of the two. The mechanical interlocking phenomena accounts for the adhesion when a matrix penetrates into the pores, holes and crevices or other irregularities of the substrate (fiber), and locks mechanically to it. A good wetting of the resin (thermoplastic) on the substrate (fiber) is essential for all the mentioned adhesion phenomena's to exist in an appreciable amount.

The lignocellulosic fibers are hydrophilic, and apolar thermoplastics (PP, PE) are hydrophobic therefore, there is a poor wetability and lack of adhesion between the two. This results in an incompatible interface between the lignocellulosic (wood /natural) fiber and thermoplastics that causes the filler debonding from the matrix and the poor dispersion of fiber in the matrix. The stress transferred from the matrix to the fiber due to poor interface is least efficient and subsequently, results in the poor mechanical properties of the composite [90, 91]. This situation requires developing the strategies for the surface modification of the lignocellulosic fiber surfaces that could render an effective control over the fiber/polymer interface. One approach to this situation is using a compatibilizer or a coupling agent that bridges the two different surfaces of thermoplastic and fiber.

Compatiblizer has two segments in a block copolymer as depicted in figure 1.9. One segment has a similar chemical nature to the thermoplastic matrix and the other is able to adhere to the wood fibers by any of the adhesion mechanism. The segment having similar chemical characteristics to the thermoplastic matrix is miscible in it. This generates an interface, of appropriate strength, between the fiber and matrix.

The wood adhering segment of the block copolymer generally has functional groups able to form covalent bonds with hydroxyl groups on wood fiber surface. A

covalent bond forms a stronger interface than a hydrogen bond and also reduces the

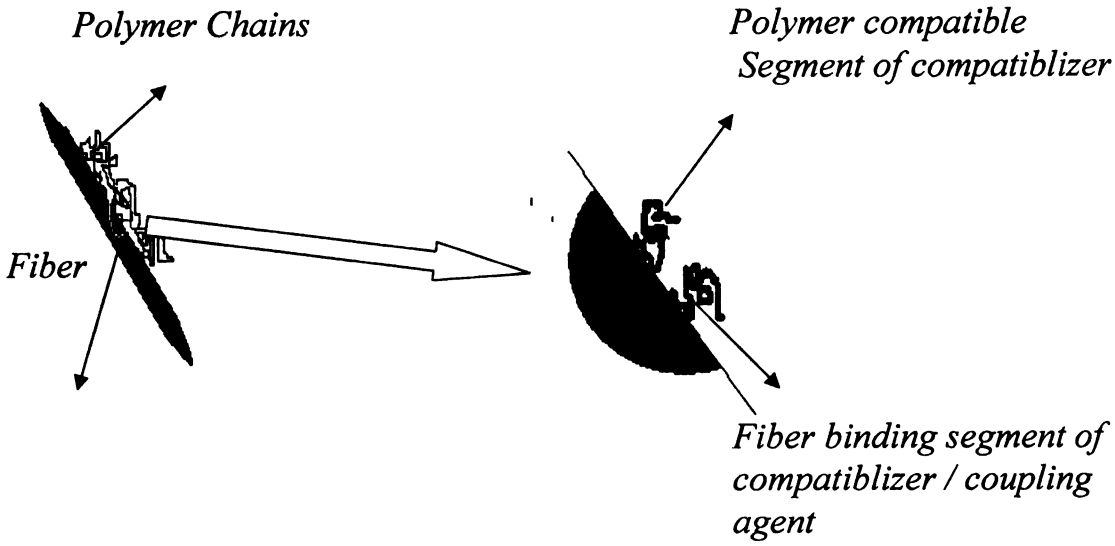

Figure 1.9: Schematic of coupling in interface region

hydroxyl groups (hydroxyl groups accounts for the water absorbing tendency of wood) on the wood fiber surface by reacting thus decreasing the hydrophilicity of wood fiber and making the composite better water-resistant than wood.

Maleated polypropylene has been the most common compatiblizer used as a coupling agent in polypropylene based WPC's that performs with the same strategy as mentioned and increases the strength of composites to a reasonable extent [92]. Surface modification of fibers using enzymes is also being looked into by various researchers and other chemical approaches to the compatiblization are carried out using silanes, isocynates, zirconates, organotitanate, grafting some polymeric chain on fiber surface (e.g MMA), impregnating fibers with the polymer compatible with the polymer matrix and alkali treatment of fibers to change morphology and enhance mechanical interlocking. Some fiber surface modifications using physical sources like plasma treatment, sputtering and corona discharge have also been mentioned [93] .

Strength of fiber-matrix interface in composites is often related with the mechanical dampening (Tan δ) in the dynamical mechanical analysis (DMA). Strong fiber-matrix adhesion lowers the mechanical dampening (Tan δ) value due to the reduced friction at fiber-matrix interface. Mechanical damping (Tan δ_c) within the composite system is given as $\text{Tan } \delta_c = \Theta_p \text{ Tan } \delta_p + \Theta_i \text{ Tan } \delta_i + \Theta_f \text{ Tan } \delta_f$

where Θ with subscript f, p, i are the respective volume fractions of the fiber, matrix and interface. Tan δ with subscript f, p, i are the mechanical dampening of the respective, fiber, matrix and interface. The adhesion factor (A) of the interface strength can be related to Tan δ as following.

$$A = \{(\text{Tan } \delta_c / \text{ Tan } \delta_p) / (1 - \Theta_f)\} - 1$$

The molecular mobility surrounding the fiber is reduced; when the fiber-matrix interface adhesion is increased. Low values of the adhesion factor (A) suggest improved interactions at the fiber-matrix interface.

It has been assumed that adhesion factor is reasonable only if the development of a transcrystallinity layer surrounding the fiber at the interface is ignored [94].

A significant amount of research, focusing to improve the compatibility between the hydrophilic natural fiber and the hydrophobic thermoplastics, is referred [95-98]. Nano-reinforcement using inorganic material like clay in wood-PP composites has also been reported elsewhere [99]. The only major limitation these composites have is their limited dimensional stability when exposed to moisture [100]. When comparing their moisture absorbance with the wood and plastic alone, these have a better moisture resistance than wood but lesser than plastics.

1.2.2 Wood as a natural reinforcing component

Wood has always been an essential part of human economy, since the beginning of any civilization. It has been used in several ways as a structural material, furnishing, tools etc., until recently, when it has found a new application as reinforcement in plastic composite. Wood fibers are used most abundantly in thermoplastic based composite, and in low severity applications for thermoset composites. There use as has been increasing with the growth of WPC market. This biomass industry is projected to become a $1.5 billion fiber market by 2012 [101, 102]. These fibers invite attention of the market due to their low cost, low density, easier to handle in production and abundance, but their renewabilty and eco-friendliness also allow them to be used as a sustainable material for future growth.

Wood fiber, also known as wood cells, forms the basic structural elements of the wood. These fibrous cells are hollow, elongated, spindle shaped cells that are arranged parallel to each other along the trunk of a tree. Their characteristics and their arrangements essentially, affect the properties such as strength and shrinkage of the wood. Woods are by and large classified in to hardwood (deciduous trees) and softwood (coniferous trees), which is based on the cellular structure of the wood. Hardwoods have four types of cells. Bulk of the wood is made from small wood fibers, and large cells function's to conduct sap up the tree through the mass of fibers , which on the end grain appear as holes or pores,. These are also called tracheids, hardwoods are also referred to as porous woods in contrast to nonporous softwoods. Other cells are largely used to store food and are the strength-giving elements of hardwoods. They are spindle shaped cells usually having small cavities and relatively thick walls. Softwoods

do not have vessels and have a simpler fibrous structure based on only two cell types. The length of wood fibers is highly variable within a tree and among species. Hardwood fibers average about 1 mm (1/25 in.) in length; softwood fibers range from 3 to 8 mm (1/8 to 1/3 in.) in length [103, 104].

These fibrous cells have cell wall of the thickness, which may vary up to 100 μm, and this makes the cell rigid. The supportive framework of the cell wall surrounds the cell. This constitutes a layers cellulose microfibrils network that are embedded in a matrix of lignin and hemicellulose. Dry wood is primarily composed of approximately 50% cellulose, which is the major component, 23% to 33% lignin in soft wood and 16% to 25% in hardwoods, hemicelluloses, and 5% to 10% of extraneous materials [104].

The structure of cell wall is layered; a primary wall is the outer most layer with a thickness of ~0.1μm, which constitutes mainly, a non cellulosic substances like waxes and pectin, but some cellulosic microfibrils that form an interwoven network; a secondary wall is the middle layer, which is the main strengthening unit of the cell wall that constitutes almost all of the cellulose in form of cellulose fibrils. To toughen the structure, the fibrils are aligned at 10 to 30° to the tree trunk axis of the cell wall. Lumen is the central canal, which chiefly holds the proteinaceous materials [104-106].

The secondary wall is actually an entity on three sub layers. First sub layer is adjacent to primary layer, which act as a transitioning sub layer of thickness ~ 0.2 μm. It consists of microfibrils, forming a lamina, crisscrossing each other and making an angle of 40 to 50° to a fiber axis. Second sub layer is the central one with a thickness of ~ 1 to 5 μm, which has micriobrils arranged parallel or making small angle with the

fiber axis. The third and the innermost sub layer adjacent to the lumen is also called tertiary wall. It has no fibrillar structure at all, but only a series of granules.

Cellulose, which forms a 50 to 55 % by wt. of the wood constituents, is a polysaccharide. The monomeric unit of this polymer is an unbranched poly-β-(1,4)-D-glucopyranose. In the cell walls these polymeric chains arrange to form ordered crystalline structures and cellulose is up to 90% crystalline. These crystalline regions form microfibrils, but less ordered or amorphous domains also exist. This is Important to mention that in these crystalline domains, the hydroxyl groups of the glucose units engage in ordered hydrogen bond systems, both within and between the cellulose chains. Intramolecular hydrogen bonding holds the accountability of the individual chain conformation, while intermolecular hydrogen bonding is responsible for microfibrils formation. The metastable cellulose-I is the most common allomorphic form of crystalline cellulose. It is a parallel arrangement of polymeric chains in a form of flatribbon conformation with a strong intramolecular hydrogen bonding. The two sub-allomorphs, I-α and I-β coexist in a cell wall and their ratio of prevalence varies in different types of wood [105-107].

The networks of cellulose microfibrils in a cell wall are embedded in a matrix of lignin and hemicellulose. Although, some fraction of lignin is distributed in the cell wall, but major portion of it is concentrated around and between the fibrous cell, and act as a binder or matrix for fibers. It is quit unclear that whether lignin is chemically or physically bonded to the cellulose, but it is tightly bonded to one of the constituent of the wood. Lignin is a three-dimensional phenylpropanol polymer and softens at the temperature of about $170^{o}C$ / $340^{o}F$. Wood lignins are predominantly an aromatic

mixture, and not fully soluble in the known solvent. Maple wood used in this research has 23 % lignin in it [104, 108].

Hemicellulose is another prime constituent of the wood, which is associated with the cellulose and lignin in a cell wall. It is a mixture of polysaccharides from different kinds of sugar monomer. In hardwoods glucose and xylose sugar monomers are more prevalent.

Other than three above mentioned major constituents wood has extraneous compounds and mixtures like, waxes, essential oils, fats, resins, coloring matter, gums, starch, and simple metabolic intermediates. These may vary from 5 to 30 % depending upon the species and growth of a tree.

The density of the dry cell wall is in the vicinity of 1.53 gm/cc, and may vary from specie to specie and other factors like growth conditions etc. The Young's modulus of wood cell wall has measured values ranging from 10 to 60 GPa, which again varies from species to species.

1.2.3 Talc as a reinforcing inorganic filler/component

Talc is a significant industrial mineral, and has an application in material for paints, rubber, plastics, insecticides, etc. It is a soft, platy, water repellent and chemically inert mineral, and practically no two talc from two different sources are same. It is available in various colors depending on the source ranging from white, brown and green to blue. Talc is a 2:1 layer phyllosilicate mineral, and chemically, an hydrated magnesium sheet silicate with the unit structure $Mg_3Si_4O_{10}(OH)_2$ and molecular weight, 379.27 gm. Crystal structure of talc is monoclinic or triclinic with the space group C-1 and unit cell dimension of a=5.2900 Å, b=9.1730 Å, c=9.4600 Å

α=90.460, β=98.680, γ=90.090

Z=2. The elementary sheets are composed of magnesium ion in an oxygen and hydroxyl octahedra that is sandwiched between the two layers of silicon and oxygen tetrahedral. The elementary sheet thickness is ~ 6.6 Å and the inter-sheet distance is ~2.8 Å. The hydroxyl groups are not located on the basal faces of the sheets, rather these are located within the sheets, i.e. on the lateral faces, which accounts for the talc's hydrophobicity and inertness. The elementary sheets are stacked, and the binding forces among these elementary sheets are weak Vander Wall forces. A few thousand elementary sheets constitute to form a platelet and these platelets slides apart at the slightest touch, which imparts the characteristic of softness to the talc. The dimensions of the individual platelet can range from 10 to 100 μm depending on the deposit source. The individual platelet dimensions determine the talc's platyness or lamellarity. Large individual platelet size will give a lamellar morphology and a much smaller platelet dimensions would result in microcrystalline talc. Generally, it is classified on the basis of mineralogy, morphology, and geographic source[109].

It is relatively chemically inert and thermally stable. Its melting point is at 1500°C, and re-crystallises into different forms of enstatite (i.e., anhydrous magnesium silicate) above 1050°C, after loosing the hydroxyl groups at 900°C.

Talc is used as an effective reinforcing agent in plastics because of its lamellar structure, which can disperse uniformly in the matrix, although it requires an advance and efficient milling technology to produce finest talc without compromising the aspect ratio of the lamellar structure. Talc also act as a nucleating agent in the semi-crystalline polymers. It is very commonly used in polypropylene to improve upon stiffness and

dimensional stability for food packaging, automotive and house hold appliance. In LDPE it is used as an anti blocking agent. Other uses of talc are predominant in rubber, paper, personal care, ceramic and coating industry. In rubber it is used as a processing aid and a viscosity modifier, and in decorative coatings as extenders to improve upon the hiding power and titanium dioxide efficiency.

1.3 Reference:

1. *http://www.principiaconsulting.com/publishing/reports.cfm?rpt=32 Date accessed 10/17/ 2008.*

2. *http://www.allbusiness.com/marketing-advertising/market-research-analysis/5695798-1.html Date accessed 10/17/2008.*

   http://www.plasticstrends.net/index.php?option=com_content&task=view&id=33&Itemid=31. Date Accessed 10/17/2008.

4. *http://composite.about.com/od/inthenews/a/bpr_principia2.htm Date accessed 10/17/2008.*

5. Aggarwal B.D. and Broutman L.J., *"Analysis and Performance of Fiber Composites"*. 1980, New York: JOHN WILEY & SONS.

6. Hull and Clyne, *"Introduction to Composite Materials" Chapter 6*. 1996, Great Britain: Cambridge University Press. 105-131.

7. *U.S. Congress, Office of Technology Assessment, Biopolymers: MakingMaterials Nature's Way-Background Paper, OTA-BP-E-102 (Washington, DC: U.S. Government Printing Office, September 1993)."Technical Overview of Biopolymer Field", Biopolymers: Chapter 2 www.princeton.edu/~ota/disk1/1993/9313/9313.PDF Date accessed 12/1/2009.*

8. Bernd H. A. and Rehm, "Polyester synthases: natural catalysts for plastics". *Biochem. J.*, 2003(376): p. 15-33.

9. Dixon M. and Carey, "A Review of Biodegradable Polymer Technology and Recommendation for Introduction of Pilot Scale Collection and Composting Infrastructure in Lexington Kentucky". 2004.

10. Zinn M. and Hanny R., "Taiolered material properties of PHAs". *Advance engineering materials*, 2005.7(5): p. 408.

11. Hanny R. and Zinn M., "Taiolered Material Properties of PHAs". *Advance engineering materials*, 2005.7(5): p. 408.

12. Green P. R., Noda I., Satkowski M.M., and SchechtmanL. A., "Preparation and Properties of a Novel Class of Polyhydroxyalkanoate Copolymers". *Biomacromolecules*, 2005.6: p. 580-586.

13. Marchessault L., "Review "Bacterial Polyesters: Biosynthesis, Biodegradable Plastics and Biotechnology"". *Biomacromolecules*, 2005.6(1).

14. Pohlmann A., Fricke W.F., Reinecke F., and Kusian B., "Genome sequence of the bioplastic-producing ''Knallgas'' bacterium Ralstonia eutropha H16". *Nature Biotechnology*, 2006.24(10).

15. Lee.S.Y., "Deciphering bioplastic production". *NATURE BIOTECHNOLOGY*, 2006.24(10).

16. Pol D'Haene., Remsen E. E., and Asrar J., "Preparation and Characterization of a Branched Bacterial Polyester". *Macromolecules*, 1999.32: p. 5229-5235.

17. Jawed. A. and Hill.J. C., "Biosynthetic Processes for Linear Polymers". *Journal of Applied Polymer Science*, 2002(83): p. 457-483.

18. Padermshoke A., *Polymers Journal of Applied Polymer Science*, 2004.45: p. 6547-6554.

19. Hong S.G. and Chen W. M., "The Attenuated Total Reflection Infrared Analysis of Surface Crystallinity of Polyhydroxyalkanoates". *e-Polymers*, 2006.24.

20. Chen C., Bin Fei, Chen S., Peng S., ZhuangY., Yuxian An., and Lisong Dong., "Crosslinking of poly[(3-hydroxybutyrate)-co-(3-hydroxyvalerate)] using dicumyl
peroxide as initiator". *Polymer International*, 2004.53: p. 937-943.

21. Tang H., Zhang L., Hou G., Shen Y., and Deng F., "The Domain Structure and Mobility of Semi-Crystalline Poly(3-Hydroxybutyrate) and Poly(3-Hydroxybutyrateco- 3-Hydroxyvalerate): A Solid-State Nmr Study". *Polymer International*, 2007.48: p. 2928-2938.

22. Holden D. A., Bloembergenf S., Bluhm T. L., Hamer G. K., and Marchessault R. H., "Stereoregularity in Synthetic ,&Hydroxybutyrate and P-Hydroxyvalerate Homopolyesters". *Macromolecules . : p. 1656-1663.*, 1989.22.

23. Holden Gordon D. A., Bloembergen S., Hamer K., Bluhm T. L., and Marchessault R. H., "Studies of Composition and Crystallinity of Bacterial Poly(3-hydroxybutyrate-co-3-hydroxyvalerate)". *Macromolecules*, 1986.19: p. 2865-2871.

24. Tamaki A., Kunioka M., and Yoshiharu D., "Crystalline and Thermal Properties of Bacterial Copolyesters: Poly(3-hydroxybutyrate-co-3-hydroxyvalerate) and Poly(3- hydroxybutyrate-co-4-hydroxybutyrate)". *Macromolecules*, 1989.22( ): p. 694-697.

25. Karlsson S., Renstad R., Albertsson A.C., Werner P.E., and Westdahl M., "Influence of Processing Parameters on the Mass Crystallinity of Poly(3-

hydroxybutyrateco-3-hydroxyvalerate)". *Polymer International* 1997.43: p. 201-209.

26. Shanks R.K. and Gunaratne L.M.W.K., "Multiple melting behaviour of PHBV using DSC". *European Polymer Journal*, 2005.41: p. 2980-2988.

27. Focarete M. L., Gazzano M., Riekel C., Ripamonti A., and Scandola M., "Structural Investigation of Poly(3-hydroxybutyrate) Spherulites by Microfocus X-Ray Diffraction". *Macromol. Chem. Phys.*, 2001.8(202).

28. Sato H., Zhang J., Noda I., and Ozaki Y., "Conformation Rearrangement and Molecular Dynamics of Poly(3-hydroxybutyrate) during the Melt-Crystallization Process Investigated by Infrared and Two-Dimensional Infrared Correlation Spectroscopy". *Macromolecules*, 2005: p. 4274-4281.

29. Briassoulis D., "An Overview on the Mechanical Behaviour of BiodegradableAgricultural Films". *Journal of Polymers and the Environment April*, 2004.12(2).

30. Stoll B., El-Taweel S. H., Ho¨hne G. W. H., Mansour A. A., and Seliger H., "Stress-Strain Behavior of Blends of Bacterial Polyhydroxybutyrate". *Journal of Applied Polymer Science*, 2004.94: p. 2528-2537.

31. McCarthy S., Zhang J., and Whitehouse R., "Reverse Temperature Injection Molding of Biopol™ and Effect on Its Properties". *Journal of Applied Polymer Science*, 2004.94 p. 483-491.

32. Keller A. Barham P. J., Wills H.H., "The Relationship between Microstructure and Mode of Fracture in Polyhydroxybutyrate". *Journal of Polymer Science: Polymer Physics Edition*, 1986.24: p. 69-77.

33. Prof. Dr. Marchessault R. H. and Prof. Dr. Ga-er Yu., *"Crystallization and Material Properties of Polyhydroxyalkanoates" Biopolymers.* December 2001 ed. Biopolymers, ed. Y.S. Doi and Alexander. Vol. Polyesters II - Properties and Chemical Synthesis. 2001, Weinheim: Wiley-VCH. 468.

34. McChalicher W.J.C. and Srienc F., "Investigating the structure–property relationship of bacterial PHA block copolymers". *Journal of Biotechnology*, 2007.132: p. 296-302.

35. Valentin H. E., Berger P. A., and Gruys J.K., "Biosynthesis and Characterization of Poly(3-hydroxy-4-pentenoic acid)". *Macromolecules*, 1999.32: p. 7389-7395.

36. Tsuge T., Yano K., and Imazu S., "Biosynthesis of Polyhydroxyalkanoate (PHA) Copolymer from Fructose Using Wild-Type and Laboratory-Evolved PHA Synthases". *Macromol. Biosci.*, 2005.5: p. 112-117.

37. Liangqi Z. and Jingfan X., "Synthesis of poly (3-hydroxybutyrate-co-3-hydroxyoctanoate) by a Sinorhizobium fredii strain". *Letters in Applied Microbiology*, 2006.42.

38. Noda I. and Green P.R., "Preparation and Properties of a Novel Class of Polyhydroxyalkanoate Copolymer". *Biomacromolecules*, 2005.6: p. 580-586.

39. Ching-Yee Loo. and Wing-Hin Lee., "Biosynthesis and characterization of poly(3-hydroxybutyrate-co-3-hydroxyhexanoate) from palm oil products in a Wautersia eutropha mutant". *Biotechnology Letters* 2005.27: p. 1405-1410.

40. Chen G. Q. and Zhang G., "Industrial scale production of poly(3-hydroxybutyrateco-3-hydroxyhexanoate)". *Appl Microbiol Biotechnol*, 2001.57: p. 50-55.

41. Dai Y. and Yuan Z., "Production of targeted poly(3-hydroxyalkanoates) copolymers by glycogen accumulating organisms using acetate as sole carbon source". *Journal of Biotechnology* 2007.129: p. 489-497.

42. Dai Y. and Lambert L., "Characterisation of polyhydroxyalkanoate copolymers with controllable four-monomer composition". *Journal of Biotechnology* 2008.134: p. 137-145.

43. Lutke-Eversloh T. and Bergander K., "Identification of a new class of biopolymer: bacterial synthesis of a sulfur-containing polymer with thioester linkages". *Microbiology-UK* 2001.147 Part 1: p. 11-19.

44. Ritter H. and Astrid Grafin von Spee, "Bacterial production of polyesters bearing phenoxy groups in the side chains, 1 Poly(3-hydroxy-5-phenoxypentanoate-co-3-hydroxy-9 -phenoxynonanoate) from Pseudomonas oleovorans". *Macromol. Chem. Phys.*, 1994.195: p. 1665 -1672.

45. Sanguanchaipaiwong V. and Gabelish C. L., "Biosynthesis of Natural-Synthetic Hybrid Copolymers:Polyhydroxyoctanoate-Diethylene Glycol". *Biomacromolecules* 2004.5: p. 643-649.

46. Soma Pal Saha, Patra A., and Paul A.K., "Incorporation of polyethylene glycol in polyhydroxyalkanoic acids accumulated by Azotobacter chroococcum MAL-201". *J Ind Microbiol Biotechnol* 2006.33: p. 377-383.

47. Zibiao Li and Shaoting Cheng, "Novel amphiphilic poly(ester-urethane)s based on poly[(R)-3-hydroxyalkanoate]: synthesis, biocompatibility and aggregation in aqueous solution". *Polym. Int.* , 2008.57: p. 887-894.

48. Jee-Wei Cheea. and Amirul A. A., "The influence of copolymer ratio and drug loading level on the biocompatibility of P(3HB-co-4HB) synthesized by Cupriavidus sp. (USMAA2-4)". *Biochemical Engineering Journal*, 2008.38: p. 314-318.

49. Caballerot K.P. and Karel S.F., "Biosynthesis and characterization of hydroxybutyrate-hydroxycaproate copolymers". *Int. J. Biol. Macromol*, 1995.17(2): p. 86-92.

50. Ilter S. and Hazer B., "Graft Copolymerisation of Methyl Methacrylate onto a Bacterial Polyester Containing Unsaturated Side Chains". *Macromol. Chem. Phys.* , , , 2001.202: p. 2281-2286.

51. Wong M. S., Causey T.B., and Mantzaris N., "Engineering Poly(3-hydroxybutyrate-co-3-hydroxyvalerate) Copolymer Composition in E. coli". *Biotechnology and Bioengineering*, 2008.99(4): p. 919.

52. Kemavongse K. and Prasertsan P., "Poly-b-hydroxyalkanoate production by halotolerant Rhodobacter sphaeroides U7". *World J Microbiol Biotechnol* 2008.24(5): p. 2073-208.

53. Davis R. and Anilkumar P. K., "Biosynthesis of polyhydroxyalkanoates co-polymer in E. coli using genes from Pseudomonas and Bacillus". *Antonie van Leeuwenhoek*, 2008.94: p. 207-216.

54. Nomura C.T. and Taguchi K., "Expression of 3-Ketoacyl-Acyl Carrier Protein Reductase (fabG) Genes Enhances Production of Polyhydroxyalkanoate Copolymer from Glucose in Recombinant Escherichia coli JM109". *Applied and Environmental Microbiology*, 2005.71(8): p. 4297-4306.

55. Ling-Fang Qin and Xue Gao, "Biosynthesis of polyhydroxyalkanoate copolyesters by Aeromonas hydrophila mutant expressing a low-substrate-specificity PHA synthase PhaC2Ps". *Biochemical Engineering Journal* 2007.37: p. 144-150.

56. Nomura C.T. and Taguchi S., "PHA synthase engineering toward superbiocatalysts for custom-made biopolymers". *Appl Microbiol Biotechnol* 2007.73: p. 969-979.

57. Valappil S.P. and Rai R., "Polyhydroxyalkanoate biosynthesis in Bacillus cereus SPV under varied limiting conditions and an insight into the biosynthetic genes involved". *Journal of Applied Microbiology*, 2008 104: p. 1624-1635.

58. Dionisi D. and Beccari M., "Storage of biodegradable polymers by an enriched microbial community in a sequencing batch reactor operated at high organic load rate". *J Chem Technol Biotechnol* 2005.80: p. 1306-1318.

59. Haynes D., Abayasinghe K.N., and Harrison G.M., "In Situ Copolyesters Containing Poly(L-lactide) and Poly(hydroxyalkanoate) Units". *Biomacromolecules*, 2007.8: p. 1131-1137.

60. Kunze C. and Freier T., "Anti-inflammatory pro drugs as plasticizers for biodegradable implant materials based on Poly(3-hydroxybutyrate)" *Journal of Material Science: Material in medicine*, 2002.13: p. 1051-1055.

61. Bibers I. and Tupureina V., "Improvement of the Deformative Characteristics of Poly-beta-hydroxybutyrate by Plasticization". *Mechanics of Composite Materials*, 1999.35(4).

62. Ishikawa K. and Kawaguchi Y., "Plasticization of Bacterial Polyester by the addition of Acylglycerols and its Enzymatic degradability". *Kobunshi Ronbunshu* 1991 48(4): p. 221-226.

63. Parra D.F. and Fusaro J., "Influence of poly (ethylene glycol) on the thermal, mechanical, morphological, physical-chemical and biodegradation properties of poly (3-hydroxybutyrate)". *Polymer Degradation and Stability* 2006.91(9): p. 1954-1959.

64. Choi J.S. and Park W.H., "Effect of biodegradable plasticizers on thermal and mechanical properties of poly (3-hydroxybutyrate)". *Polmer Testing*, 2004.23(4): p. 455-460.

65. Choi J.S. and Park W.O., "Thermal and Mechanical Properties of Poly(hydroxy-3-butyrate-co-3-valerate) Plasticized by Biodegaradble Soyabean oils". *Macromolecules Symposia*, 2003.197: p. 65-76.

66. Wang L. and Zhu W., "Processability Modifications of Poly(3-hydroxybutyrate) by Plasticizing, Blending, and Stabilizing". *Journal of Applied Polymer Science*, 2008.107: p. 166-173.

67. Azuma Y., Yoshie N., Sakurai M., Inoue Y., and Chujo R., "Thermal behavior and miscibility of poly(3-hydroxybutyrate)/poly(vinyl alcohol) blends". *Polymer Degradation and Stability*, 1992.33: p. 4763-4767.

68. Avella M. and Martuscelli E., "Poly-(3-hydroxybutyrate)/poly(ethyleneoxide) blends: phase diagram, thermal and crystallization behavior". *Poymer Degradation and Stability* 1988.29: p. 1731-1737.

69. Avella M., Martuscelli E., and Greco P., "Crystallization behavior of poly(ethylene oxide) from poly(3-hydroxybutyrate)/poly(ethylene oxide) blends: phase structuring, morphology and thermal behavior". *Polymer Degradation and Stability*, 1991.32: p. 1647-1653.

70. Blümm E. and Owen A.J., "Miscibility, crystallization and melting of poly(3-hydroxybutyrate)/poly(L-lactide) blends". *Polymer*, 1995.36: p. 4077-4081.

71. Koyama N. and Yoshiharu D., "Miscibility of binary blends of poly[(R)-3-hydroxybutyric acid] and poly[(S)-lactic acid]". *Polymer*, 1997.38(7): p. 1589-1593.

72. He Y., Masuda T., Cao A., Yoshie N., Doi Y., and Inoue Y., "Thermal, crystallization, and biodegradation behavior of poly(3-hydroxybutyrate) blends with poly(butylene succinate-co-butylene adipate) and poly(butylene succinate-co-ε-caprolactone)" *Polymer Journal*, 1993(31): p. 184-192.

73. Koyama N. and Doi Y., "Miscibility, thermal properties, and enzymatic degradability of binary blends of poly[(R)-3-hydroxybutyric acid] with poly(ε-caprolactone-co-lactide)". *Macromolecules*, 1996.29: p. 5843-5851.

74. Wang T., Cheng G., Ma S., Cai Z., and Zhang L., "Crystallization Behavior, Mechanical Properties, and Environmental Biodegradability of Poly(hydroxybutyrate)/Cellulose Acetate Butyrate Blends". *Journal of Applied Polymer Science*, 2003.89: p. 2116-2122.

75. Yoon J., Oh S., and Kim M., "Compatibility of poly(3-hydroxybutyrate)/ poly(ethylene-co-vinyl acetate) blends". *Polymer*, 1998.39: p. 2479-2487.

76. Gonzalez A., Iriarte M., Iriondo P.J., and Iruin J.J., "Miscibility and carbon dioxide transport properties of blends of bacterial poly(3-hydroxybutyrate) and a poly(vinylidene chloride-co-acrylonitrile) copolymer". *Polymer*, 2002.43: p. 6205-6211.

77. Kumagai Y. and Doi Y., "Enzymatic degradation and morphologies of binary blends of microbial poly(3-hydroxybutyrate) with poly(ε-caprolactone), poly(1,4-butylene adipate) and poly(vinyl acetate)". *Polymer Degradation and Stability*, 1992.36: p. 241-248.

78. Gassner F. and Owen A.J., "Physical properties of poly(β-hydroxybutyrate)-poly(ε-caprolactone) blends". *Polymer*, 1994.35: p. 2233-2236.

79. Koller I. and Owen A. J., "Starch-Filled PHB and PHB/HV copolymer". *Polymer International*, 1996.39: p. 175-181.

80. Paglia D.E., Beltrame P. L., Canetti M., Seves A., Marcandalli B., and Martuscelli E., "Crystallization and thermal behaviour of poly (3-hydroxybutyrate)/poly(epichlorohydrin) blends". *Polymer*, 1993.34(996-1001).

81. Yoon J.C., Choi C.S., Maing S. J., Choi H. J., Lee H., and Choi S. J., "Miscibility of poly-image(−)(3-hydroxybutyrate) in poly(ethylene oxide) and poly(methyl methacrylate)". *European Polymer Journal*, 1993.29: p. 1359-1364.

82. Greco P. and Martuscelli E., "Crystallization and thermal behaviour of poly(3-hydroxybutyrate)-based blends". *Polymer*, 1989.30: p. 1475-1483.

83. Avella M., Immirzi B., Malinconico M., Martuscelli E., Orsello G., Pudia A., and Ragosta G., "Poly(butyl acrylate) inclusive polymerization in the presence of bacterial polyesters, 1. Synthesis and preliminary mechanical and morphological characterization" *Die Angewandte Makromolekulare Chemie*, 1993.205: p. 151-160.

84. Rosa D.D, Gaboardi F, Guedes C.D.F, and Calil R.M, "Influence of oxidized polyethylene wax (OPW) on the mechanical, thermal, morphological and biodegradation properties of PHB/LDPE blends". *J Mater Sci*, 2007.42(19): p. 8093-8100

85. A.J. Owen F. Gassner, Physical properties of poly(β-hydroxybutyrate)-poly(ε-caprolactone) blends. *Polymer*, 1994.35: p. 2233-2236.

86. Principia partners presentation. in *7th international conference of wood fiber-plastic composites* 2003. Madison (WI).

87. *http://www.principiaconsulting.com/consulting/news.cfm*. date accessed 05/15/2006,

88. Karus M., Ortmann S., and Vogt D. (2004-10) *"Use of natural fibers in composites in the German automotive production 1996 till 2003"* http://www.nachwachsende-rohstoffe.info Date Accessed 12/4/06,

89. Jamal M., Mehdi T., John C., Hermanson, and Ismaeil G., "Tensile Properties of Wood Flour/Kenaf Fiber Polypropylene Hybrid Composites". *Journal of Applied Polymer Science*, 2007.105: p. 3054-3059.

90. Jungil S., Douglas J., Gardner, Shane O'Neill., and Costas M., "Understanding the Viscoelastic Properties of Extruded Polypropylene Wood Plastic Composites". *Journal of Applied Polymer Science*, 2003.89: p. 1638-1644

91. William T. Y. T., Shane C. O'Neill, Carl P. T., Duglas J. G., and Stephen M. S., "Evaluation of Load Transfer in the Cellulosic-Fiber/ Polymer Interphase using

a Micro-Raman Tensile test". *Wood and Fiber Science*, 2007.39(1): p. 184 - 195.

92. Hristov V. N. and Vasileva S.T., "Deformation Mechanisms and Mechanical Properties of Modified Polypropylene/Wood Fiber Composites". *Polmer Composite*, 2004.25(5).

93. Shreeleka M.S., George J., and Thomas S., "A Review on Interface Modification and Characterization of Natural Fiber Reinforced Plastic Composites". *Polymer Engineering and Science* 2001.41(9).

94. Correa C.A., Razzino C.A.S, and Hage E., "Role of Maleated Coupling Agents on the Interface Adhesion of Polypropylene—Wood Composites". *Journal of Thermoplastic Composite Materials*, 2007.20: p. 323.

95. Ferrer F.M., Vilaplan F., Greus A.R., Borras A.B., and Box C.S., "Flour rice husk as filler in block copolymer polypropylene: Effect of different coupling agents". *Journal of Applied Polymer Science*, 2006.99: p. 1823-31.

96. Huda M.S., Mohanty A.K., Drzal L.T., Shut E., and Misra M., ""Green" composites from recycled cellulose and poly(lactic acid): Physico-mechanical and morphological properties evaluation" *Journal of Material Science*, 2005.40: p. 4221 - 4229.

97. Rana A.K., Mitra B.C., and Banerjee A.N., "Short jute fiber-reinforced polypropylene composites: Dynamic mechanical study". *Journal of Applied Polymer Science*, 1999.71: p. 531-539.

98. Lu J.Z., Negulescu I. I., and Wu Q., "Maleated wood-fiber/high-density-polyethylene composites: Coupling mechanisms and interfacial characterization". *Composite Interfaces*, 2005.12(1-2): p. 125-140.

99. Yeh., Shu-Kai., Casuccio., Mary E., Al-Mulla., and Adam., *Annual Technical Conference - Society of Plastics Engineers*, 2006.64: p. 209-213.

100. Khalil H.P.S.A. and Shahnaz S.B.S., "Recycle Polypropylene (RPP) - Wood Saw Dust (WSD) Composites - Part 1: The Effect of Different Filler Size and Filler Loading on Mechanical and Water Absorption Properties". *Journal of Reinforced Plastics and Composites*, 2006.25(12): p. 1291-1303.

101. *http://www.risiinfo.com/technologyarchives/risi-international-woodfiber-report-biomass-2012.html Date Accessed 10/23/2008.*

102. *http://findarticles.com/p/articles/mi_m0EIN/is_/ai_94439333 Date accessed 10/23/2008.*

103. *http://www.farmforestline.com.au/pages/2.1.2.1_wood.html Date accessed 10/23/2008*

104. Wood handbook: Wood as an engineering Material, USDA, Agriculture handbook; 72;US Government Printing Office, Washington DC; 1987 .

105. *http://www.msm.cam.ac.uk/doitpoms/tlplib/wood/structure_wood_pt1.php Date accessed 10/24/2008*

106. The chemistry of wood, Browning B.L., New York, Interscience Publishers, 1963.

107. Schmidt M., Gierlinger N., Schade U., Rogge T., and Grunze M., "Polarized Infrared Microspectroscopy of Single Spruce Fibers: Hydrogen Bonding in Wood Polymers". *Biopolymers*, 2006.83: p. 546-555.

108. *http://koti.kapsi.fi/hvartial/wood/wood2.htm Date accessed 10/17/2008*

109. *http://www.ima-na.org/about_industrial_minerals/talc.asp Date accessed 10/20/2008*

Chapter 2

Wood Fiber Reinforced Bacterial Bioplastic Composites: Fabrication and Performance Evaluation

2.0 Introduction

Wood reinforced plastics (WPC) are the fastest growing sector of the plastic industry, ratcheting up with the quarter percent growth rate and reflecting a strong market demand in the near future [1, 2]. The wide, global acceptance of these has been due to the reduced cost, weight, superior properties over wood and plastic alone, recycling ability, assimilation to the existing plastic processing techniques and a mounting awareness regarding the sustainable and eco-friendly products. WPC, as a structural material, predominantly exist in decking, railing, automotive and housing interiors. Several kinds of WPC, using wood fiber and conventional polymers like PE, PVC and PP, had been developed and researched [3-6]. Emerging issues with the conventional petroleum based polymers such as, non-renewability, environmental sustainability are the major challenges that needs to be addressed in the near future. Renewable, bio-based, eco-friendly and fully green WPC are the potential alternative to the conventional WPC.

Polyhydroxyalkanoates (PHAs) can be a new found renewable resource based substitute to conventional polymers as a matrix in WPC. Polyhydroxybutyrate (PHB) and polyhydroxybutyrate-co-valerate (PHBV) are prominent examples of PHAs bioplastics. The potential benefit of these polymers as matrix in WPC is because of their comparative properties to conventional polymers such as polypropylene coupled with their eco- friendly properties like biodegradability, biocompatibility and

environmental sustainability. Among PHAs, PHBV was developed to compensate for poor mechanical properties and process ability of PHB by introducing hydroxy valerate (HV) units in PHB segments thereby, producing a PHBV copolymer. [7-9]. PHBV produced through fermentation gives a good command on stereoregularity of the polymer therefore, giving a highly isotactic and crystalline thermoplastic [10-11]. Increase of HV content in PHBV decreases its brittleness by limiting secondary crystallization to some extent. Low HV content restricts segmental dynamics in the amorphous region of PHBV thereby, showing reduced flexibility, elongation and impact strength [12].

Natural fibers are the emerging reinforcing agent in the polymer matrix due to their abundant availability, low cost, low density and compatibility with the nature [13]. Wood fibers, which fall in category of natural fiber, have been used to reinforce thermoplastics [3-6]. The mechanical properties of PHBV were found to improve when reinforced with cellulosic natural fibers [14-16]. PHBV can be reinforced with high content of cellulosic wood fiber in order to enhance its mechanical properties and to reduce the cost of molded product. Although, there are a few hydroxyl and carboxylic groups on PHBV molecular chain ends, but some degree of dipolar interactions among moderately polar (>C=O) and polar groups (-OH and –COOH) of PHBV and hydroxyl group (-OH) of cellulosic wood fiber can provide an opportunity for an interfacial interaction between the fibers and the matrix. [17,18]

The objective of this study was to fabricate maple wood fiber reinforced PHBV composites and evaluate their mechanical and thermomechanical properties as a function of wood fiber weight content in PHBV. The composites were fabricated by

extrusion-injection molding process. Efforts have been made to develop a theoretical understanding of the experimental findings by correlating them with theoretical models presented by Halpi-Tsai and Tsai-Pagano. The morphological aspects of the composites such as fiber dispersion and fiber-matrix interface were investigated using scanning electron microscopy (SEM).

2.1 Experimental Section

2.1.1 Materials:

Polyhydroxybutyrate-co-valerate (PHBV) with the trade name Biopol (Zeneca Bio Products) was obtained from Biomer, Germany. Maple wood fiber, trade name 2010 MAPLE wood flour was supplied by American Wood Fibers, Schofield, WI. Length and diameter of the wood fibers were between 1600-1650 μm and 300-400 μm, respectively. The aspect ratio (l/d) of the wood fiber was ~ 4 [19].

2.1.2 Fabrication of composite employing micro-compounding technique:

Maple wood fiber was dried at a 110 ^{o}C under the vacuum for 2 hrs. PHBV was dried at 80 ^{o}C for 4 hrs under similar vacuum conditions. Both, PHBV and wood fiber were dried in order to avoid any moisture content during processing. The dried wood fiber and PHBV were kept in a zip lock plastic bags until processing. Processing was carried out in a micro extruder (manufactured and designed by DSM Research, Netherlands) with a barrel volume of 15 cc. It was equipped with a co-rotating twin-screw system with screw length of 150 mm and L/D (length/diameter) of 18. Temperature, in the three respective zones of micro extruder, was set at 165,160 and 155 ^{o}C, for all the different compositions of PHBV and wood fiber. Processing

temperature was optimized between 155 and 165°C, to achieve low melt flow, and to avoid thermal degradation of PHBV. The screw rotating speed was 100 rpm. Different mix ratios of PHBV and wood fiber along with some other processing parameters are mentioned in Table 2.1. Wood fiber and PHBV pellets were physically mixed, and fed to the DSM extruder. After the fixed extrusion time, the molten mix was transferred to a preheated mini-injection molding machine and the testing specimens were molded. The optimized injection pressure for all PHBV-wood fiber composites was 551.5 KPa and the temperature was 155 °C. Residence/ Extrusion time, in the DSM extruder, of compositions with 30 and 40 wt% was increased to 10 minutes in order to provide better mixing and dispersion of the wood fiber in the matrix.

Table 2.1: Processing parameters of various PHBV-wood fiber compositions

PHBV (wt %)	Wood fiber (wt %)	Processing temp. (°C)	Retention time (min.)
100	0	160	3
90	10	160	5
80	20	160	5
70	30	160	10
60	40	160	10

2.1.2 Testing and Characterization

2.1.2.1 Mechanical properties: Tensile and flexural properties of the specimens were measured using a United Calibration Corp. SFM 20 testing machine as per ASTM D638 and ASTM D790 standards, respectively. The tensile testing was carried out at a rate of 2.54 mm/min with a pre load value of 0.023 kg. The system controls and data analysis were performed using Datum software. The notch Izod impact testing was carried out on a Testing Machine Inc. (TMI) 43-02-01 as per ASTM D256.using pendulum of impact energy 1.35 J. The number of specimens used for testing were five.

2.1.2.2 Thermomechanical properties:

2.1.2.2.1 Dynamic Mechanical Analysis (DMA): The storage modulus, loss modulus and tan delta of the specimens were evaluated using DMAQ800 supplied by TA Instruments. The specimens were heated from -30 to 125 ^{o}C at a heating rate of 2 ^{o}C/min. A single cantilever mode was used to test the specimens at the oscillating amplitude of 15 μm and frequency of 1 Hz.

2.1.2.2.2 Heat deflection temperature (HDT): DMA Q800, TA instruments was used to find the HDT of various specimens as per ASTM D648 standards. The rectangular bars, 1.99 ×12 × 58 mm in three-point bending mode with an applying load of 66 psi were used for testing. Samples were heated at the rate of 2^{o}C/ min from the room temperature, i.e., 20^{o}C to the required temperature.

2.1.2.2.3 Coefficient of linear thermal expansion (CLTE): CLTE of the composites was determined using TMA 2940, TMA was equipped with an expansion probe. Heating

rate of specimens was 3 °C/min under a constant applied load of 0.15 N. Testing was performed in the temperature range from 30 to 90 °C.

2.1.2.3 Thermogravimetric analysis (TGA): TGA was tested, using TGA 2950 instrument, with the heating rate of 20 °C/min from the room temperature to 600 °C, i.e., the temperature of complete thermal degradation. All TGA runs were performed in N_2 atmosphere.

Data analysis of all the thermo mechanical properties was performed using Universal analysis software and the number of specimens used for testing were five.

2.1.2.4 FTIR analysis: Perkin Elmer, system 2000 FTIR Spectrometer, was used to carry out FTIR spectra, using an attenuated total reflectance (ATR) accessory of all the specimens.

2.1.2.5 .Morphological studies: Morphological studies were conducted using a JEOL scanning electron microscope (model JSM-6400). Specimens were sputter-coated with gold to a thickness of ~10 nm before the surface characterization. The SEM instrument has a lanthanum hexaboride (LaB_6) crystal as electron emitter. An accelerating voltage of 13 KV was used to collect SEM photomicrographs.

2.2 Results and Discussion

2.2.1 Tensile Properties: Tensile properties of neat PHBV and its wood fiber loaded composites are depicted in Figure 1.1. A gradual increase in the Young's modulus of PHBV-wood fiber composites was observed with the uniform increment of wood fiber loading in the total composition of composite. Young's modulus ratcheted up by ~ 28 % with every 10 wt% increase of wood fiber loading in the composite. The tensile modulus of PHBV based composite was increased by 167 %, when reinforced with 40 wt% of wood fiber as compared to neat PHBV. The modulus of neat PHBV was found to be 1.02 ± 0.09 GPa, while for the PHBV-wood composite with 40 wt% for wood fiber was 2.73 ± 0.22 GPa. The increasing trend of the modulus could be attributed to the compatibility between the wood fiber and PHBV. Wood fiber has polar groups in the cellulose structure, and PHBV also has abundant moderate polar groups in its chemical makeup, this may provide some opportunity of having a reasonable interaction at the interface of the two. A uniform dispersion of the filler in the matrix is also a crucial parameter in determining the final properties of a composite. Based on the visual observation of the processed specimens, the uniform dispersion of the fibers in matrix allowed the fibers to share an evenly distributed load. Figure 1, shows a slender decreasing trend in the tensile strength, with the increase in wood fiber content. Tensile strength of neat PHBV decreased to 16.75 ± 0.51 MPa from 21.42 ± 1.5 MPa, when loaded with 40 wt% of the wood fiber. There was an average decrease of 6.3 % tensile strength with each subsequent increment of 10 wt% wood fibers in the composite. The decreasing trend could be explained by taking the dewetting effect in to account. The theory pertaining to the composite behavior under external loading suggested that the

interface region of fiber and matrix experiences the stress concentration around the filler particle as a result; the interaction between the filler and the matrix weakens up thus, gradually leading to debonding at the interface [20]. The phenomenon becomes more predominant with the increase of fiber to matrix volume ratio. Comparing the tensile modulus and strength of the PP based wood fiber composites with PHBV–wood fiber composites, PP based composites have a higher order of tensile properties. The modulus of the 30 and 40 wt% wood fiber-PP composites, as reported in literature, have values of 3.33 and 4.72 GPa, respectively, and the strength of the same wood fiber content composites are 27.1 and 25.6 MPa , respectively [6]. The experimental data of tensile properties were compared with the most commonly, applied theoretical models. Halpin -Tsai and Tsai-Pagano equations and Nicolais - Nicodemo model were used to evaluate the modulus and tensile strength of the composites [21-23, 14].

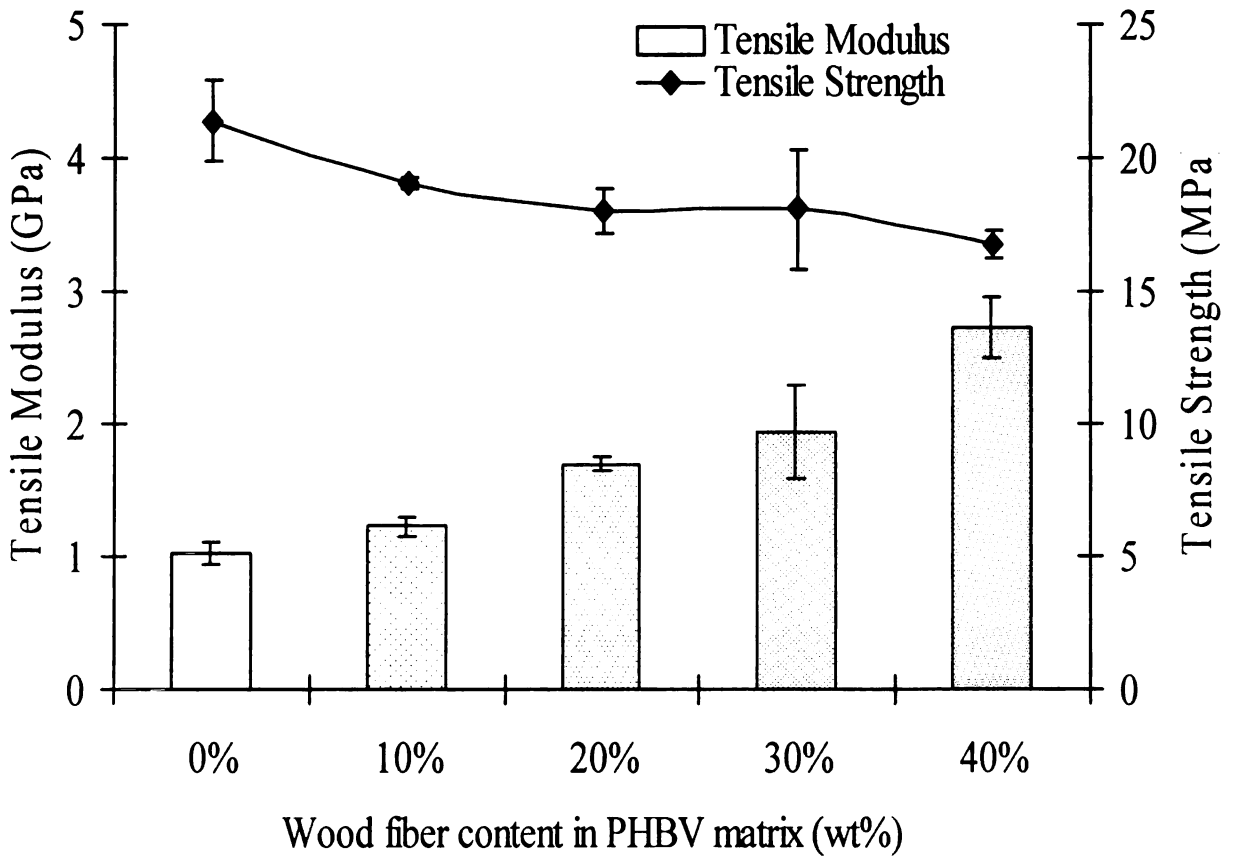

Figure 2.1: Tensile properties of PBV-wood fiber composites with different loading level of wood fiber

Halpin-Tsai and Tsai-Pagano equations:

Halpin –Tsai and Tsai-Pagano proposed equations for calculation of tensile modulus of composites. Elastic modulus of the maple wood is 11.3 GPa [24]. The density of the PHBV and wood fiber are 1.25 and 1.4 gm/cm^3 respectively. Aspect ratio *(l/d)* of the wood fiber loaded in the composite is 4.02. Halpin-Tsai equation predicts the longitudinal (E_L) and transverse (E_T) modulus of the aligned short fiber composite. Longitudinal modulus (E_L) and Transverse modulus (E_T) are given by following equations.

$$E_L = E_m \frac{1+\xi\eta_L V_f}{1-\eta_L V_f}$$

$$E_T = E_m \frac{1+2\eta_T V_f}{1-\eta_T V_f}$$

ξ is the measure of geometry of reinforced fiber and if the fiber has rectangular

η_L and η_T are given by the following equations.

$$\eta = \frac{(E_f / E_m) - 1}{(E_f / E_m) + \xi}$$

$$\eta_T = \frac{(E_f / E_m) - 1}{(E_f / E_m) + 2}$$

The following Tsai-Pagano equation predicts the moduli of the composite for a randomly oriented and uniformly distributed fiber by taking in to account 5/8th of the transverse moduli and 3/8th of the longitudinal moduli of composites with fibers oriented in a single specified direction.

$$E_{random} = (3/8)E_L + (5/8)E_T$$

E_{random}, is the tensile modulus of the randomly oriented fibers. Figure 2.2 depicts the experimental and theoretical values of the tensile modulus. The experimental tensile modulus values were, significantly, close to the theoretical data points. This suggested that the wood fibers were randomly oriented in the PHBV matrix. The embedding of wood fiber has stiffened the PHBV under the given processing conditions, thereby increasing the tensile modulus. This could be attributed to an appropriate assumption of model in respect to the fabricated composites i.e. short fiber length and random distribution of fibers in matrix.

Nicolais and Nicodemo model:

Nicolais and Nicodemo proposed a model that proposes an equation for tensile stress as a function of filler fraction, assuming no adhesion between filler and matrix

with $$\sigma_c = \sigma_m(1 - a\phi^b)$$

b = 2 / 3. ϕ is the volume fraction of filler while, a is a constant. (Figure 2.3) The tensile strength data fit very well with the proposed model assuming the value of a = *0.45. "a"* is assumed to be a function of aspect ratio (l/d) of the fiber which decreases

with increasing aspect ratio. Similar values of "*a*" was reported by Maiti and Singh [25].

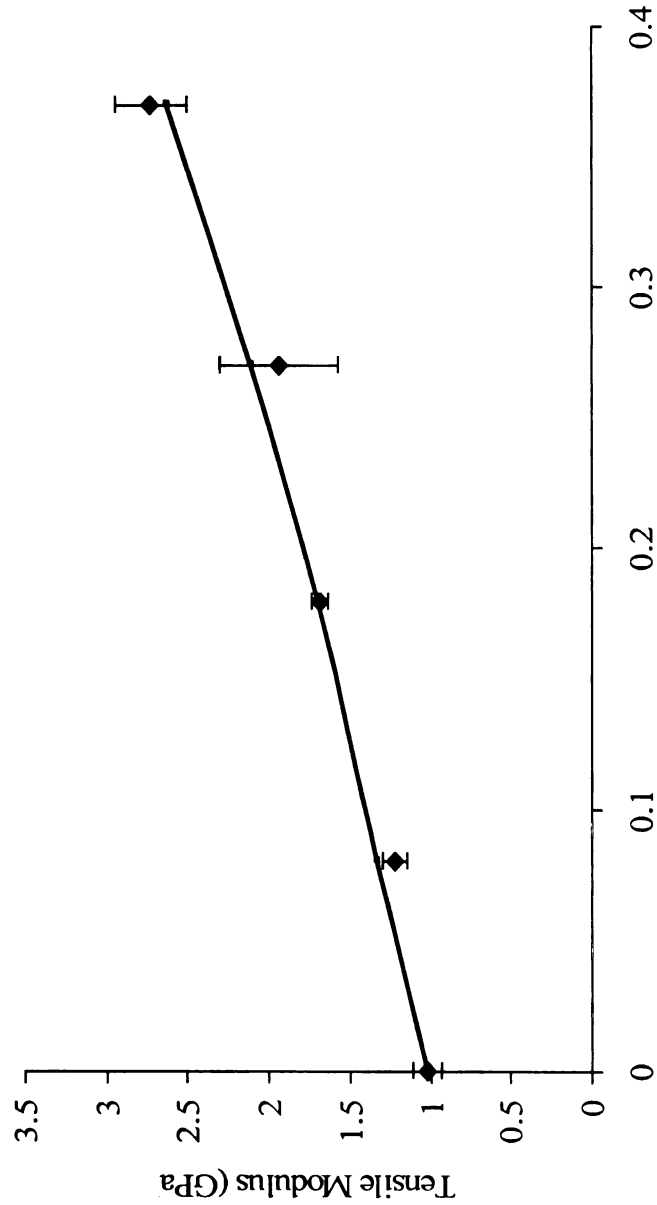

Figure 2.2: Comparison of Tensile modulus (-) Halpin-Tsai and Tsai-Pagano relation data (◆) experimental data points

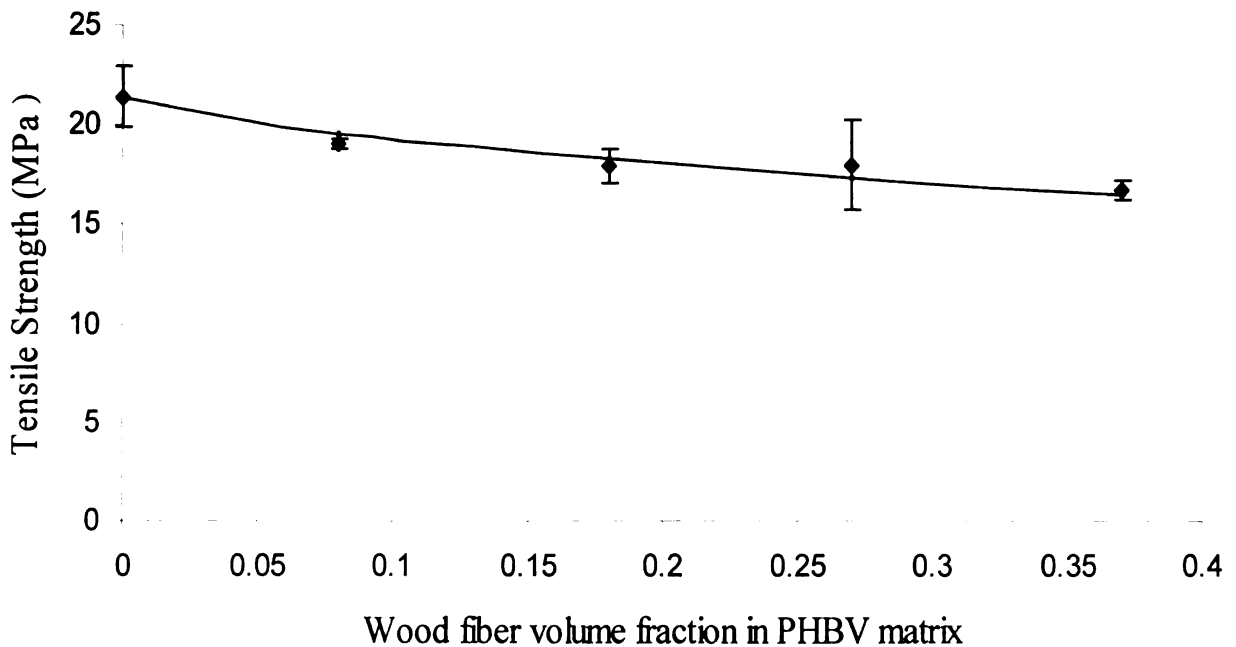

Figure 2.3: Comparison of Tensile strength (-) Nicolais and Nicodemo relation data (♦) experimental data points

2.2.2 Flexural properties: Flexural properties of PHBV-wood fiber composite with varying wood fiber content from 10 to 40 wt% are shown in Figure 2.4. Flexural modulus of the composite exhibited an increasing trend with increasing wood fiber content in the PHBV-wood composites. The flexural modulus showed an average increase of 28 % with every 10 wt% rise of wood fiber in the PHBV matrix. PHBV based composite having 40 wt% of wood fiber content showed a notable increase of 168 % when compared with neat PHBV. The flexural modulus of neat PHBV was 1.28 ± 0.02 GPa while, for PHBV-wood composite with 40 wt% of wood fiber it was 3.44 ± 0.17 GPa. During the flexural testing, stress is more localized in the region of applied load, which is in contrast to the tensile testing, where stress is distributed through out the specimen. Therefore, the increase in the flexural modulus of the PHBV-wood composite contribute to the assumption that a reasonable amount of interfacial interaction existed between fiber and matrix, which allowed the transmission of stress from matrix to fiber thereby, increasing the stiffness of the specimen. Flexural strength of the PHBV-wood composite did not show any significant improvement with the increase of wood fiber in PHBV-wood composition (Figure 2.4). Flexural strength of composites remained at 30 MPa with a little variation of ±1 MPa on adding wood fiber to PHBV, which could be accounted in the standard deviation. Fiber alignment also plays an important role in determining the flexural strength. The uniaxially aligned fibers can give a better strength property than the randomly oriented fibers [18]. Flexural modulus of PP based wood fiber composite at 30 and 40 wt% was 3.4 and 4.6 GPa and strength at the same wt% was 51.4 and 55.1 MPa published by Huda [19].

Both the flexural properties have a higher order of values than the PHBV-wood fiber composites.

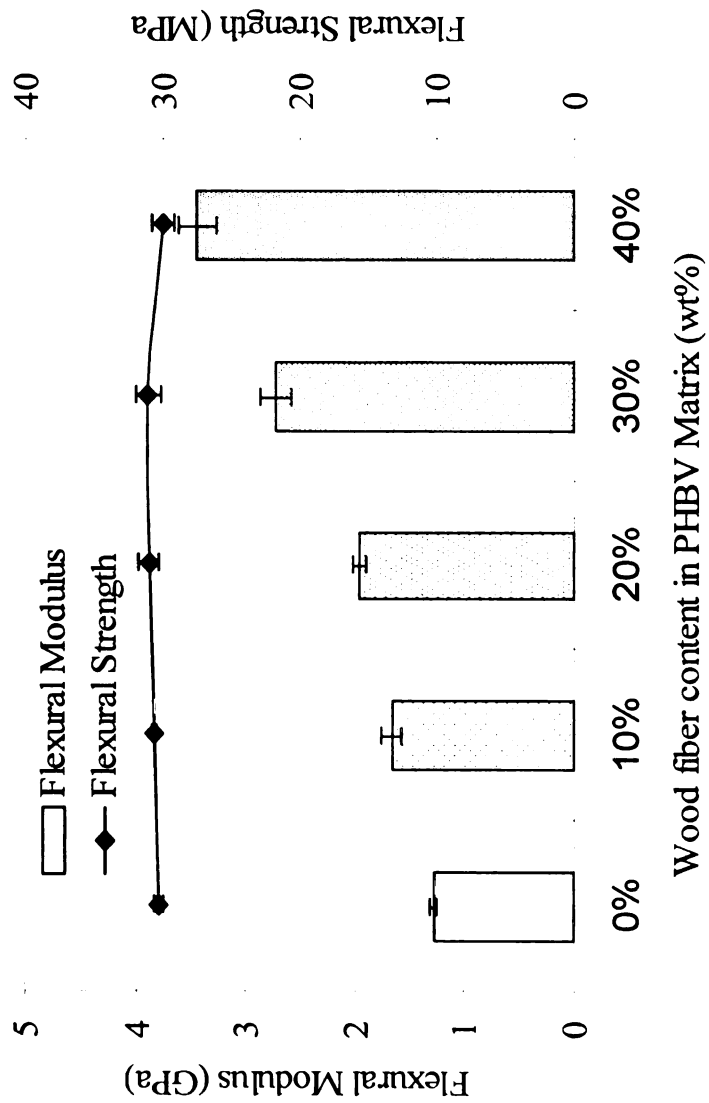

Figure 2.4: Flexural properties of PHBV-wood fiber composites with different loading level of wood fiber

2.2.3 Dynamic Mechanical Properties:

Storage Modulus: The effect of temperature on the storage modulus of PHBV-wood composites having differing wood fiber content is depicted in Figure 2.5. A general trend of increase in storage modulus with the increasing fiber content in the composites was observed. An average increase of 21 % in storage modulus was observed with every 10 wt% increment of wood fiber in the PHBV. The storage modulus of PHBV-wood composite having 40 wt% of wood fiber was improved by around 168 % higher than that of neat PHBV at 25 ^{o}C. The storage modulus of all PHBV-wood composite decreased with an increase in temperature and converged to a narrow range at high temperature (Figure 2.5). The reduction in E' with increasing temperature was due to the softening of matrix and initiation of relaxation process. At temperatures above Tg, the molecular mobility and thermal expansion increases thus reducing the interfacial interaction as a result E' decreased sharply. Storage modulus is associated with the elastic response of the composite and indicates the stiffness of the material. Being an inherent property of a material, it is more associated with the molecular response and therefore, can give a better estimation of the fiber to matrix interaction. The increasing fiber concentration had increased the storage modulus because of the mechanical limitation posed by the fibers embedded in the viscoelastic matrix thereby, reducing the mobility and the deformation of the matrix with the increasing temperature [26]. Interfacial interaction due to the dipolar nature of hydroxyl group on cellulose (wood fiber) and carbonyl group on PHBV can not be ruled out [15]. A uniform dispersion of fiber in matrix had also synergistically acted in the increase of storage modulus of

PHBV-wood composite. The effectiveness of the fibers on the modulus of the composite can be represented by a coefficient factor "C"

$$C = \frac{(E'_g / E'_r)_c}{(E'_g / E'_r)_m}$$

where E'_g and E'_r are the storage modulus in the glassy and rubbery state[26]. The subscripts 'c' represent composite and 'm' matrix. Lower the value of 'C', higher is the effectiveness of the reinforcement. The measured storage modulus at -20 and 20°C at a frequency of 1 Hz were taken as, E'_g and E'_r, respectively. The results are listed in Table 2.2. The 'C' value was found to be least in case of PHBV-wood composite having 40 wt% of the wood fiber content. This showed that wood fiber had a good reinforcing ability in the PHBV based composites.

Table 2.2: Value of coefficient "C" with different loading levels of wood fiber

Wood fiber Content in PHBV (wt %)	Coefficient factor "C"
10	1.07
20	0.87
30	0.82
40	0.75

Loss modulus: The Loss modulus of the material is associated with the viscous response or the dampening effect of the material. It is the out of phase component of the complex modulus and is associated with the dissipating energy, which is unrecoverable and lost to the system. Figure 2.6 shows the effect on loss modulus (E'') of the composite with the varying wood fiber content and temperature. E'' increased with the increasing fiber concentration and gave a peak in the transition region. This peak can be assigned as a glass transition temperature (T_g) of the semi-crystalline material. The peak shifted slightly towards the higher temperature thus indicating a small rise in T_g of PHBV-wood composites with the increasing wood fiber content.

Tan δ : The Tan δ is a ratio of the loss modulus to the storage modulus. It gives a peak in a region, which has rate of decrease in storage modulus higher than that of loss modulus, and after attaining the maxima, vice-versa happens, thus an emergence of peak indicates a transition of material from one region to the other. The height of tan δ peak decreased with an increase in the fiber content in the composite i.e., the dampening effect had reduced with the increased fiber content in the matrix (Figure 2.7). This suggested that some degree of interfacial bonding existed between the fibers and matrix in PHBV-wood composites, which increased with the addition of fibers to the PHBV matrix. The higher wood fiber level induced a better fibers packing in the matrix, and resulted in efficient stress transfer form the PHBV matrix to wood fibers, thereby decreasing the dampening effect. Widening of the Tan δ peaks with the increasing fiber content in the PHBV–wood composite suggested the increased fiber to matrix interfacial regions in the fiber rich matrix as well as an increased molecular relaxation in the composite system as compared to the neat polymer [26]. The

broadening of the peaks at higher level of fiber loading in the system reflects the heterogeneity generated in it.

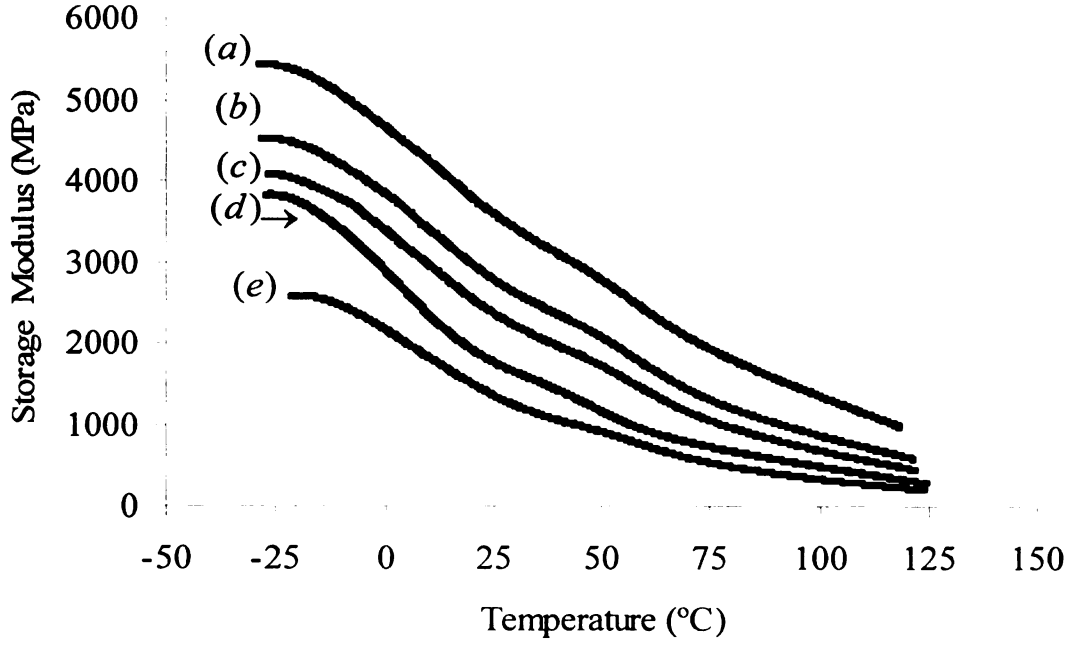

Figure 2.5: Temperature dependency of storage modulus with varying loading level of wood fiber in PHBV matrix. (a) PHBV-wood fiber (60:40), (b) PHBV-wood fiber (70:30), (c) PHBV-wood fiber (80:20), (d) PHBV-wood fiber (90:10), (e) PHBV-wood fiber (100:0).

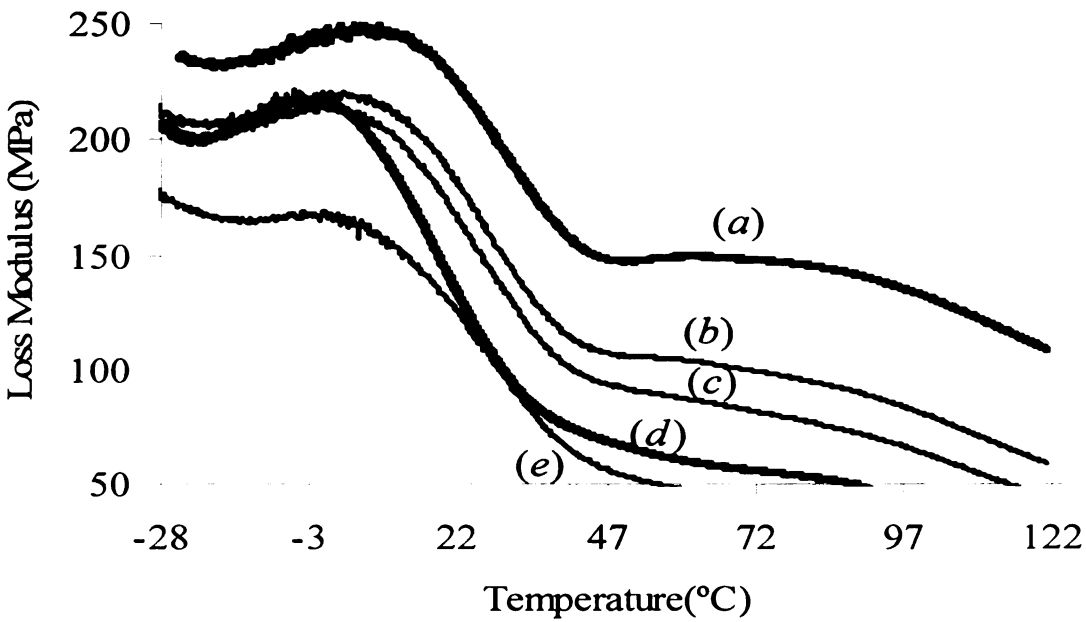

Figure 2.6: Temperature dependence of Loss Modulus with varying loading level of Wood fiber in PHBV matrix. (a) PHBV-wood fiber (60:40), (b) PHBV-wood fiber (70:30), (c) PHBV-wood fiber (80:20), (d) PHBV-wood fiber (90:10), (e) PHBV-wood fiber (100:0).

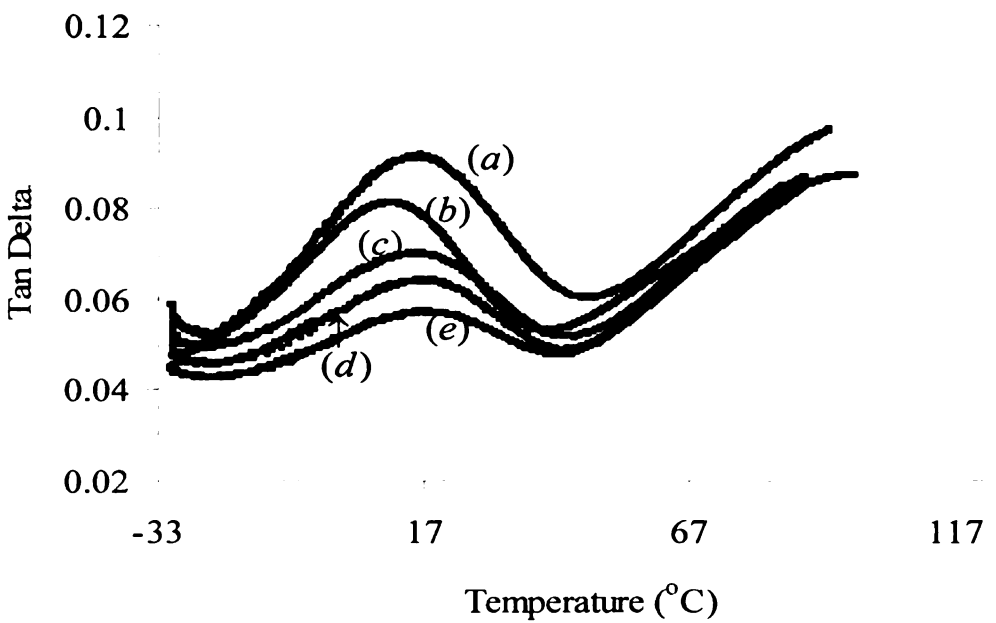

Figure 2.7: Temperature dependency of Tan Delta with varying loading level of Wood fiber in PHBV matrix. (a) PHBV-wood fiber (60:40), (b) PHBV-wood fiber (70:30), (c) PHBV-wood fiber (80:20), (d) PHBV-wood fiber (90:10), (e) PHBV-wood fiber (100:0).

2.2.4 FTIR analysis: Figure 2.8 (a) shows FTIR spectrum of the specimen from processed neat PHBV, (b) and (c) are of 30 and 40 wt% wood fiber-PHBV composites, respectively. Bands appearing at 1275, 1226, and 1180 cm^{-1} (marked with arrows) in FTIR spectra of PHBV are sensitive to degree of crystallinity. [27]. In addition, bands at 1130,1100,and 1060 cm^{-1} are also sensitive to degree of crystallization, but to a lesser extent. Comparing the intensities of the bands at 1226 and 1180 cm^{-1} of neat PHBV and 30 wt% and 40 wt% wood fiber loaded PHBV, it is observed that the intensity of the band at 1226 cm^{-1} increases and that of 1180 cm^{-1} decreases thus giving an inference of the rise in degree of crystallinity in PHBV with the addition of the wood fiber. Crystallinity index (CI) is a relative measure of degree of crystallization and is defined as a ratio of the intensity at band 1378 cm^{-1} (marked with asterisk) to the band at 1176 cm^{-1} (i.e., ratio of the intensity of the band insensitive to crystallization to the band sensitive to crystallization) [26]. CI is not be confused with absolute crystallinity. CI of neat processed PHBV was calculated to be 0.66 and that of PHBV with 30 wt% and 40 wt% wood fiber was 0.95 and 0.9. Higher CI value of PHBV-wood fiber than neat PHBV indicates the higher order in degree of cyrstallinity of the PHBV matrix in presence of wood fiber.

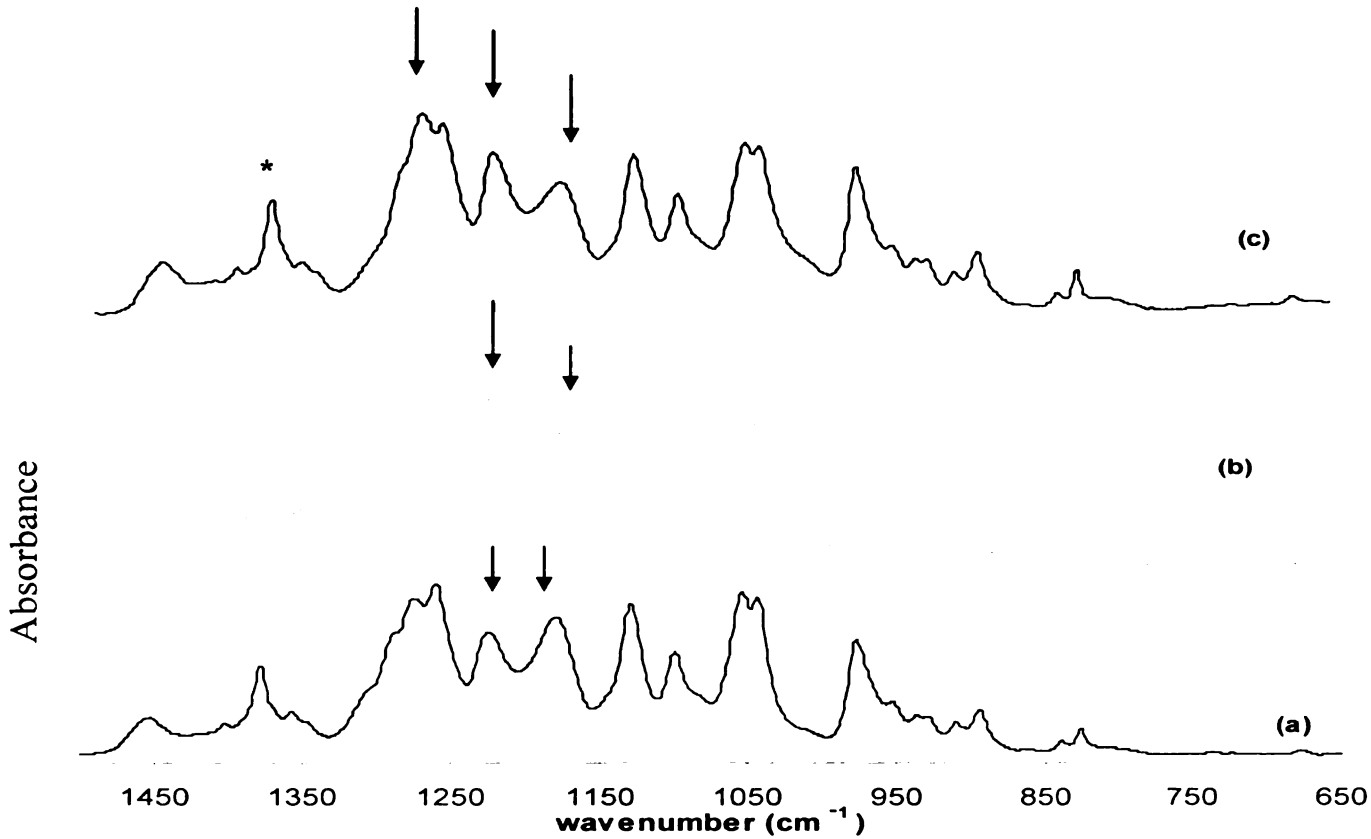

Figure 2.8: FTIR spectra of (a) PHBV (b) PHBV-Wood fiber (70:30) (c) PHBV-Wood fiber (60:40)

2.2.5 *Heat Deflection Temperature (HDT):* The effect of wood fiber reinforcement on the HDT of the composite is of significant importance for the reason that HDT is considered as an upper temperature limit of a material. HDT of crystalline polymers depends on thermal history of polymer, crystallite sizes and presence of impurities or other nucleating agents, which enhance crystallinity [28]. The HDT values of PHBV-wood fiber composites with different wood fiber loading are depicted in Figure 2.9. The HDT of PHBV-wood composite, loaded with 40 wt% of wood fiber, was improved by 24 ^{o}C as compared to neat PHBV. The major contribution to the improved HDT with enhanced fiber content is the fiber reinforcement, which has higher HDT than the matrix. The increased HDT can also be attributed to an increase in the degree of crystallinity in PHBV due to addition of wood fibers, the fiber surface acted as nucleating sites therefore, increasing the crystallinity of the wood fiber filled PHBV composite [29,30]. This is supported by the FTIR analysis of the PHBV- wood fiber composite. HDT is directly proportional to the modulus, and inversely proportional to the applied load at which deformation occurs therefore, an increased storage modulus of PHBV based composites, at higher temperature, was also the contributing factor in the increase of HDT with the increasing fiber content in matrix [14, 16, 31].

2.2.6 Coefficient of linear thermal expansion (CLTE): Coefficient of linear thermal expansion (CLTE) is a vital property for composites in structural applications. A low CLTE value is a desirable property in order to achieve dimensional stability. CLTE of crystalline polymers depends on various parameters like processing conditions, thermal history, and degree of crystallinity and crystallite size. Filler aspect ratio, volume fraction, orientation and distribution in matrix also play a deciding role in determining

the CLTE of composites [16, 30]. Figure 2.9 give the details of the CLTE with the varying wood fiber level in matrix. The wood fiber lowered the CLTE of PHBV. The CLTE value of PHBV-wood composite was reduced from 182 x 10^{-6} / ^{o}C (i.e., neat PHBV) to 173 and 154 x 10^{-6} / ^{o}C, when reinforced with 30 and 40 wt% of wood fiber, respectively. CLTE of a composite is affected by the mismatch of the high CLTE of the matrix and low CLTE of the fibers. The fibers are tightly squeezed in the matrix during mold cooling because of which the fiber poses a mechanical restrain on the opening of the polymer chain during heating, and thus reduce the overall CLTE of the composite. As the ratio of fiber to matrix volume increases the decrease in CLTE of the composite is mainly due to the lower CLTE of the fiber. Surface of the wood fiber acted as an additional nucleating site for the formation of crystallite of PHBV matrix therefore, enhancing the crystallinity of the matrix as revealed from the FTIR spectra of the PHBV-wood fiber composite [11]. The increased crystallinity would pack the matrix more densely, thus resulting in reduction of CLTE. This can be another identifiable reason for the reduction of CLTE of a semi-crystalline polymer like PHBV when filled with wood fiber.

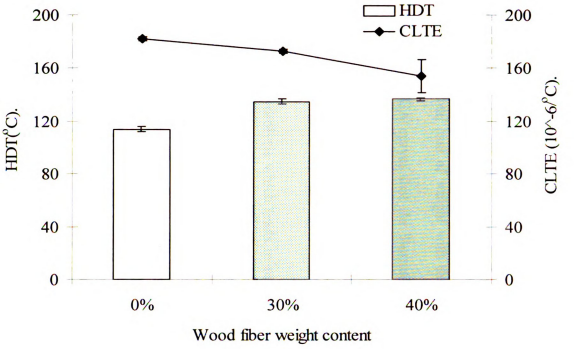

Figure 2.9: Effect of wood fiber content on heat deflection temperature (HDT) and coefficient of linear thermal expansion (CLTE) values of PHBV-wood fiber composites.

2.2.7 *Thermogravimetric analysis (TGA)*: Figure 2.10 shows the wt% loss of PHBV, wood fiber and their composites with increasing temperature. The TGA curve of wood fiber indicated that the actual thermal degradation of wood initiates at 250°C, and its maximum loss percent occurred at 390°C, completely degrading at 500°C. The TGA of neat PHBV showed a gradual loss of weight with the increase in temperature. It could be inferred from the TGA curves that the thermal degradation of PHBV was uniform with maximum degradation occurring at 310 °C and onsets at 250°C. It has been reported that PHBV is thermally unstable above 250°C. The degradation process involves chain scission and hydrolysis which leads to reduction in molecular weight and formation of crotonic acid [32], the presence of moisture can enhance hydrolytic degradation of PHBV. The PHBV-wood fiber composites of PHBV having 30 and 40 wt% of the wood fiber showed similar trends of thermal degradation giving a little information of any effect of increased wood fiber content on the thermal stability of PHBV-Wood fiber composites. TGA curves of composites indicated that thermal degradation of composite is a collective thermal degradation phenomenon of PHBV and wood fiber. Degradation of the PHBV-wood composites onsets around 250 °C, which is also an onset point of both wood fiber and PHBV, and completes at 390 °C. The TGA of PHBV-wood composites also showed that wood fiber was the final content to degrade in composite. Maximum degradation of composites occurred at the temperature, which corresponds, to the maximum degradation temperatures of PHBV and wood fiber. Figure 2.11 shows the derivative weight loss of neat PHBV, wood fiber

and PHBV-wood fiber composite. TGA curve peak of the composites shifted towards the lower temperature from that of neat PHBV, which indicated that the presence of wood fiber made PHBV a little more thermally unstable than neat PHBV. This could be due to presence of some other constituent in wood fiber or degradation effect of hydroxyl groups on the cellulose in wood fiber [33].

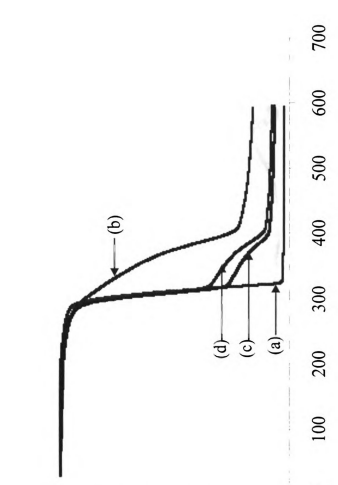

Figure 2.10: Thermogravimetric analysis of PHBV, wood and their composites; (a) PHBV-wood fiber (100:0), (b) Wood fiber (c) PHBV-wood fiber (70:30), (d) PHBV-wood fiber (60:40).

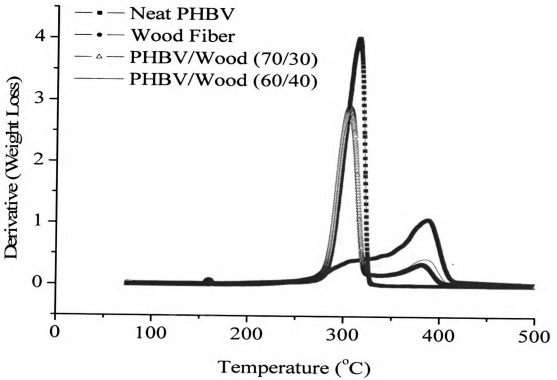

Figure 2.11: Derivative weight loss of PHBV, wocod fiber and their composites

2.2.8 Impact Strength: The Impact test measures the energy required to completely break the specimen. This energy is a combination of crack initiation and crack propagation phenomena, which depends on various factors like fiber to matrix adhesion, toughness of the matrix and fiber alone, defects in the packing of fiber/matrix, crystalline morphology etc [34]. The notch izod impact strength test basically measures the energy to propagate an existing crack. 2.12 represents the results of the notched izod impact strength of PHBV and its wood fiber filled composites with various concentration levels. The impact strength of PHBV decreased with the increase of wood fiber content in the PHBV matrix. The impact strength of PHBV-wood composite decreased from 34 ± 2.7 J/m i.e. neat PHBV to 30 ± 0.5 and 24.4 ± 1.2 J/m when reinforced with 30 and 40 wt% of the wood fiber, respectively. The crystalline polymers are brittle, and the increase in degree of crystallinity further decreases the impact strength [18].The crystallinity of PHBV increases with the addition of wood fiber because the surface of cellulosic wood fiber acted as the additional nucleating sites for the PHBV matrix. This increased the spherulite prominence in the matrix around the fibers and constraining it thus, resulting in the reduced impact strength. The reduced impact strength at a higher fiber loading of 40 wt% due to some fiber clustering in specimens can not be ruled out. The molecular weight reduction due to higher processing time (10 min.) of 30 and 40 wt% wood fiber composite as compared to that of neat PHBV (3 min.) may also be a contributing factor to the reduced impact strength of wood fiber-PHBV composite. [18, 32, 35].

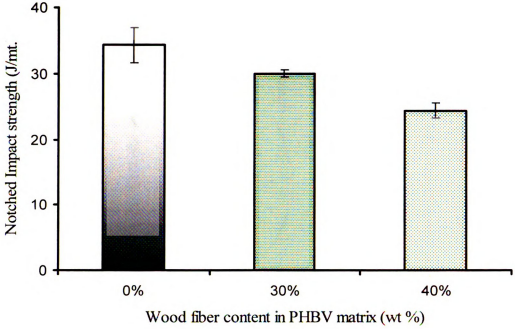

Figure 2.12: Notch Impact strength of PHBV-wood fiber composites with different loading levels of wood fiber.

2.2.9 *Morphology:* Figure 2.13 and 2.14 shows the photomicrographs of the PHBV-wood fiber composites with 30 and 40 wt% of wood fiber. Scanning electron microscopy (SEM) was used to characterize the morphology of the composites. The surface characterized under SEM was the fractured surface obtained as a result of the notched impact test. Fiber pull out fiber breakage were the failure mode of the fractured surface. Figure 2.13 (A) of 30 wt% wood fiber shows a good dispersion of wood fiber in the PHBV matrix and relatively lesser number of pullouts to the fractured fibers. Fiber breakage contributes much lesser energy than the fiber pullouts in the net fractured energy. As can be observed from the SEM micrographs, fiber fracture was predominant in the fractured surface of the specimen. This is consistent with the low impact strength at 30 and 40 wt% wood fibers. A lesser amount of fiber dispersion is observed in Figure 2.14 (A) of 40 wt% fiber than that of 30 wt% fiber specimen. More number of fiber pullouts were observed on the fractured surface of a specimen with 40 wt% wood fiber content than the specimen with 30 wt% wood fiber content. More fiber pullouts at 40 wt% of wood fiber should have had given more impact energy than at 30 wt% however, this did not happen because of higher fiber content at 40 wt% wood fiber there was not sufficient fiber to matrix contact therefore, fiber to fiber contact dominated in the matrix. Thus insufficient adherence of fiber to matrix lead easy fiber pullout during the impact. Fiber matrix adhesion remained below the critical adhesion limit due to which impact energy decreased with increased fiber loading [36]. Figure 2.13 (B) and 2.14 (B) are the photomicrographs at higher magnification which shows that a significant amount of interfacial interaction exist between fiber and matrix. An

interface adhesion allowed better stress transfer from matrix to fiber, which accounted for superior tensile and flexural modulus.

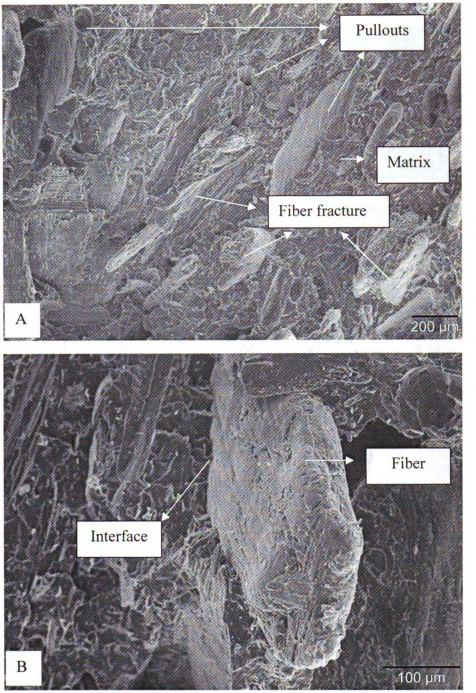

Figure 2.13: SEM photomicrographs of impact - fractured samples of PHBV-wood (70:30) composite;(A): 60x, 200µm, (B): 200x, 100µm.

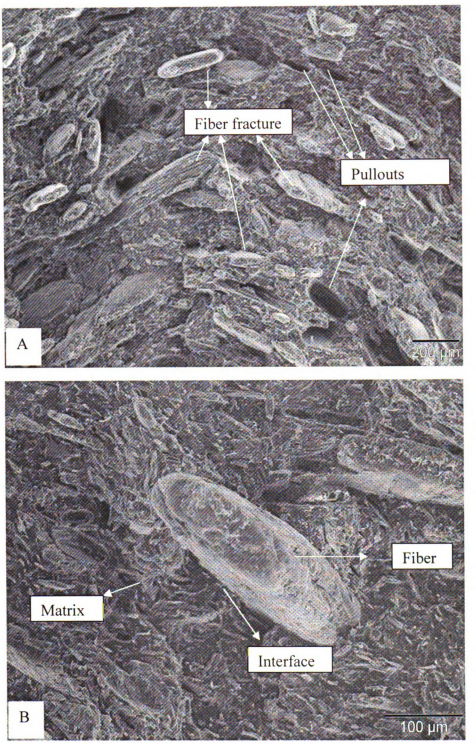

Figure 2.14: SEM photomicrographs of impact-fractured samples of PHBV-wood (60:40) composite; A: 60x, 200µm, B: 200x, 100µm.

2.3 Conclusion

Biodegradable composite from polyhydroxybutyrate-co-hydroxyvalerate (PHBV) and wood fiber were fabricated using extrusion followed by injection molding. The fabricated PHBV based biocomposites contained 10 to 40 wt% of the maple wood fiber. The effects of increasing wood fiber weight contents on mechanical, thermomechanical and morphological properties of the PHBV based biocomposites were evaluated. The tensile and flexural modulus of PHBV based biocomposites reinforced with 40 wt% of wood fiber was improved by ~167% when compared with neat PHBV. The theoretical tensile modulus values of PHBV based biocomposites obtained from Halpin-Tsai and Tsai-Pagano equations were consistent with the experimental tensile modulus values. The storage modulus values of the PHBV based biocomposites also exhibited the increasing trend with the enrichment of wood fiber in PHBV matrix. The effectiveness of fibers on the storage modulus of the composite was evaluated by a coefficient factor, C. The heat deflection temperature was increased by 21%, and the coefficient of linear thermal expansion reduced by 18 % of the biocomposite at 40 wt% of wood fiber content in PHBV. Scanning electron microscopy (SEM) photomicrographs exhibited the existence of interfacial interaction between wood fiber and PHBV thus, providing the compatibility between the two.

2.4 References

1. Principia Partners presentation at 7th International Conference of Wood fiber-Plastic composites May 19-20, 2003; Madison, WI.

2. http://www.principiaconsulting.com/consulting/news.cfm?article=78 (accessed date 05/15/2006).

3. Selke S E, Wichman I .Wood fiber/polyolefin composites. Composites Part A; 2004; 35; 321-326.

4. Harper D, Wolcott M. Interaction between coupling agent and lubricants in wood-polypropylene composites. Composites Part A; 2004; 35; 385-395.

5. Li T Q, Wolcott M P. Rheology of HDPE-wood composites. I. Steady state shear and extensional flow. Composites Part A; 2004; 35; 303-311.

6. Stark N M, Berger M J. Effect of Species and Particle Size on Properties of Wood-Flour-Filled Polypropylene Composites; 1997.

7. Lenz R W, Marchessault R H. Bacterial Polyesters: Biosynthesis, Biodegradable Plastics and Biotechnology. Biomacromolecules; 2005; *6*(1); 1-8.

8. http://www.nature.com/news/1999/990930/full/990930-5.html (accessed date 5/15/2006)

9. http://www.mhhe.com/biosci/pae/botany/botany_map/articles/article_28.html (accessed date 5/15/2006).

10. Hao Y, Zhu M, Zhang Y, Chen Y. Mechanism of the Formation of Concentric ring like Patterns on PHBV Spherulites. Polymer-Plastics Technology and Engg.; 2004; 43(1); 1-15.

11. Reinsch V E, Kelley S S. Crystallization of Poly (hydroxybutyrate-co-hydroxyvalerate) in Wood Fiber Reinforced Composites. Journal of Applied Polymer Science; 1997; 64 (9); 1785-1796.

12. Sics I, Ezquerra T A, Nogales A, BaltaC F J, Kalnins M, Tupureina V. On the Relationship between Crystalline Structure and Amorphous Phase Dynamics during Isothermal Crystallization of Bacterial Poly(3-hydroxybutyrate-*co*-3-hydroxyvalerate) Copolymers. Biomacromolecules; 2001; *2*(2); 581-587.

13. Mohanty, A K, Misra M, Drzal LT. Sustainable Biocomposites from Renewable Resources: Opportunities and Challenges in Green Materials World. Journal of Polymer and Environment; 2002; 10.

14. Bhardwaj R, Mohanty A K, Drzal L T, Pourboghrat F, Misra M. Renewable Resource-Based Green Composites from Recycled Cellulose Fiber and Poly(3-hydroxybutyrate-*co*-3-hydroxyvalerate).Biomacromolecules; 2006;(Published on web 04/26/2006).

15. Dufresne A, Dupeyre D, Paillet M. Lignocellulosic Flour-Reinforced Poly(hydroxybutyrate-covalerate) Composites. J Appl Polym Sci ; 2003; 87;1302–1315.

16. Luo S, Netravali A N. Interfacial and mechanical properties of environment-friendly "green" composites made from pineapple fibers and poly(hydroxybutyrate-co- valerate) resin. Journal of Material Sc.; 1999; 34; 3709 – 3719.

17. Jotier. J.J, Limieux. E, Prud'homme. E.R. Miscibility of polyester/Nitrocellulose blends: A DSC and FTIR study. Journal of Polymer Science: Part B: Polymer Physics; 1988; 26;1313-1329.

18. Fie.B, Chen.C, Wu.Hang, Peng.S, Wang. X, Dong.L. Comparative study of PHBV/TBP and PHBV/BPA blends. Polymer International; 2004; 53; 903- 910.

19. Huda M S, Drazal L T, Mohanty A K, Misra M. Wood fiber reinforced Poly (Lactic acid) composites. 5th Annual SPE Automotive Composition conference, Troy, MI, USA, 2005, Sept 12-14.

20. Nielsen E L. Mechanical properties of Polymers and Composites. In: Marcel Dekker, editor.vol.2. New York, 1976.

21. Tsai S W, Pagano N J, Composite Material Workshop, Technology Publishing Co., New York; 1968.

22. Karrad S, Cuesta J, Crespy M L. Influence of a fine talc on the properties of composites with high density polyethylene and polyethylene/polystyrene blends., Journal of Material Sc;1998; 33; 453-461.

23. Nicolais.L, Nicodemo.L. The Effect of particle shape on tensile properties of glassy thermoplastic composite; Intern.J.Polyeric Mater.;1974; 4; 229-243.

24. Wood Handbook: Wood as an Engineering Material; Forest Products Laboratory Forest Service, USDA; 1987.

25. Maiti.S.N, Singh.K. Influence of wood flour on polypropylene: J. Applied Polymer Sc.;1986; 32;4285-4289.
26. Pothana L A, Oommenb Z, Thomas S. Dynamic mechanical analysis of banana fiber reinforced polyester composites. Composites Science and Technology; 2003; 63; 283–293.

27. Bloembergen. S, Holden.D.A, Hamer.G.K, Bluhm.T.L, Marchessault.R.H; Studies of Composition and Crystallinity of Bacterial Poly(β-hydroxybutyrate-co-β-hydroxyvalerate; Macromolecules; 1986;19;2865-2871

28. Takemori M T. Towards an Understanding of the Heat Deflection Temperature of Thermoplastics; Polymer Sc. and Engg.;1979;19(15);1104-09.

29. Avella M, Martuscelli E, Raimo M. Properties of blends and composites based on poly(3-hydroxy)butyrate (PHB) and poly(3-hydroxybutyrate -hydroxyvalerate) (PHBV) copolymers; J. of Material Sc.; 2000; 35;523-545.

30. Tan J K, Kitano T, Hatakeyama T J. Crystallization of carbon reinforced polypropylene. Mater Sci; 1990; 25; 3380-84.

31. Kardos J L, Raisoni J, Piccarolo S. Prediction and Measurement of the Thermal Expansion Coefficient of Crystalline Polymers. Polymer Sc. and Engg.; 1979; 19; 5; 1004-09.

32. Gatenholm P, Mathiasson A. Biodegradable Natural Composites. II. Synergistic effect of processing cellulose with PHB. Journal of Applied Polymer Sc.,1994; 51; 1231-1237.

33. Fernandes E G, Pietrini M, Chiellini E. Bio-Based Polymeric Composites Comprising Wood Flour as Filler. Biomacromolecules; 2004; 5(4); 1200-1205.

34. Kamdem.P, Jiang H C, Freed J W, Matuana M L. Properties of wood plastic composite made of recycled HDPE and wood flour from CCA-treated wood removed from service. Composites: Part A 35; 2004; 35; 347-355.

35. Zhang J, McCarthy S, Whitehouse R. Reverse temperature Injection Molding of Biopol™ and effect on its properties. Journal of Applied Polymer Science; 2004; 94; 483-491.

36. Agarwal. B. D, Broutman. L. J .Analysis and Performance of Fiber composites. In. Jhon Wiley and Sons. Editor; New York, 1980.

Chapter 3

Renewable Resource Based Biocomposites from Natural Fiber i.e., Bamboo Fiber, and Polyhydroxybutyrate-Co-Valerate (PHBV) Bioplastic and its Analogy to Wood Fiber Reinforced Bioplastic Composites

3.0 Introduction

In the established market of plastic composites there has been a dynamic emergence of wood and natural fiber plastic composite (W/NF PC). These have a proven market in outdoor and indoor applications like decking, railing, fencing, furniture, etc., and they also hold a large share of the European market in automotive applications [1]. Most of the thermoplastic used in W/NF PC are recyclable and is being look to as a profitable opportunity for these materials. Contemporary, W/NF PC are based on conventional thermoplastics and naturally available cellulose fiber, with the fiber content varying from 30 to 70 wt.%. Various kinds of naturally available fibers and wood fiber have been used to achieve good mechanical properties of W/NF PC. A significant amount of research is focused on improving the compatibility between the hydrophilic natural fiber and the hydrophobic thermoplastics [2-5]. Nano-reinforcement using inorganic material like clay in wood-PP composites has also been reported elsewhere [6]. The major limitation these composites encompass is their limited dimensional stability, when exposed to moisture [7].

The environmental concerns due to the accumulated plastic wastes over the last few decades have obligated the biodegradable green plastics to surrogate petroleum based polyolefins. Polyhydroxyalkanoates (PHAs), a family of natural, biodegradable

polyesters, differ from petroleum-based synthetic polymers such as polypropylene and polyethylene by their synthesis from renewable resources, and by their unproblematic biodegradability. The similarity of some of its mechanical properties to the polyolefins indicates that it may be a substitute for polyolefins. The biodegradability and biocompatibility of PHBV has given it a remarkable breakthrough and application in biomedical applications [8, 9]. Its composites with natural fiber have been studied extensively [10-12]. Wood and other naturally available fibers are generally used to reinforce thermoplastics due to their low cost, abundant availability, high performance and low density [12]. Among the existing WPC products, maple wood fiber is the most widely used fiber commercially; whereas among the naturally available fibers in Asia, bamboo fiber has the most abundant applications [13, 14]. Therefore, these two fibers, obtained from two different categories of lignocellulose-based sources are the most used fibers in the commercial sector. In the previous chapter wood fiber was evaluated for its reinforcing ability in PHBV.

The prime focus of the study in this chapter was to fabricate and evaluate bamboo fiber based PHBV biocomposites. Bamboo is a more sustainable source of natural fiber than wood fiber due to the short growth period of 3 to 5 years, regrowth from its shoot therefore, avoid deforestation, and higher strength. In fact, bamboo is the commonly used structural material in housing construction in south-east Asia. Fundamental aspects of these bamboo based biocomposites were measured using differential scanning calorimetry (DSC), thermogravimetric analysis (TGA), Fourier transform infrared spectroscopy (FTIR), and their morphology was also explored. Furthermore, the experimental results of tensile modulus were compared with the

existing theoretical model. Comparative analysis of the processed bamboo fiber biocomposites with the earlier reported wood fiber-PHBV biocomposites [15] in the previous chapter has been discussed; along with performing a two-way ANOVA on their mechanical properties.

3.1 Experimental Section

3.1.1 Materials

Polyhydroxybutyrate-co-valerate (PHBV) under the trade name Biopol (Zeneca Bio Products) was obtained from Biomer, Germany. Madake bamboo fiber with lengths of ~ 500 μm and diameters between 10- 100 μm was supplied by the Kyoto Institute of Technology, Japan.

3.1.2. Fabrication of composites employing micro-compounding technique:

In order to avoid any moisture induced degradation during processing, the bamboo fiber and PHBV were dried at a 110 ^{o}C and 80 ^{o}C under vacuum for two and four hours, respectively. The dried fibers and PHBV were kept in air-tight plastic bags until the time of processing. The composites were prepared using a micro-extruder (DSM Research, Netherlands) with a barrel volume of 15 cc. The extruder was equipped with co-rotating twin-screws having a length of 150 mm and L/D of 18. The temperatures in three heating zones of the micro-extruder (top, center and bottom) were 165, 160 and 155 ^{o}C. The processing temperature was kept between 155 and 165 ^{o}C in order to achieve low melt flow and avoid thermal degradation at higher temperature. The screw rotation speed was 100 rpm. After fixed processing time in the micro–extruder, the molten mix was transferred to a preheated mini-injection molding machine for specimen fabrication. The optimized injection pressure for all PHBV-

bamboo fiber composites was 551.5 KPa and the temperature was 155 °C. The different mix ratios of PHBV and fibers along with some other processing parameters are given in Table 3.1.

Table 3.1: Processing parameters of PHBV and fiber compositions

PHBV (wt%)	Fiber (wt%)	Processing temperature (°C)	Retention time (min)
100	0	160	3
70	30	160	10
60	40	160	10

3.1.3 Testing and Characterization

3.1.3.1 Mechanical Properties

Tensile and flexural properties of specimens were measured using a United Calibration Corp. SFM 20 testing machine as per ASTM standards D638 and ASTM D790, respectively. Tensile testing was carried out at a rate of 2.54 mm/min with a pre-load of 0.023 kg. The system controls and data analysis were performed using the supplied Datum software. The notched Izod impact testing was carried out on a Testing Machine Inc. (TMI) model 43-02-01 as per ASTM D256 with a pendulum of impact energy 1.35 J.

3.1.3.2 Thermo-mechanical Properties

3.1.3.2.1 Dynamic mechanical analysis (DMA)

The storage modulus, loss modulus and tan delta of PHBV and its natural fiber composites were measured using a TA Instruments model Q800 DMA. The specimens were heated from -30 to 125 ^{o}C at a heating rate of 2 ^{o}C/min. The single cantilever mode was used to test the specimens at amplitude of 15 μm and frequency of 1 Hz.

3.1.3.2.2 Heat deflection temperature (HDT)

The DMA was used to determine the HDT as per ASTM D648. Rectangular bars 2 × 12 × 58 mm in three-point bending mode with an applying load of 66 psi were used for testing. Samples were heated at the rate of 2 ^{o}C/min from room temperature to the temperature required to produce 0.195% strain.

3.1.3.3 Thermal Properties

3.1.3.3.1 Thermogravimetric analysis (TGA)

TGA was tested using TGA 2950 instrument with a heating rate of 20 °C/min from room temperature to 600 °C, the temperature of complete thermal degradation. All TGA runs were performed under a nitrogen purge.

3.1.3.3.2 Differential Scanning Calorimetry (DSC)

DSC of the samples was performed using a model Q100 DSC, TA Instruments. The heat/cool method was adopted for all specimens testing. Specimens were heated to 190 °C at a ramp rate of 10 °C/min and cooled with the same ramp. The data for melting points and heat of crystallization were collected during the heating cycle. The crystallization temperature and heat of fusion were obtained from the cooling cycle.

Data analyses of DMA, HDT, TGA and DSC results were performed using the supplied software *Universal Analysis.*

3.1.3.4 FTIR analysis

A Perkin-Elmer system 2000 FTIR Spectrometer was used with an attenuated total reflectance (ATR) accessory to gather the IR spectra of neat PHBV and its natural fiber composites.

3.1.3.5 Morphological studies

Morphological studies were conducted using a JEOL scanning electron microscope (model JSM-6400). Specimens were sputter-coated with gold to a thickness of ~10 nm before surface characterization in order to make minimize charging. The

SEM was equipped with a lanthanum hexaboride (LaB_6) crystal as electron emitter source. An accelerating voltage of 13 KV was used to collect the SEM images.

3.1.3.6 Statistical Analysis

Statistical analysis of tensile and flexural modulus results was carried out by performing two-way ANOVA on the PHBV and its composites with wood and bamboo fiber at 30 and 40 wt.% using MINITAB® software.

3.2 Results and Discussions

3.2.1 Tensile Properties: Figure 3.1 shows the Young's modulus of PHBV and its composites with bamboo fiber at 30 and 40 wt.% loadings. The modulus of the PHBV composites increased steadily with the fiber loading. At 30 wt.% fiber loading, it increased by 67%, and at 40 wt.% the increase was 175%. The tensile properties of short fiber composites depend on fiber length, distribution, orientation and their interfacial bond strength with matrix. The fiber orientations have been assumed to be random; as observed visually, and the composites behavior isotropic. The increased modulus of the composites can be ascribed to uniform dispersion of fibers in the PHBV matrix, which leads to the even distribution and transfer of stress from matrix to fiber. Uniform dispersion of fibers was physically visible in the specimens. The tensile strength of PHBV decreased with addition of the bamboo fibers. This can be attributed to the lack of sufficient interfacial interaction between the fiber and matrix. The presence of polar group on the lignocellulosic natural fibers and the abundant moderate polar groups in the chemical makeup of PHBV lead to an expectation of some interfacial interaction between the two; although from the FTIR analysis, no chemical or hydrogen bond interactions between the moderately polar groups of the two

components were observed. Reader may refer figure 3.7 for this purpose. Therefore, the only possible interactions responsible for the load transfer from matrix to fiber were frictional and Van der Waal forces. To increase the interfacial bonding between the fiber and matrix use of compatiblizer lies under the scope of future work.

Christensen's Model

The theoretical Young's modulus of the composites has been estimated using Christensen's model of equations [16, 17]. It provides a solution for the elastic properties of composites with randomly oriented short fibers. The following expression predicts the elastic modulus of composites below and above the critical length (l_c) of the fiber.

$$E_c \approx \frac{1}{6} v_f E_f \left(1 - \frac{l_c}{2l}\right) + v_m E_m \qquad \text{at} \quad l > l_c$$

$$E_c \approx \frac{1}{6} v_f E_f \frac{l}{2l_c} + v_m E_m \qquad \text{at} \quad l < l_c$$

E_c denotes the modulus of the composite, E_f and E_m that of fiber and matrix (in this case bamboo fiber and PHBV), v_f and v_m are the volume fractions of fiber and matrix, respectively, l is the fiber length and l_c the critical fiber length which is given by an expression of the Rosen model. For a bamboo fiber $l_c < l$.

$$\frac{l_c}{d_f} \approx 1.15 \left[\frac{1 - v_f^{1/2}}{v_f^{1/2}} \left(\frac{E_f}{G_m} \right)^{1/2} \right] \qquad d_f \text{ is the diameter of the fiber}$$

G_m has been estimated from a general relation

$$G = \frac{E}{2(1+\nu)}$$ ν is Poisson's ratio

Figure 3.2 depicts the theoretical and experimentally determined values of the modulus. Theoretical values of lignocellulosic natural fibers (bamboo) and the PHBV matrix have been approximated to be 25 GPa [18] and 1.02 GPa, respectively. Volume fraction of the fiber and the matrix at 30 and 40 wt.% were calculated using general equations

$$v_f = \frac{\frac{m_f}{\rho_f}}{\frac{m_f}{\rho_f} + \frac{m_m}{\rho_m}} \quad \text{and} \quad v_m = (1 - v_f) \quad \text{assuming density}$$

of natural fiber (ρ_f) and matrix (ρ_m) to be ~ 0.84 gm/cm^3 [19] for bamboo fiber and 1.25 gm/cm^3 for PHBV. The modulus of bamboo fiber-PHBV composites as predicted by Christensen's model are in close approximation to the experimental results. This was due to the uniform and narrow size distribution of bamboo fibers, although not quantified but observed visually. The difference between the theoretical and experimental data can be due to the agglomeration of the fillers at high volume fractions, which results in the higher modulus than the expected. The agglomeration was visible in SEM microphotographs. Although the composites have been assumed to be isotropic; anisotropy of the fibers cannot be ruled out. The model does not account

for the effect of filler and processing conditions on the matrix (PHBV) e.g. change in the degree of crystallinity, which had been noted from the FTIR and DSC analysis.

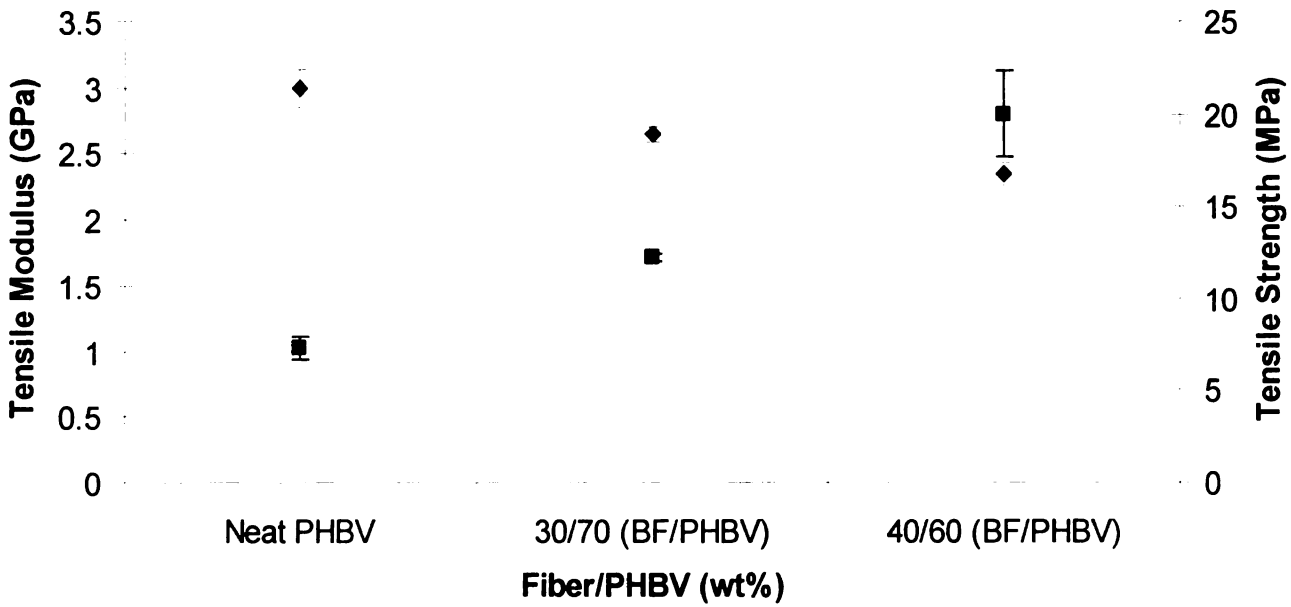

Figure 3.1 : Tensile properties of Bamboo fiber-PHBV composites at 30 and 40 wt% fiber(■) Tensile modulus, (♦) Tensile Strength.

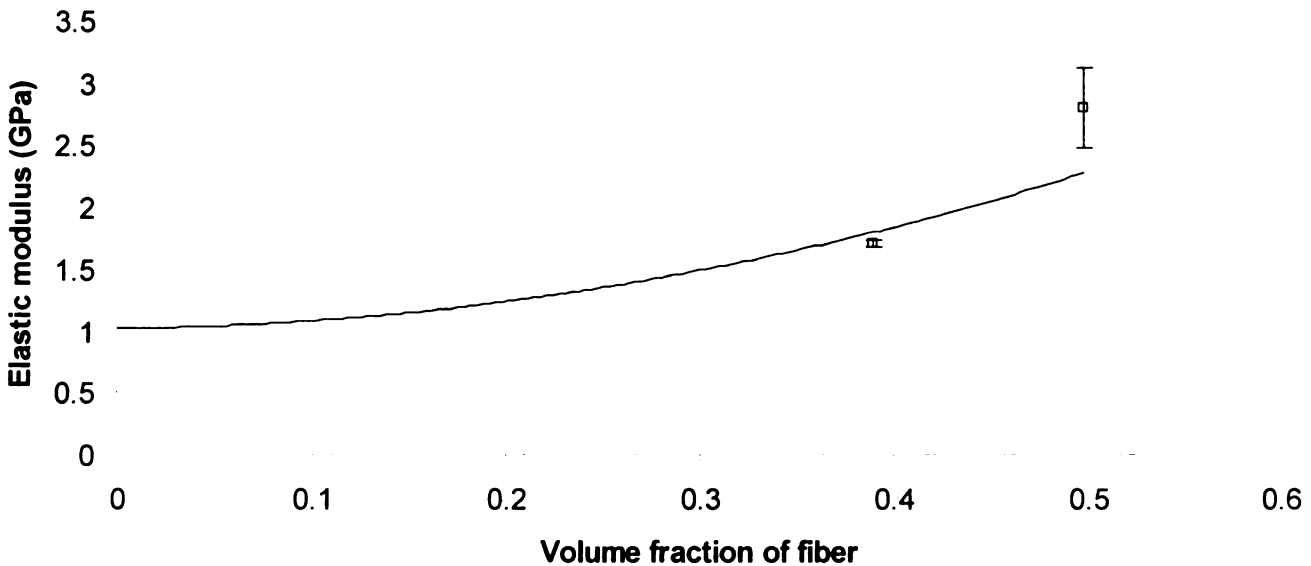

□ PHBV-Bamboo fiber Composite (——) Theoritical PHBV-Bamboo fiber Composite

Figure 3.2: Experimental and Theoritical data plots

3.2.2 *Flexural Properties:* Flexural modulus and strength of PHBV and its bamboo fiber composites with different fiber loadings are shown in Figure 3.3. In general, the modulus increased with incorporation of fibers. At 30 wt.% of fiber content the PHBV modulus improved by 100% and the increase was greater at 40 wt.% fiber with the modulus leap of 154%. The flexural strength of PHBV remained unchanged upon the addition of fibers. The improved flexural modulus and retained strength of the composites validated the reasonable amount of compatibility and interfacial interaction of cellulose fiber to the natural polyester PHBV. Fiber orientation in the matrix plays vital role in determining the flexural properties. Unlike tensile testing, where induced tensile stress plays crucial role, the flexural testing incorporates both compression and tensile stresses on the fiber, matrix and their interface across the specimen cross section, therefore, the strength response to the stress during flexural testing would be higher than during tensile testing. The tensile strength is chiefly govern by the dewetting of matrix from the fiber under tensile load and also is more sensitive to the defects originated at the interfaces of matrix and fiber.

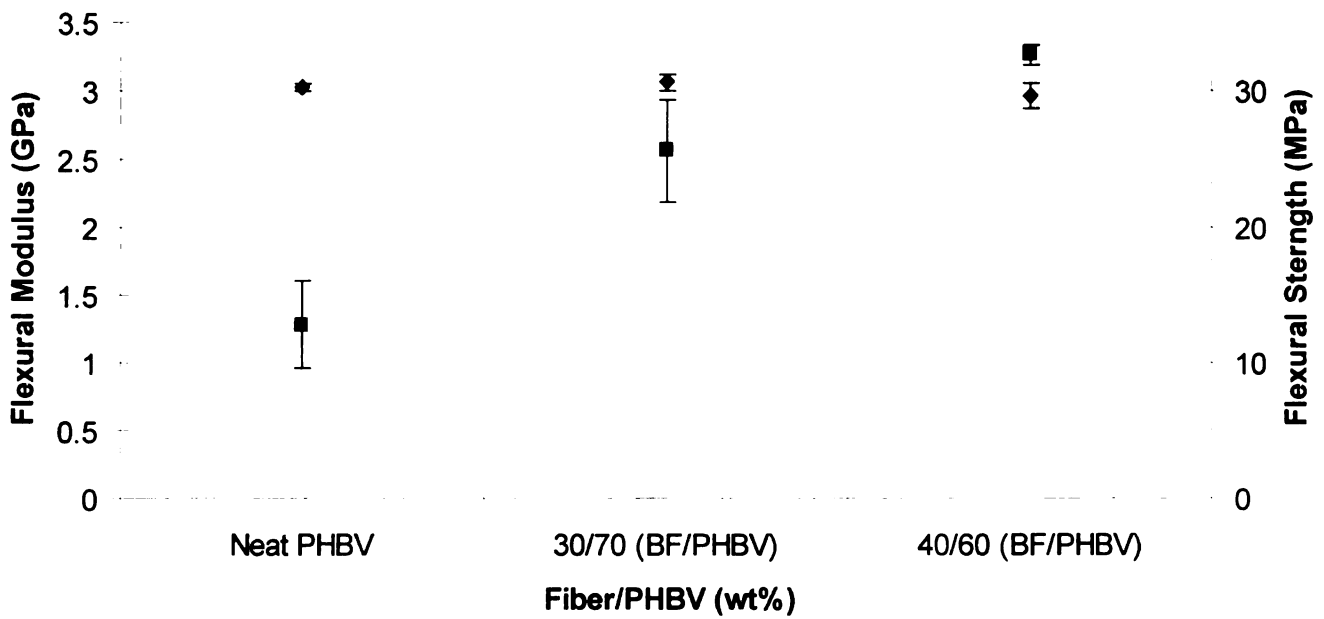

Figure 3.3 : Flexural properties of Bamboo fiber/PHBV composites having 30 and 40 wt% fiber (■) Flexural modulus, (♦) Flexural Strength.

3.2.3 Dynamic Mechanical Analysis (DMA)

The viscoelastic characteristics of the materials were measured using DMA. It is a complex quantity defined with elastic (storage) and viscous (loss) components; denoted E' and E", respectively. In DMA, the effect of temperature on the viscoelastic properties of the composites was studied. This gives more distinct insight to the interactions at the molecular level of the materials.

Figure 3.4, depicts the change in the E' of PHBV, and its composites with temperature. Like a generic tendency of thermoplastic composites, E' of PHBV and its composites decreases with rising temperature. E' of PHBV increased with the fiber loading up to 40 wt.%. The difference between the modulus values of bamboo fiber composites at 30 and 40 wt.% was not significant. E' of bamboo fiber composites improved by 157 and 173% at 30 and 40 wt.% fiber content at 25 $^{\circ}$C, respectively. The increase in E' of the fiber filled PHBV with respect to neat PHBV was greater below T_g than above it. This can be attributed to the temperature sensitivity of the natural fiber. The slope of the E' vs. temperature curve around the glass transition (T_g) temperature (~ 1 $^{\circ}$C) of PHBV increases with the fiber loading. This gave an indication of increased brittleness of these composites. A small bump in the curve of PHBV at 52 °C is indicative of the cold crystallization region. During the heating cycle as the specimen enters the cold crystallization region, the increasing crystallinity leads to decrease in the reduction rate of E', as a result a small bump in the curve emerges in this region. The cold crystallization temperature (T_{cc}) decreases with fiber loading. The T_{cc} decreases

to 46 °C in case of bamboo fiber composites. This could be due to very low diameter or high aspect ratio of the bamboo fiber versus the wood fibers which gave it a better opportunity to act as nucleating agent in PHBV matrix. Among the dynamic mechanical properties, dampening is most sensitive to the structural heterogeneity, morphological and transitions changes of system, and fiber-matrix interfacial interactions. Figure 3.5 shows the dampening of the PHBV and its fiber composites. Tan δ expressed as the ratio of E" to E' gives account of the energy dissipated as heat during the dynamic testing. Tan δ peak occurs approximately 10 to 20 °C above the T_g of the PHBV and its fiber composites. Increased stiffness of the PHBV with the fiber loading decreases the tan δ peak value thus reflecting the reduced energy losses in the interfacial regions. Low dampening of the composites in the transition region is attributed to the fineness of the bamboo fibers, which allows their uniform distribution and crystallinity effect on the matrix. The widening of the tan δ curve also indicates the increased heterogeneity of the specimens which was observed from the SEM photomicrographs. The maxima of the loss modulus of PHBV and its composites (Figure 3.6) occur in the glass transition temperature region. The enhanced response of molecular chains to the temperature in the amorphous region increases the viscous characteristic of the material in the glass transition domain. The fiber incorporation into the PHBV slightly increases its T_g towards higher temperature, thus delaying the increasing viscosity component of the composites. This can be due to the restriction imposed by the fibers on the movement of the expanding molecular chains in the amorphous region.

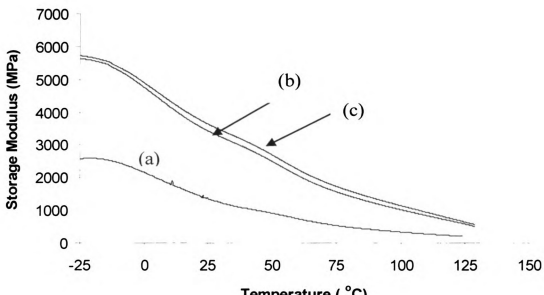

Figure 3.4: Storage modulus *vs* temperature of PHBV with varying loading level of fiber (a) PHBV (b) PHBV/Bamboo fiber (70:30) wt% (c) PHBV/Bamboo fiber (60:40) wt%

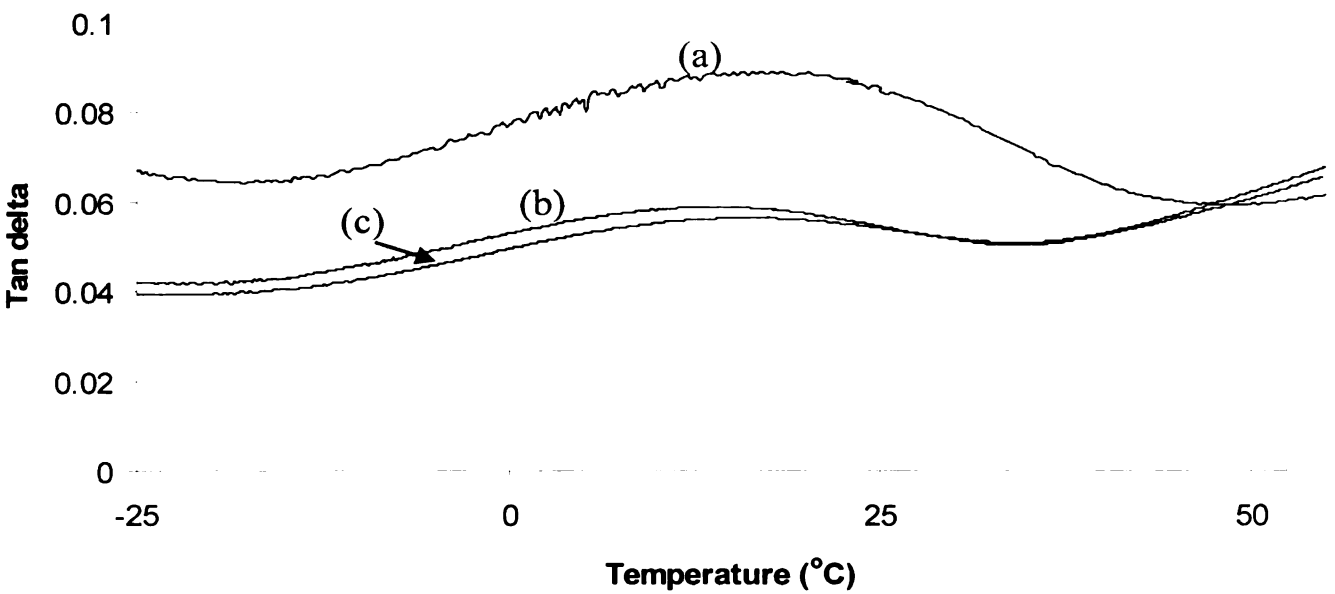

Figure 3.5: Tan Delta *vs* temperature of PHBV with varying loading level of fiber (a) PHBV (b) PHBV/Bamboo fiber (70:30) (c) PHBV/Bamboo fiber (60:40)

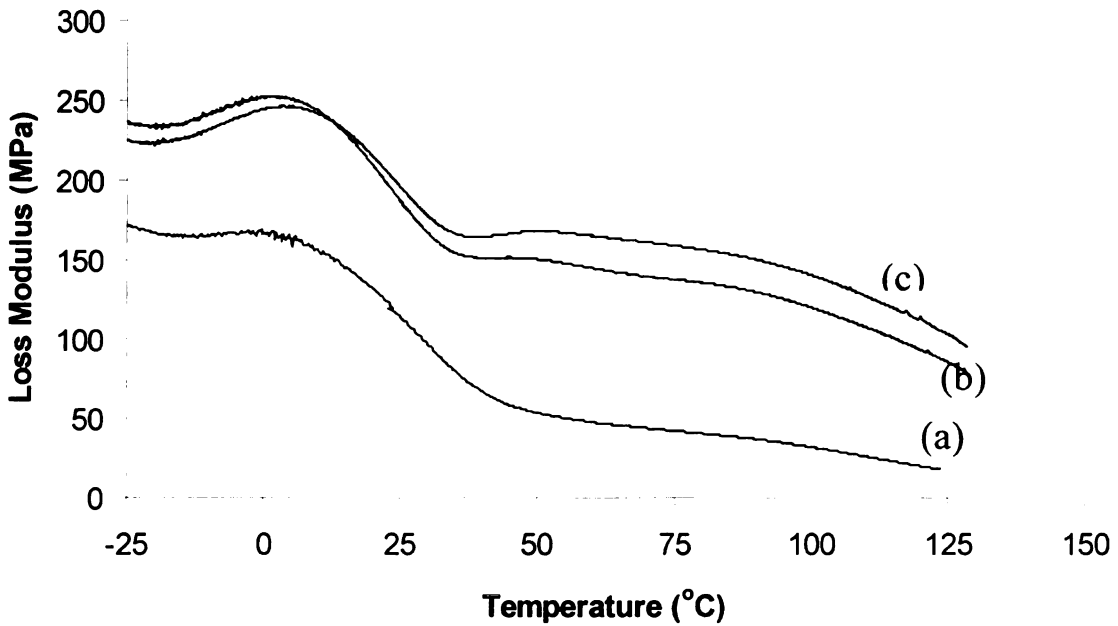

Figure 3.6: Loss modulus *vs* temperature of PHBV with varying loading level of fiber (a) PHBV (b) PHBV/Bamboo fiber (70:30) wt% (c) PHBV/Bamboo fiber (60:40) wt%.

3.2.4 FTIR analysis

In the PHBV IR spectra, Figure 3.7(a), the band at 1720 cm^{-1} was the C=O stretch of the ester group present in the molecular chain of highly ordered crystalline structure [20]. A slight shoulder emerging at 1740 cm^{-1} was of the C=O stretch in the amorphous region of semicrystalline PHBV. Characteristic peaks of symmetric –C–O–C– stretching vibration were present from 800 cm^{-1} to 975 cm^{-1} and the antisymmetric –C–O–C–stretching between 1060 cm^{-1} and 1150 cm^{-1} [21]. The band around 1378 cm^{-1} corresponds to the symmetrical wagging of CH_3 groups and at 1453 cm^{-1} was due to asymmetric deformation of methylene groups, the intensity of both the peaks is independent of crystallinity or in other words insensitive to crystallinity. The absorption bands at 1720, 1276, 1228, and 980 cm^{-1} crop up from the crystalline regions (designated with arrows) and bands at 1740, 1453, 1176 cm^{-1} from the amorphous regions (designated with two face arrows) of PHBV. Peak at 1228 cm^{-1} was purely of the conformational band of crystalline helical molecular chains and therefore, are absent in amorphous region [22]. The crystallinity index (*CI*) gives the relative measure of degree of crystallinity in PHBV. It is given as

$$CI = \frac{I_{at1378cm^{-1}}}{I_{at1176cm^{-1}}}$$ (*ratio of intensity of the band insensitive to crystallization to the band sensitive to crystallization*), where *I* is intensity of the peak at a given wave number. Figure 3.7 (b), (bamboo and PHBV composites) depicts the IR spectrum of

fibers and PHBV composites. On the comparison of the intensity of peaks at 1228 cm^{-1} and 1176 cm^{-1} of PHBV and its fiber composites, it is observed that these vary inversely to one another with the changing degree of crystallization. The *CI* of PHBV 0.66 increased to 0.74 with the addition of 30 wt.% bamboo fiber indicating the increase in the crystallinity of PHBV more, when the bamboo fiber was induced. *CI* value of similar order was obtained even though when a 40 wt.% bamboo fiber was added to the PHBV.

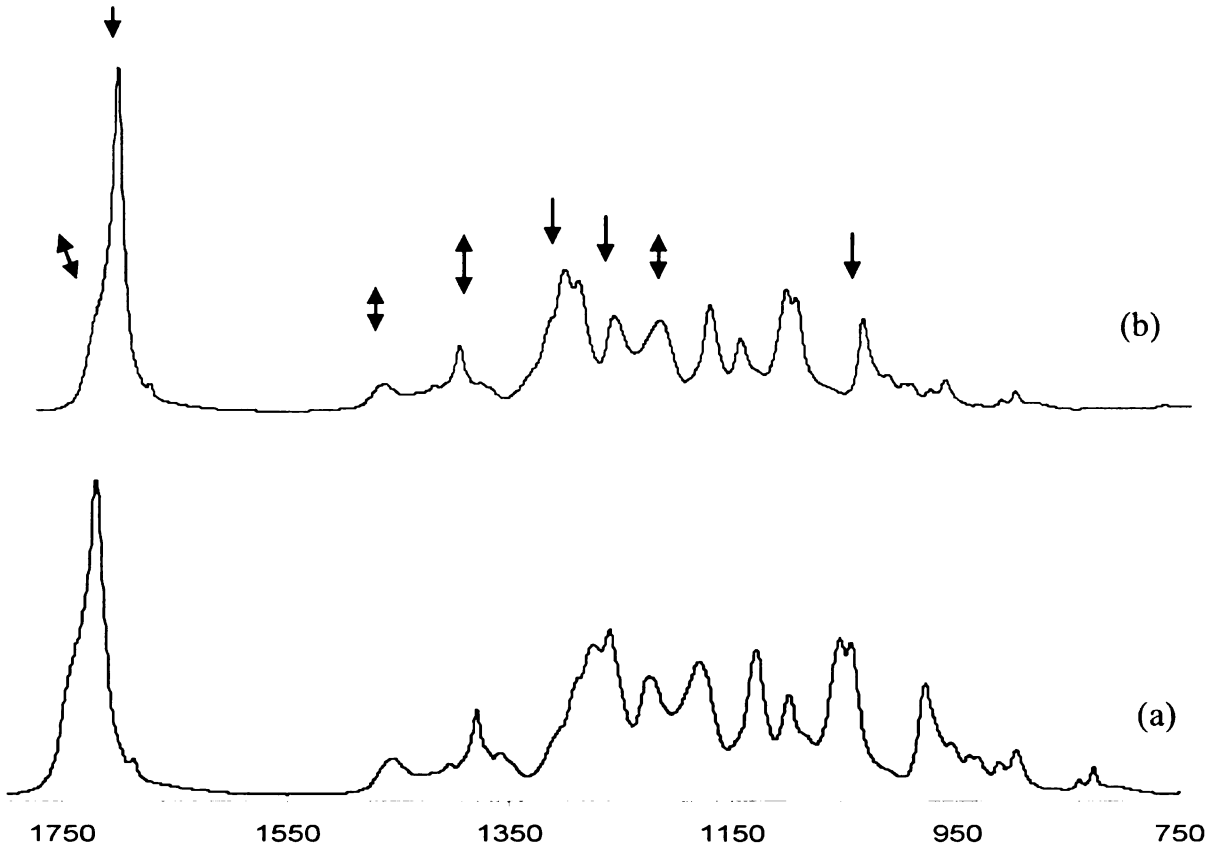

Figure 3.7: FTIR spectra of (a) PHBV (b) PHBV/Bamboo fiber (70:30) composite

3.2.5 Thermogravimetric Analysis (TGA)

The TGA curves in Figure 3.8 depict the weight loss of fibers, PHBV and its composites with temperature. Bamboo fibers began to thermally degrade at 250 ^{o}C, reaching the maximum at 380 ^{o}C and entirely degrading at around 500 ^{o}C. The PHBV lost weight gradually with the increasing temperature and its thermal degradation occurred maximum at 316 ^{o}C while insetting at 250 ^{o}C. Its thermal instability above 250 ^{o}C has earlier been reported stating that the degradation process involves chain scission and hydrolysis which leads to reduction in molecular weight and formation of crotonic acid [23] and the presence of moisture further promotes hydrolytic degradation. The thermal degradation of biocomposites appeared to be cumulative phenomena of thermal degradation of matrix (PHBV) and fiber alone. Degradation of composites initiated around 250 ^{o}C in case of both, fiber and PHBV and ceased around 400 ^{o}C. The TGA of composites also showed the fibers to be final constituent to undergo degradation in composites. The composite degradation maxima occurred at the temperature, a little higher than that of PHBV. Figure 3.9 illustrates the derivative weight loss of PHBV, fibers and their composites at 30 wt.% fiber. Maximum degradation temperature peak of the composite shifted to the higher temperature from that of PHBV indicating it to be a slightly more thermally stable than PHBV. Thus the presence of bamboo fiber (a lignocellulosic fiber) did not had any degradation effect on PHBV.

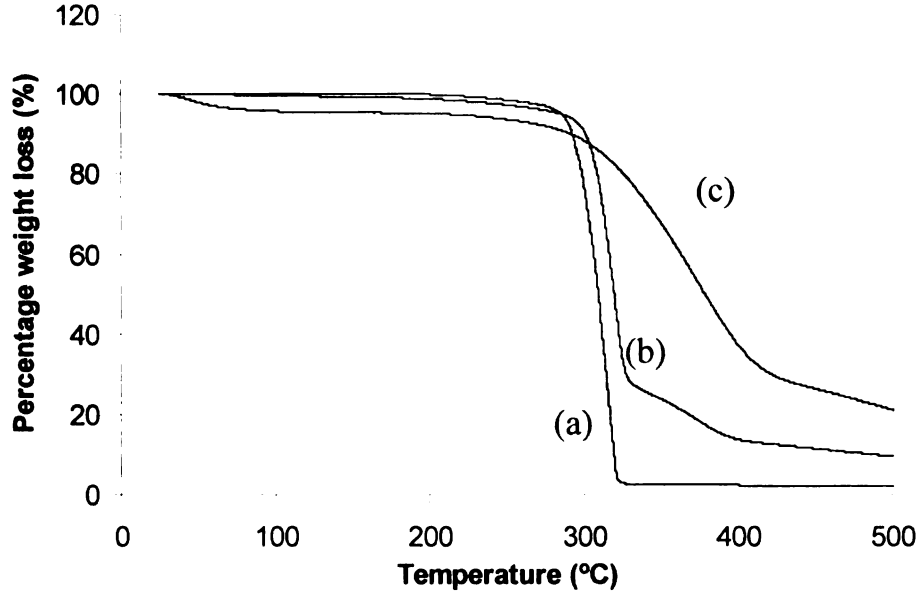

Figure 3.8: Percentage weight loss of (a) PHBV, (b) PHBV/Bamboo fiber (70:30) (c) Bamboo fiber.

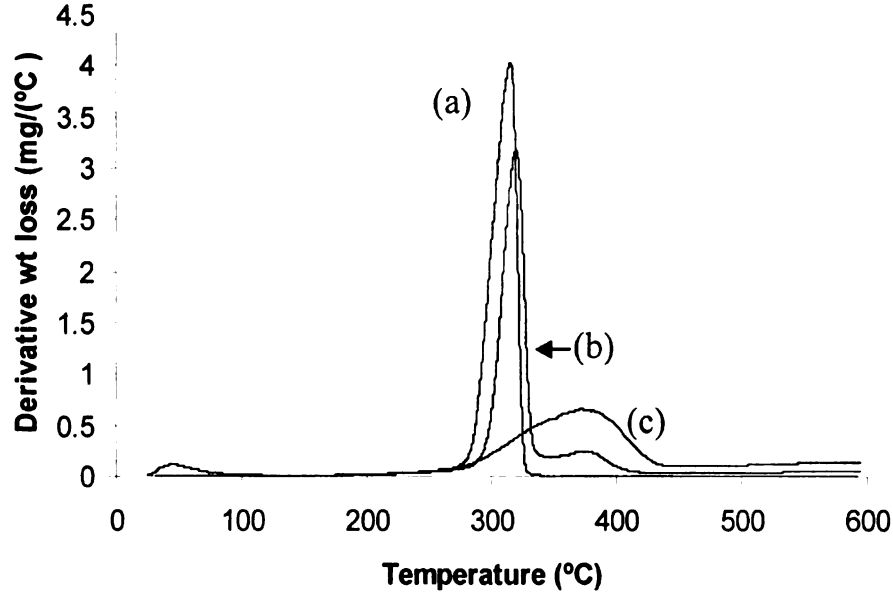

Figure 3.9: Derivative weight loss of (a) PHBV, (b) PHBV/Bamboo fiber (70:30) (c) Bamboo fiber.

3.2.6 Heat Distortion Temperature (HDT)

The HDT is an upper use temperature limit of a material, therefore, the effect of fiber type and loading in composites has a considerable importance in their structural applications. The HDT of semicrystalline polymers like PHBV depends on thermal history, crystallite sizes and distribution along with the presence of impurities and other nucleating agents which affects their crystallinity [24]. Figure 3.10 has a description of the HDT values of PHBV and its composites with bamboo fibers at 30 and 40 wt.% fiber content. The HDT of PHBV was enhanced by addition of fibers at 30 and 40 wt.% from 114 ^{o}C to 120 ^{o}C and 123 ^{o}C, respectively. The major contributing factor to the improved HDT with higher degree of fiber content was the fiber reinforcement which had better HDT than the matrix. The increased storage modulus of composites at higher temperatures also contributed to the increased HDT. Similar types of observations have been earlier reported [11, 15].

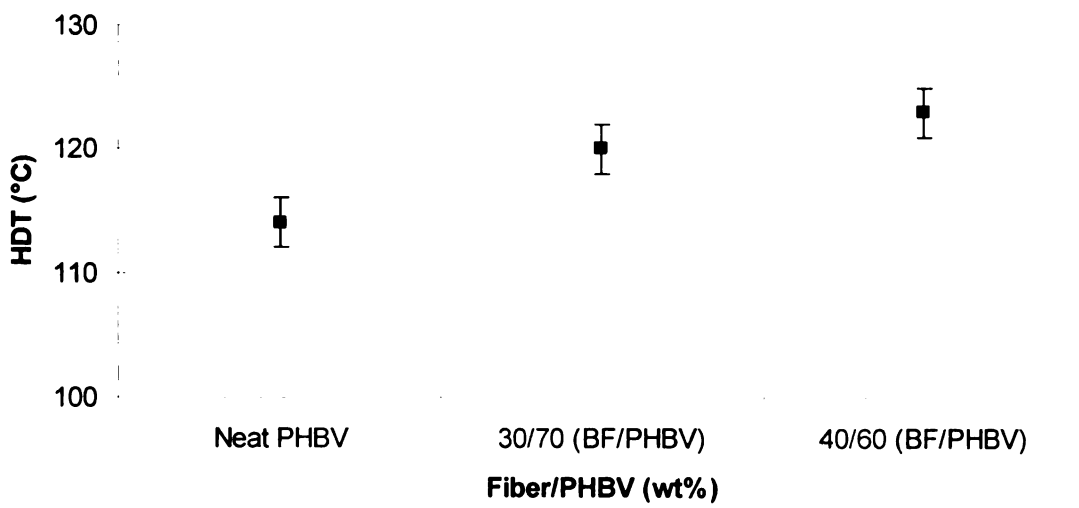

Figure 3.10 : HDT of Bamboo fiber/PHBV composites having 30 and 40 wt% fiber .

3.2.7. Impact Strength

Impact strength depends on various factors like fiber-matrix adhesion, toughness of the matrix and fiber, defects in the packing of fiber/matrix, crystalline morphology, etc. [25]. The notch Izod impact strength test measures the energy to propagate an existing crack. Figure 3.11 depicts the notched Izod impact strength of bamboo fiber composites with PHBV. The impact strength of PHBV (34.3 ± 2.7 J/mt) decreased with the addition of fiber but there was no significant reduction when the fiber content was increased from 30 to 40 wt.%. The higher fiber volume in matrix gave manifold fiber to fiber contact (fiber clustering) with respect to fiber to matrix contact, which did not allow the sufficient fiber matrix interfacial interactions to develop. As seen from the micrograph discussed in the following section majority of the fracture occurred through the fiber rather than through the matrix or the interface of matrix and fiber.

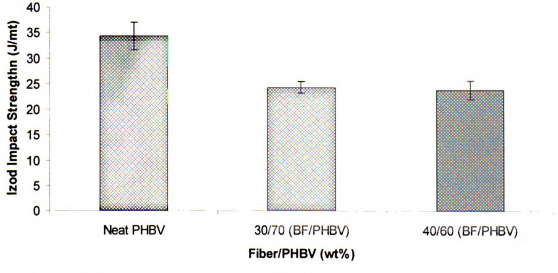

Figure 3.11: Notch impact strength of PHBV/ Bamboo fiber composites at 30 and 40 wt% loading levels.

3.2.8 Morphology

Figure 3.12a and 3.12b shows the micro photographs characterized under SEM at different magnifications of the impact fractured surfaces at 30 wt.% of bamboo fiber composites. The failure modes observed during the fracture were fiber pull-out and fiber breakage. Due to the higher volume fraction of bamboo fiber the majority of the surface could be seen dispersed with the fibers along with the clustering. A number of voids were also visible on the fractured surface that had contributed to the low impact and tensile strength with the fiber loading. Fiber separation in the clusters contributes much lesser to the energy than the fiber pull-outs from the matrix in the total fractured energy during the impact. This was consistent with the observation of low impact strength of the bamboo-PHBV composites, (Figure 3.13). At 40 wt.% fiber content fiber clustering dominated over the fiber matrix adhesion thus giving insufficient adherence of fiber to matrix which lead easy fiber pull-out and separation during impact. Fiber-matrix adhesion remained below the critical adhesion limit, due to which, the impact energy decreased [26].

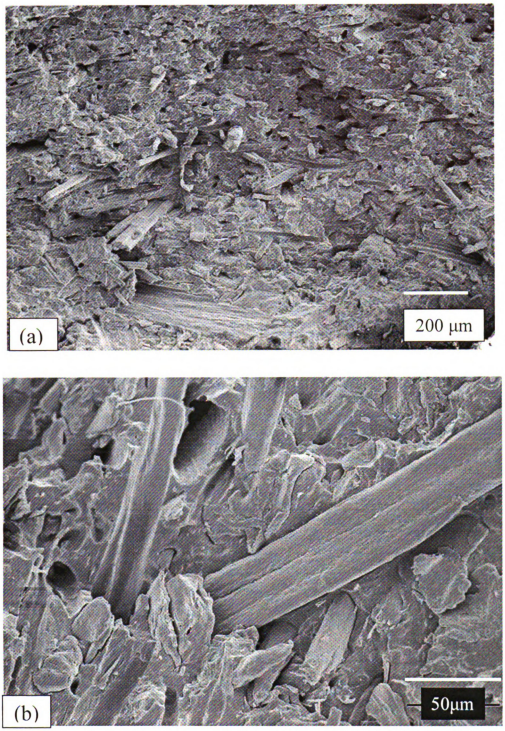

Figure 3.12 SEM photomicrographs of impact-fractured samples of PHBV/Bamboo (70:30) composite: (a) 90×, 200 µm, (b) 450×, 50 µm

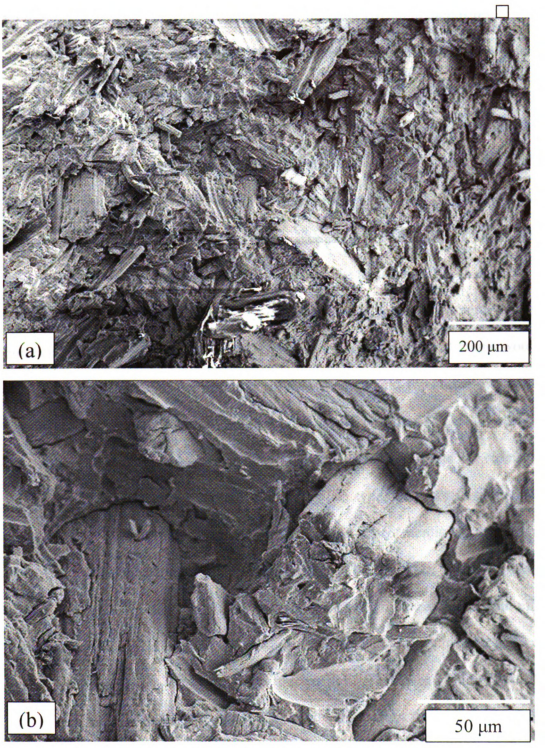

Figure 3.13 SEM photomicrographs of impact-fractured samples of PHBV/Bamboo (60:40) composite: (a) 90×, 200 μm, (b) 500×, 50 μm

3.2.9 Analogy of Bamboo fiber-PHBV and Wood fiber-PHBV biocomposites

There wasn't any significant difference among the tensile properties of bamboo and wood fiber based composites at the same loading level even though the aspect ratios of the two fibers were different (length and diameter of the wood fibers were between 1600-1650 μm and 300-400 μm [15] and that of bamboo fiber were ~500 μm and 10-100 μm, respectively). Table 3.2 lists various mechanical properties of the two biocomposites at 30 and 40 wt.% fiber. The flexural strength of both types of biocomposites remained somewhat unaltered with the addition of fibers up to 40 wt.%, and the modulus in case of wood fiber composites was greater than the bamboo fiber composites by 14 % .This may be due to the higher order stiffness of maple wood fiber versus bamboo fiber. Furthermore, the effect on tensile and flexural modulus of fiber type (wood and bamboo) and loading level (30 and 40 wt.%) of natural fibers in PHBV was statistically analyzed by performing a two-way ANOVA. Table 3.3 represents the F , F critic and P values on the effect of fiber type, their loading level and an interaction of the type and loading levels on the afore mentioned characteristics. ANOVA was performed at a significance level (α) of 0.05. From the above mentioned values, it can be inferred that the type of fiber does not have any significant effect on the elastic and flexural modulus of composites whereas, the fiber loading at 30 and 40 wt% have significant effect on both the moduli. The interaction effect of both parameters on tensile and flexural modulus varies. For the tensile modulus the interaction effect of fiber class and loading was significant but for the flexural modulus it was insignificant. This is consistent with the experimental results because the tensile

properties are more sensitive to the defects (stress concentration) originated during processing or fabrication of the specimens.

Table 3.2: Description of Bamboo and Wood* fiber based PHBV biocomposites properties

wt% of fiber in PHBV matrix	Type of fiber	Tensile Properties		Flexural Properties		Impact Strength (J/mt.)	HDT (°C)
		Strength (MPa)	Modulus (GPa)	Strength (MPa)	Modulus (GPa)		
0 (neat PHBV)	--	21.4	1.02	30.27	1.28	34.3	114
30	Bamboo	18.9	1.71	30.6	2.56	24.28	120
30	Wood	18.08	1.94	31.09	2.72	30.0	135
40	Bamboo	16.74	2.8	29.59	3.26	23.75	123
40	Wood	16.75	2.73	29.97	3.44	24.4	137

* The data of the wood fiber-PHBV composites has been adapted from the earlier publicatior of the authors for the purpose of comparison [15].

Table 3.3: Description of P and F values

	Tensile Modulus			Flexural Modulus		
	P- value	F	F *critic*	P- value	F	F *critic*
Fiber type	0.247	1.41	4.259	0.058	3.95	4.259
Fiber loading	0	235.42	3.402	0	474.23	3.402
Interaction between fiber type and fiber loading	0.031	4.03	3.402	0.386	0.99	3.402

The HDT of the wood fiber biocomposites was greater than that of the bamboo fiber biocomposites by 15 ^{o}C at both the loadings levels, whereas the increase from 30 wt% to 40 wt% was a marginal of 2 ^{o}C in both the natural fibers biocomposites. The difference between the HDT of bamboo and wood fiber composites can be attributed to the more uniform distribution of low density and small fiber size of bamboo fiber which increased the volume of fiber with respect to matrix in the composite. This did not allow the sufficient matrix packing and crystallite size growth as it happened in case of wood fiber based composites. This was supported by the FTIR and DSC analysis depicting the increased crystallinity of wood fiber based composite versus the bamboo fiber based PHBV composite.

From the comparative TGA of both kinds of composites, the thermal stability of PHBV-Bamboo fiber composites was a little more than that of PHBV-Wood fiber composites [15]. The reduced thermal stability of PHBV in presence of wood fiber has earlier been reported in publication [15]. This can be due to the lesser amount of lignin in bamboo fiber than maple wood fiber (table 3.5). The effect of delignification on the mechanical properties of PP based WPC has been reported by Alinaghi et-al [27].

The impact strength of PHBV composites with wood fiber was observed to be higher than that with bamboo fiber. This can be reasoned due to the higher volume fraction of bamboo fiber than wood fiber at same wt.%. As observed from FTIR and DSC results, low crystallinity in the bamboo fiber biocomposites may had resulted the lower impact strength than the wood fibers biocomposites. Wood fiber surface gave a nucleation growth effect thus giving a better embedment of fiber in the matrix.

Figure 3.14 are the photomicrographs at higher magnification of composites depicting the fibers embedded in the matrix and its wettability on the fiber surface indicating the similar interfacial interactions existing between the two different lignocellulosic fiber and PHBV matrix.

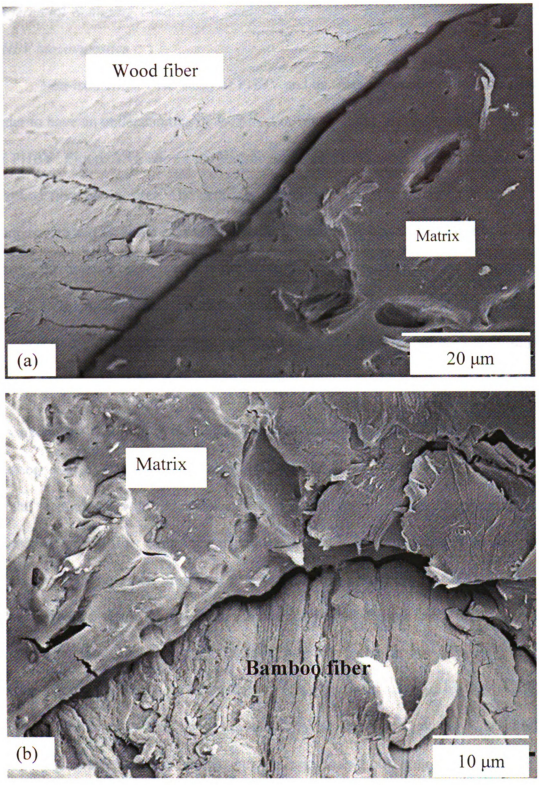

Figure 3.14: SEM Photomicrographs at high magnification (a) PHBV/ Wood fiber composite 1500X , 20 μm(b) PHBV- Bamboo fiber composite, 2300X, 10

Differential Scanning Calorimetry analysis of Bamboo fiber-PHBV and Wood fiber-PHBV biocomposites.

Non-isothermal DSC study of PHBV and its fiber composites was carried out in order to have an understanding of the effect of fibers on the nucleation and crystallinity of PHBV. Figure 3.15 shows the thermograms of PHBV and its 30 wt.% wood and bamboo fiber composites. The details are given in Table 3.4 where T_m is the melting temperature and H_c is the cold crystallization enthalpy. A bimodal endotherm of PHBV during the heating cycle is due to the crystallization phenomena of the heterogeneous crystal morphology formed during processing. Renstad et. al [28] have carried out a detailed study of this. Embedding the fibers in PHBV does not vary its melting point which remains at 154 ^{o}C for both kinds of fiber composites. The enthalpy of melting or crystallization (H_f) in both the cases of fibers composites remains same, thus depicting the degree of crystallization was unaffected by the type of fiber in the PHBV. Mergence of the second peak with the primary peak of PHBV was an observable phenomenon in 30 wt.% bamboo fiber composite which was absent in 30 wt.% wood fiber composite. The fine bamboo fiber interferes in the crystal morphology of PHBV during the processing as a result the nucleation growth of PHBV became more homogenized in presence of fine and uniformly blended bamboo fibers in the matrix. Spherulite homogenization of PBS in presence bamboo fiber had been reported by Kori et. al [29] .High volume fraction of bamboo than wood fiber at same wt.% may have increased the nucleating density of the matrix but no appreciable difference between the net crystallinity of both types of composites was observed. It is to be noted that no such effect was noticed at 40 wt.%. The melt crystallization temperature (T_c) of PHBV was

observed to be 101 °C. The addition of 30 wt.% wood fiber increased this temperature to 104 °C, whereas the bamboo fiber decreased it to 99 °C; indicating an increase in the rate of crystallization in the presence of wood fiber and decrease in the case of bamboo fiber. This may be due to slower diffusion of molecular chains though the well dispersed bamboo fiber to the nucleus thus decreasing the crystallinity rate in case of bamboo fiber composite. (Figure 3.15) Similarity in the melt crystallization peaks of PHBV and its fibrous composites during cooling provided the evidence of having any divergence in their crystalline morphologies.

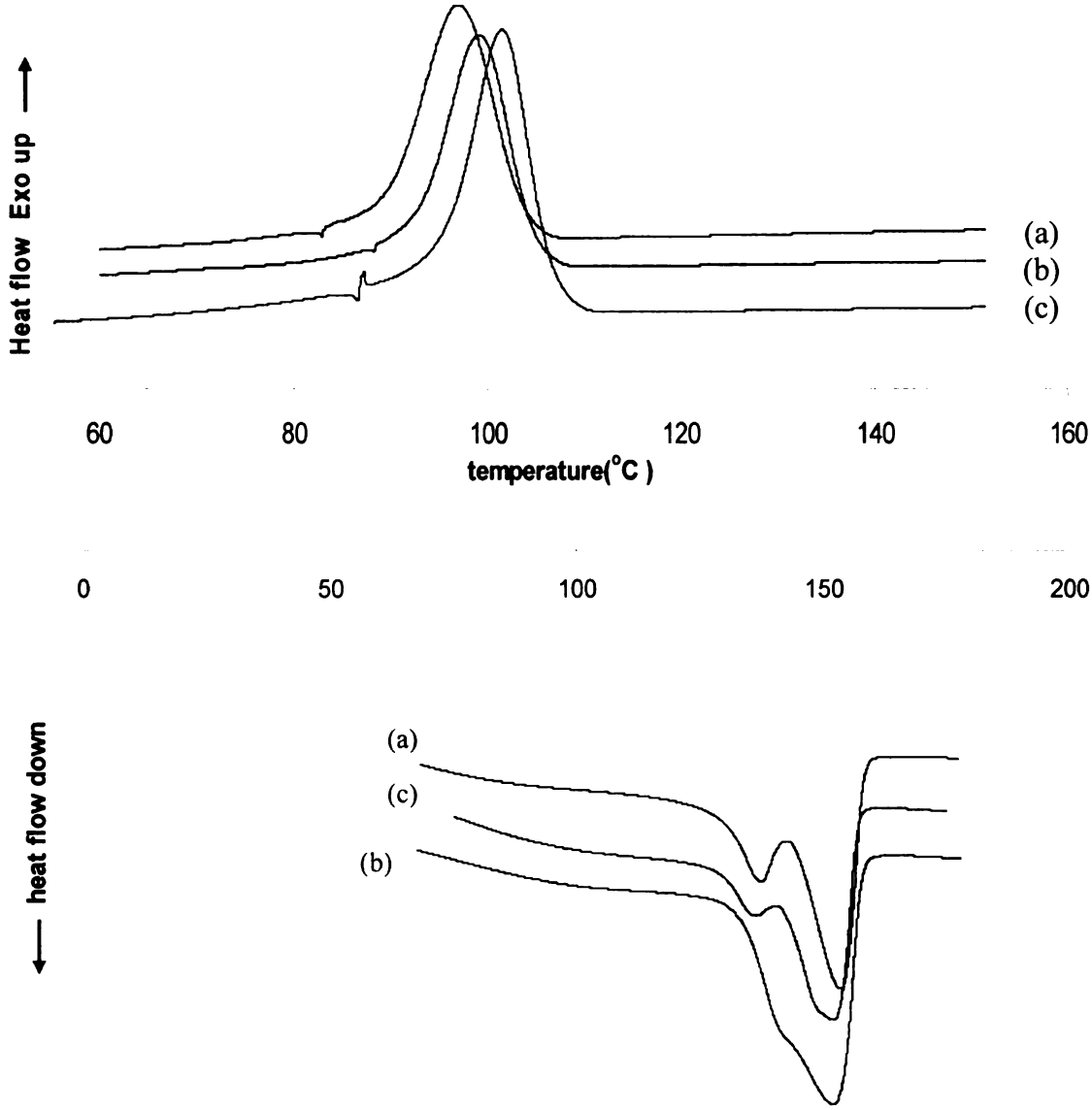

Figure 3.15: Crystallization and melting curves of (a) PHBV (b) PHBV/Bamboo fiber (70:30) composite (c) PHBV /Wood Fiber (70:30) composite

Table 3.4: Detailed Information Obtained from Differential Scanning Calorimetry of PHBV and its Composites

	T_m (^oC)	H_f(J/g)	T_c(^oC)	H_c(J/g)
PHBV	154	57.25	101.4	48.6
PHBV-Wood fiber (70:30)	153.3	63.28	104.3	35.47
PHBV-Bamboo fiber (70:30)	152.9	62.29	99.1	30.52
PHBV- Bamboo fiber (60:40)	152.7	59.44	97.2	28.92

FTIR of the bamboo and wood fiber were carried out to determine an estimate of their contents and composition. Figure 3.16 shows FTIR spectra of wood and bamboo fibers (described peaks marked with arrows). The region around 3400 cm^{-1} depicted hydrogen bonded O-H stretching and at 2900 cm^{-1} C-H stretching. The peak at 1740 cm^{-1} was the C=O stretch in hemicelluloses present in both lignocellulosic fibers. 1505 and 1600 cm^{-1} are characteristic peaks of lignin which arises due to the aromatic skeletal vibration of benzene ring in lignin. The peak at 1600 cm^{-1} has a contributions from the conjugated C=O group along with aromatic skeletal stretch [30]. The ratio of the two (1505 cm^{-1} to 1600 cm^{-1}) gives some qualitative aspects of the two different types of lignins present in different kinds of natural fibers. Similar spectrums of wood and bamboo fiber suggested the presence of same proportion of cellulose, hemicellulose and lignin in both types of natural fibers, as supported in the literature [30]. Composition of lignin and cellulose in both fibers are listed in Table 3.5 [31]. Wood fiber composites had a higher *CI* values (0.95) than bamboo fiber composites at 30 wt.% fiber content indicating greater crystallinity of PHBV in presence of wood fiber than bamboo Similar results were noticed at 40 wt.% fiber content in both type of composites [15].

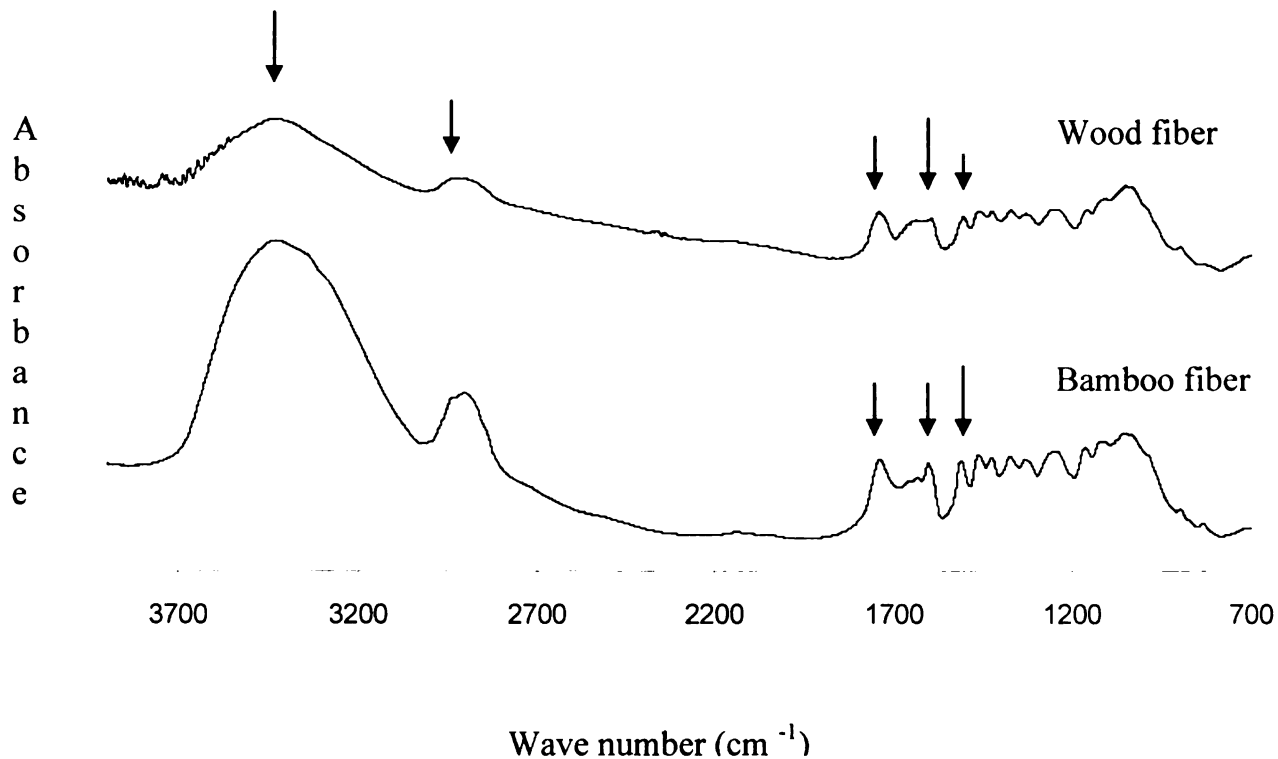

Figure 3.16: FTIR spectra of wood and bamboo fiber

Table 3.5*: Lignin and Cellulose content of Wood and Bamboo fiber

Fiber Type	Lignin (%)	Cellulose (%)
Wood	38-49	23-30
Bamboo	21-31	26-43

* Reference [31]

3.3 Conclusions

Biocomposites from a bamboo fiber and poly(hydroxybutyrate-co-hydroxyvalerate) (PHBV) were fabricated using extrusion followed by injection molding. Tensile and flexural modulus of this biocomposite increased with fiber loading. The storage modulus also improved with fiber addition and no appreciable difference among the two compositions (30 wt.% and 40 wt.% fiber) was noticed. Comparative analysis of two different type of lignocellulosic fiber (wood and bamboo) at 30 and 40 wt.% fiber loaded biocomposites were studied with respect to their mechanical, thermomechanical, thermal, FTIR and morphological aspects. Both types of lignocellulosic fibers embedded in the PHBV matrix gave an appreciable rise in tensile and flexural modulus. Statistically, there was no effect of the fiber type on mechanical properties of composites. A difference between the net crystallinity of both types of composites with different fibers was observed in differential scanning calorimetry (DSC) and infrared spectroscopy (FTIR). Notch impact strength of PHBV decreased with the fiber addition and the reduction was greater in case of bamboo fiber composites. No effect of the fiber type on the thermal stability of composites was present, but incorporation of wood fiber gave a higher heat deflection temperature (HDT) versus the bamboo fiber. Scanning electron microscopy (SEM) photomicrographs demonstrated the existence of similar kinds of interfacial interaction between the two types of fibers and PHBV

3.4 References

1) Karus M, Ortmann S, Vogt D. Use of natural fibers in composites in the German automotive production 1996 till 2003 (2004-10); http://www.nachwachsende-rohstoffe.info (date accessed: 12/4/06).

2) Ferrer FM, Vilaplan F, Greus AR, Borras AB, Box CS. Journal of Polymer Science 2006; 99 : 1823-31.

3) Huda MS, Mohanty AK, Drzal LT, Shut E, Misra M. Journal of Materials Science 2005; 40: 4221 – 4229.

4) Rana AK, Mitra BC, Banerjee AN. Journal of Applied Polymer Science 1999; 71: 531–539.

5) Lu JZ, Negulescu I I, Wu Q. Composite Interfaces 2005; 12:1-2:125–140.

6) Yeh, Shu-Kai, Casuccio, Mary E, Al-Mulla, Adam. Annual Technical Conference - Society of Plastics Engineers 2006; 64: 209-213.

7) Khalil HPSA, Shahnaz SBS. Journal of Reinforced Plastics and Composites 2006; 25:12: 1291.

8) Luzier WD. Proc. Nati. Acad. Sci. USA. Feb.1992; 89: 839-842. (Colloquium Paper).

9) Williams SF, Martin DP, Horowitz DM, Oliver P, Peoples. International Journal of Biological Macromolecules 1999; 25: 111–121.

10) Dufresne A, Dupeyre D, Paillet M. Journal of Applied Polymer Science 2003; 87: 1302–1315.

11) Bhardwaj R, Mohanty AK, Drzal LT, Pourboghrat F, Misra M. Biomacromolecules 2006; 6: 7: 2044-2051.

12) Fernandes EG, Pietrini M, Chiellini E. Biomacromolecules 2004; 5: 4: 1200-1205.

13) Kitagawa K, Ishiaku SU, Mizoguchi M, Hamada H, in Natural fibers, Biopolymers, and Biocomposites, Edited by Mohanty AK, Misra M, Drzal LT. Taylor and Francis 2006.

14) Yongli M, Xiaoya C, Qipeng G, Journal of Applied Polymer Science 1997; 64: 1267–1273.

15) Singh S, Mohanty AK, Wood fiber reinforced bacterial bioplastic composites: Fabrication and performance evaluation. Composites Science and Technology 2007; 67 (9): 1753-1763.
16) Berlin AA, Volfson SA, Enikolopian NS, Negmatov SS. Principles of Polymer Composites. Springer-Verlag. Berlin Heidelberg; 1986.

17) Christensen R. Mechanics of Composite Material. John Wiley & Sons. New York; 1979.

18) Deshpande A P, Rao MB, Rao CL. Journal of Applied Polymer Science 2000; 76; 83–92.

19) Rajulu AV, Chary K, N, Reddy GR, Meng YZ. Journal of Reinforced Plastics and Composites 2004; 23: 127.

20) Padermshoke A, Katsumoto Y, Sato H, Ekgasit S, Noda I, Ozaki Y. Polymer 2004; 45: 6547–6554.

21) Suthar V, Pratap A, Rawal H, Bulletin of Material Science 2000; 23: 3: 215–219.

22) Hong SG, Chen WM. e-Polymers 2006; 024: (www.epolymers.org , ISSN 1618-7229)

23) Gatenholm P, Mathiasson A. Journal of Applied. Polymer Science 1994; 51: 1231–7.

24) Takemori MT, Polymer Science Engineering 1979; 19: 15: 1104–9.

25) Kamdem P, Jiang HC, Freed JW, Matuana ML. Composite: Part A 2004; 35: 347–55.

26) Agarwal BD, Broutman LJ, Analysis and performance of fiber composites. John Wiley and Sons. New York.1980.

27) Alinaghi K, Saleh N, Ismaeil G, Mehdi T, Ghanbar E. Journal of Applied Polymer Science 2006; 102: 4759–4763.

28) Renstad R, Karlsson S, Albertsson AC, Werner PE, Westdahl M. Polymer International 1997; 43: 201-209.

29) Kori Y, Kitagawa K, Hamada H. Journal of Applied Polymer Science 2005; 98: 603–612.

30) Pandey K K. Journal of Applied Polymer Science 1999; 71: 1969–1975.

31) http://www.PaperListeningStudy.org (date accessed 03/03/07)

Chapter 4

Anisotropy and Characteristic Comparison of Short fiber Bioplastic Composites

4.0 Introduction

As discussed in previous chapters, bioplastics are coming up as an effective alternatives to the petro-based plastics in various commercial sectors like packaging, automotive interiors, structural, biomedical applications etc.. Among these, polyhydroxyalkanoates (PHAs), a bacterial sourced bioplastic has found some foot holds in the commercial sector. Significant serious attempts have been made to address the processing, brittleness and cost relating issues of Polyhrdroxybutyrate-co-valerate (PHBV) in past. These issues collectively have been approached either by blending, plasticizing, filling with available cheap fillers, or by altering branching of the molecular chain in order to alter its crystallinity. Fabricating PHBV based composites, using naturally available fiber or wood fiber in order to enhance its performance as a commodity material has been attempted by various researchers. The processing of the composite has been carried out using either of the techniques, compression molding, injection molding or solvent casting. In the short fiber composites, random and uniform distribution of the fibers in a matrix leads to the theoretical assumption of an isotropy in a composite material, with no preferred directional orientation of fibers. But, the anisotropy associated firstly, with the fibers itself [1] and secondly, the alignment or orientations of the fiber during the directional flow of the melt during the melt mixing and injection molding engender an intrinsic anisotropy in the specimens. Therefore, development of the anisotropy, during processing, is unavoidable in short fiber

composites. Anisotropy in short fiber composites can become a governing factor in their performance when the applied stress is not in a favorable direction during the application.

Chao-Ming Lin et al. reported the anisotropic behavior of sheet molding compound from polyester and chopped glass fiber, theromosets during processing with compression molding [2]. In another paper, Ming Tian et al. discuss the influence of two roll mill processing on an anisotropic behavior in mechanical properties of fibrillar silicate /rubber nanocomposites [3]. Bernd Lauke describes a modified rule of mixture to analyze the anisotropic strength of the short fiber composites with respect to the loading direction [4]. Different theoretical and computational analyses of short fiber composites have been made by various authors to relate anisotropy of the composites with their mechanical, thermo-viscoelastic behavior, the fiber ellipticity, and fraction [5-10]. References [11-15] discuss the various aspects of anisotropic behavior of short fiber reinforced polymeric composites associated with their mechanical characteristics.

Wanjun Liu discusses the effect of different processing methods on the kenaf natural fiber reinforced soy based biocomposites [11] and in another kenaf reinforced polypropylene composite Zampaloni elaborates the manufacturing difficulties and associated solutions [12]. None of the published papers until now compare the two different processing techniques, i.e., injection molding and compression modeling of the natural short fiber composites from PHBV in terms of the anisotropy associated with them. This chapter attempts to draw a direct comparison between the compression molded specimens and injection molded specimens of the same composite in terms of

the anisotropy associated with the specimens and their static and dynamic mechanical properties.

4.1 Experimental section

4.1.1 Materials

Polyhydroxybutyrate-co-valerate (PHBV) was obtained from Biomer, Germany with the trade name Biopol (Zeneca Bio Products). Wood fiber used was the maple wood fiber from the American Wood fiber Schofield, WI with the trade name 2010 MAPLE.

4.1.2 Fabrication of composites

Two different processes were used to fabricate PHBV and wood fiber composite with different compositions. Table 1, list the compositions and the fabrication method along with other processing parameters associated with the specific process. The wood fiber and PHBV pellets were dried at a 110 ^{o}C and 80 ^{o}C under vacuum for 2 and 4 hours respectively, to devoid of any moisture during processing.

4.1.2.1 Injection molding

Specimens were fabricated using micro-compounder, (manufactured and designed by DSM Research, Netherlands with a barrel volume of 15 cc) and a mini injection molder. This equipment was a co-rotating twin-screw extruder with the length of 150 mm, L/D (length to diameter ratio) 18 and has three consecutive heating zones. PHBV pellets and wood fiber in a fixed composition as listed in Table 1 were physically mixed and fed to the micro-extruder, allowing the two to melt- mix for a fixed time period in the extruder. The processing temperatures of the three consecutive zones were 165, 160 and 155 ^{o}C. The melt from the extruder was collected in a pre heated mini injection (at

a temperature of 155 ^{o}C), and was transferred to a mini-molding machine for specimen fabrication. The optimized injection pressure listed in Table 1 was used to extricate the melt-mix from the injection cylinder to the mold located in the molding machine. Finally, the specimen was removed from the mold and conditioned for 48 hrs before testing.

4.1.2.2 Compression molding

Both, PHBV pellets and wood fiber were physically mixed in a given proportion and spread uniformly within the periphery of 3 mm thick window frame sandwiched between the two heating platens of a Carver Press SP-F 6030 held a 160 ^{o}C. The physical mixture was pre heated for 10 minutes and compressed to a pressure of 800 KPa initially and gradually increased up to 1245 KPa. The sheets were maintained at this pressure for 15 minutes and eventually cooled to room temperature in order to remove from the press. The resulting sheets were 2.7 mm thick and 11X 11 square inches in area. The testing specimens for the appropriate test were cut from the sheets as per the dimensions listed in the next section.

Table 4.1: Processing parameters of PHBV and PHBV-Wood fiber composite

Composition	Injection Molding			Compression molding	
	Injection Pressure (KPa)	Processing time (minute)	Processing temperature (^{o}C)	Compression pressure (KPa)	Processing time (minute)
Neat PHBV	552	3	160	-	-
Wood fiber-PHBV (30-70 wt %)	825	6	160	1245	15

4.1.3 Testing and characterization

4.1.3.1 Mechanical properties

Tensile and flexural properties of specimens were tested using a United Calibration Corp. SFM 20 testing machine as per ASTM D638 and ASTM D790 standards, respectively. The system controls and data analysis were performed using Datum software.

4.1.3.2 Dynamic mechanical analysis (DMA)

The storage modulus, loss modulus and tan delta of the test specimens were evaluated using DMAQ800 supplied by TA Instruments. The specimens were heated from -30 to 125 ^{o}C with a heating rate of 2 ^{o}C/min. Single cantilever mode was used to test the specimens at an oscillating amplitude of 15 μm and a frequency of 1 Hz.

4.1.3.3 Anisotropy analysis

4.1.3.3.1 Squeeze flow test:

This test was done to determine the developed orientations of wood fibers in the specimens during injection or compression molding process. In case of injection molding, three circular discs of 13 mm diameter were incised from three different sections of the 4 mm thick specimen, i.e. gate area, middle portion and the far off end section of the specimen. In case of compression molded samples, 25 mm diameter discs were incised from the different areas of the compression molded sheet of thickness 3 mm. These discs were marked with an axis corresponding to zero degree direction and positioned at the center between two teflon sheets. Teflon sheets and disc was sandwiched between two smooth surface steel plates and this whole unit was placed between the pre heated platens at 160 ^{o}C, i.e., the thermoforming temperature. After

attaining an equilibrium temperature for 1 minute platens were compressed with a load of 500 lbs for 60 seconds. The part was unloaded and allowed to cool immediately at room temperature within the mold ensuring that it retains the deformed shape. An illustration of the test along with the pre and post shapes of specimens is given in Figure 4.1 on next page.

4.1.3.4 Morphological studies

Morphological studies were conducted using a JEOL scanning electron microscope (model JSM-6400). Specimens were sputter-coated with gold to a thickness of ~10 nm in order to prevent charging during the examination. The SEM used was equipped with a lanthanum hexaboride (LaB_6) crystal as a source of electrons. An accelerating voltage of 13 KV was used to collect SEM images.

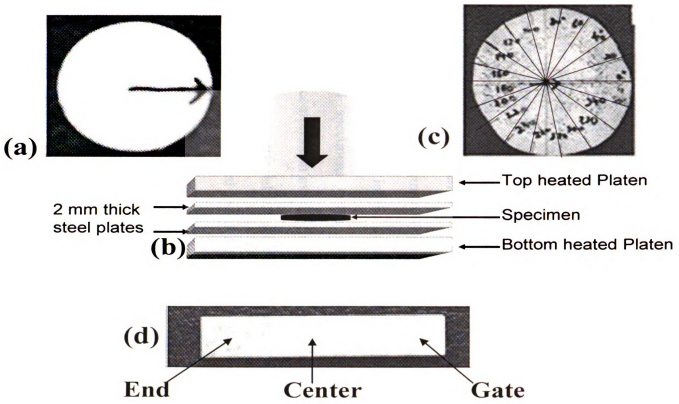

Figure 4.1: (a) Squeeze flow test specimen before test (b) Schematic of squeeze flow test (c) Squeeze flow test specimen after test (d) Section illustration of injection molded specimen.

4.2 Results and Discussion

4.2.1 Tensile properties:

Figure 4.2 illustrates the Young's modulus and tensile strength of PHBV and its 30 wt% loaded wood fiber composite with two different processing methods i.e., compression molding and injection molding. The modulus and the strength of the composite were significantly affected by the two different processing methods. The Injection molded specimens show better characteristics than the compression molded specimens. The enhancement in the modulus of injection molding specimens was 104% with respect to the neat PHBV, and practically, no loss in the strength. Where as, in case of compression molded specimens the modulus remained same as of neat PHBV with a significant loss of 50% in the strength. The wood fiber acted as filler in compression molded specimens rather than a reinforcing agent. Lower tensile characteristic of the compression molding composite than the injection molding can be reasoned due to the poor interfacial adhesion of the matrix to the fiber. The mixing of fibers in the matrix was expected to be more uniformed and percolated during the extrusion than the physically mixed and spread fiber during compression molding. More precise reason for the difference among the properties of the two methods as discernible from the SEM micrographs was the entrapment of air in the matrix during the compression molding. The entrapped air did not allow an intricate adhesion of the matrix to the fiber as a result little stress transfer occurred from matrix to fiber during loading conditions. The entrapped air lead to the formation of non-uniform and uneven cell wall foamed like structure of the PHBV matrix, thereby reducing its specific strength, and additionally, contributing to the reduction in strength.

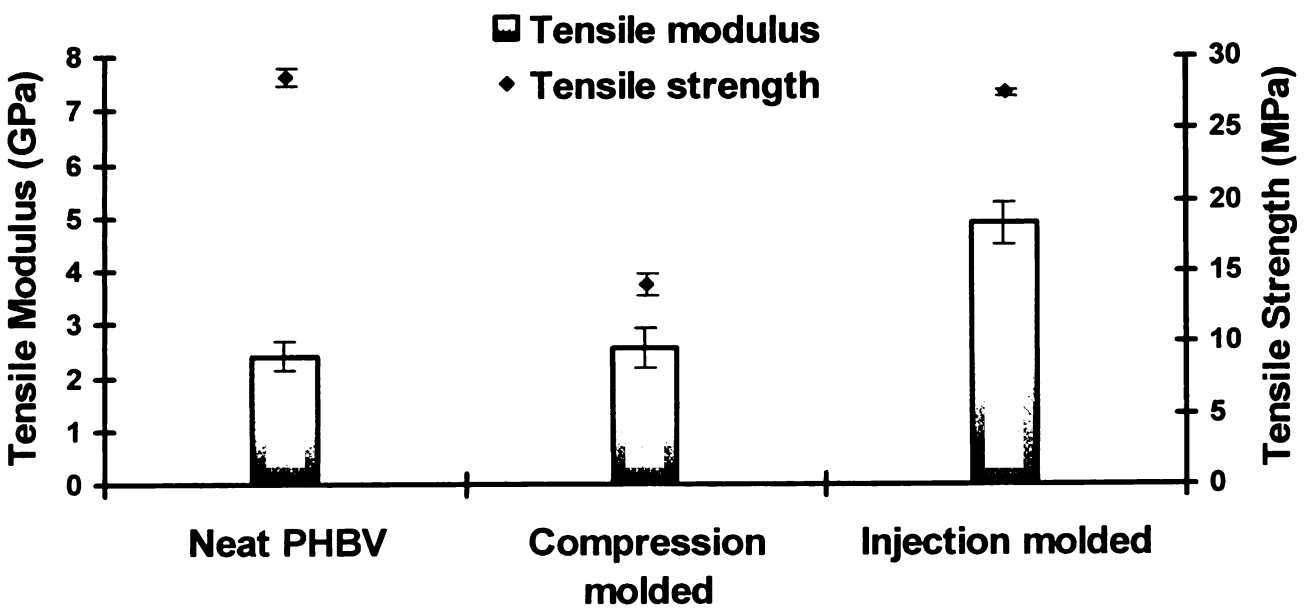

Figure 4.2 Tensile properties of PHBV and its composite loaded with 30 wt% wood fibers.

4.2.2 Flexural Properties:

Flexural properties of composites reflected no different trend than tensile properties with both the different kind of molding processes. In case of injection molding modulus doubled to 4.5 GPa from 2.2 GPa of PHBV with no deflated strength of the composite but precipitously decreased strength and modulus of the compression molded samples. Figure 4.3 show the details of the flexural strength and modulus of 30 wt% wood fiber filled PHBV composite fabricated using both the processes i.e., compression and injection molding process.

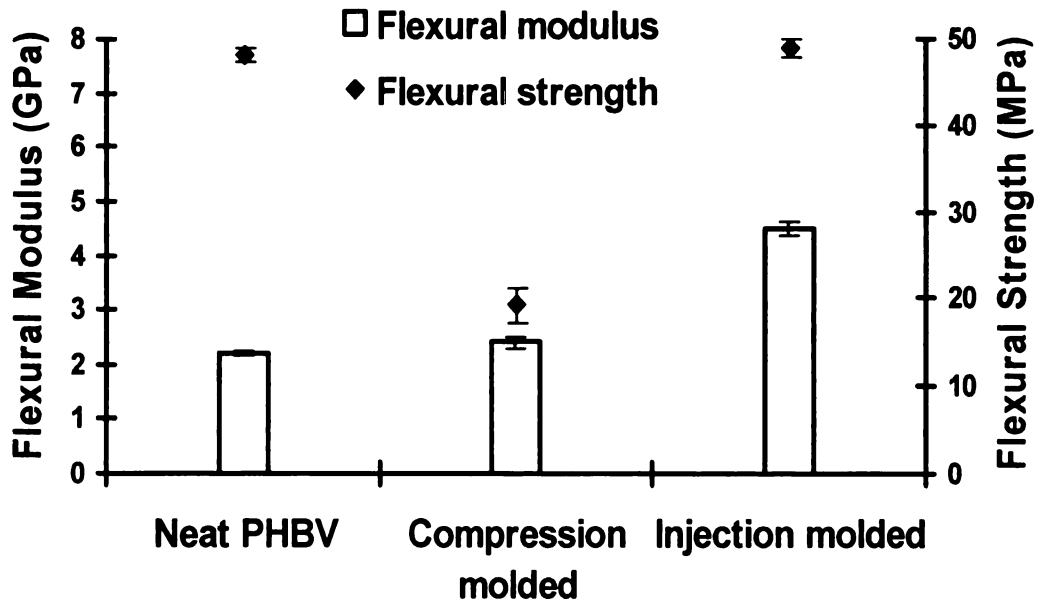

Figure 4.3: Flexural properties of PHBV and its composite loaded with 30 wt% wood fibers

4.2.3 *Dynamic Mechanical Analysis*

Dynamic mechanical analysis was carried out to characterize the fiber matrix interaction in composites. DMA allows a better estimate of interactions occurring at the molecular level of a material. In visco-elastic materials modulus is a complex quantity, which is the sum of elastic and viscous component of a material, and inherently changes with the temperature of the material. The elastic component of the material is described by the storage modulus, and the viscous component by the loss modulus. Figure 4.4 shows the change in storage modulus of composites with the increasing temperature at the rate of 2 ^{o}C/minute. The figure depicts the typical trends as of thermoplastics and their filled composites in these cases. The storage modulus of composites is higher than the neat PHBV because the high rigidity of the fiber induces an additional stiffness to the matrix. The storage modulus of injection molded specimens was higher than that of the compression molded at all the temperature. The increase with respect to neat PHBV of injection molded composite was higher than that of compression molded by 17 % before (at 0 ^{o}C) and 27 % after (at 25 ^{o}C) the glass transition temperature (T_g). This was due to the better compaction of fibers in the matrix of the injection molded composites than the compression molded ones. At a temperature above T_g in rubbery region fibers poses restrictions to the extending molecular chains in the region of influence i.e., matrix around fibers, as a result, the increase in the storage modulus in rubbery region is higher than in the glassy region, where the molecular chains are virtually immobile. In case of injection molded

composites these restriction becomes more predominant as fibers are imbedded more compactly in the matrix than the compression molded specimens.

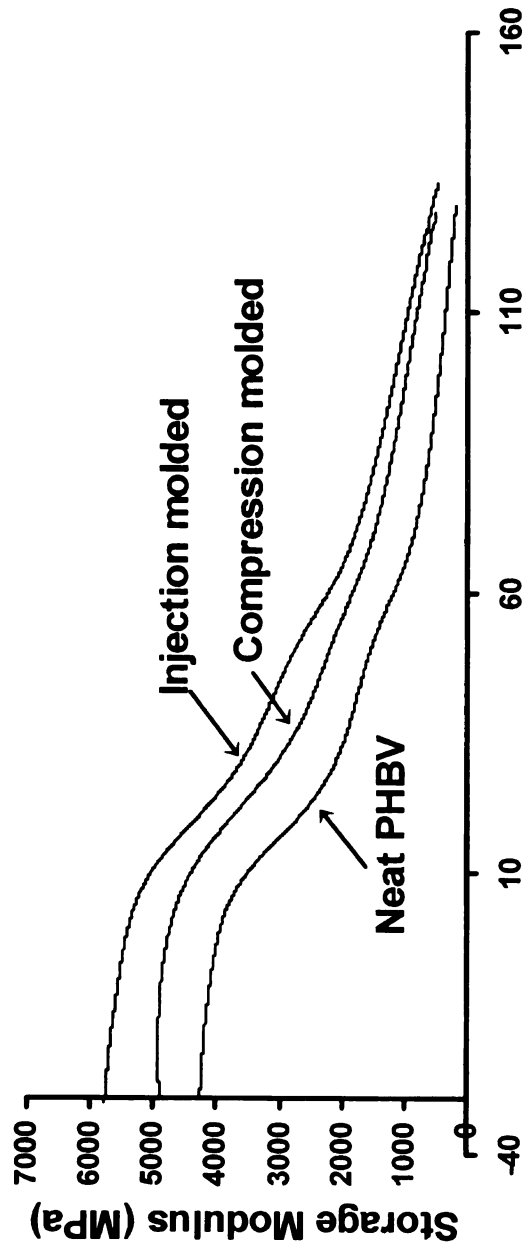

Figure 4.4: Storage modulus of PHBV and its 30 wt% wood fiber loaded composite.

In case of compression molded composites the trapped air in the matrix and the fiber interface provides an ample movement to molecular chain without much restriction imposed by the loosely imbedded fibers thus contributing in low degree to the stiffness. The trapped air in the matrix and loosely held fibers are visible in the SEM micrographs discussed in the forth written section.

Figure 4.5 & 4.6 shows the loss modulus and tan δ variation, respectively with respect to the temperature on x- axis. Loss modulus is the outcome of the loss in irrecoverable energy due to dampening effect of the molecular movements and interactions in the material. A peak of loss modulus vs temperature represents the transition region of the polymeric material from glassy to rubbery state. Dampening effect in the fibrous composite can result from the molecular chain motion in the amorphous phase, fiber-matrix interfacial regions and fiber-fiber frictional interactions in the fiber conglomerated regions. Loss modulus of compression molded composite was higher than the injection molded composite. This can be due to the more amorphous region in the compression molded composite due to morphological heterogeneity in the PHBV matrix because of air entrapment during processing as visible in the SEM micrographs. Another source of dampening was the energy loss due to friction among fibers in the fiber conglomerated regions. Compression molded composites were processed just by physically mixing the fiber and PHBV pellets.

Tan δ is the dampening factor generally decreases with the reinforcement in the composite system. The theoretical decrease in the tan δ value of the composite with respect to neat matrix is by the weight percentage of the reinforcement filler in the

composition i.e., tan δ_c = tan δ_m (1-Φ) where tan δ_c , tan δ_m are the values of composite

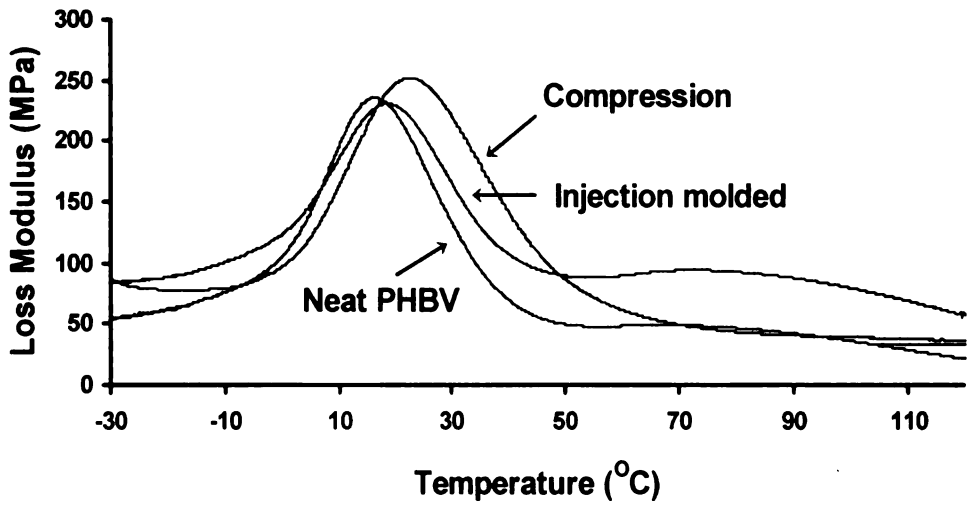

Figure 4.5: Loss Modulus of PHBV and its 30 wt% wood fiber loaded composite

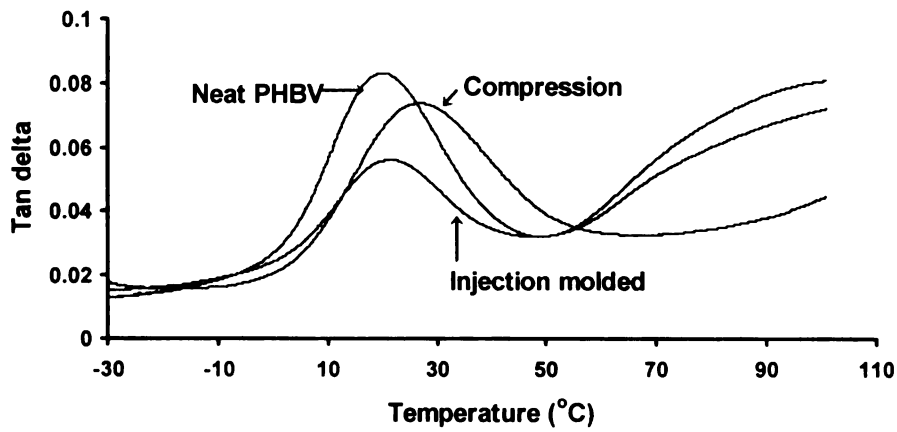

Figure 4.6: Tan δ of PHBV and its 30 wt% wood fiber loaded composite

and matrix respectively, and Φ is the weight fraction of fibers in the composite (30 wt%, Φ =0.3). The experimental decrease in the dampening factor of the injection molded composite was 32% and that in compression molded composites was just 11%. The broadening of the tan δ peak accounts for the widening of the transition region. Figure 6 depicts the broadening of the compression molded tan δ peak more than that of the injection molded composite. High tan δ peak value and wide transition region further confirms the added heterogeneity due to the trapped air and non uniform mixing of fibers in the compression molded composite.

4.2.4 Squeeze flow testing

Short fiber thermoplastic composites are assumed to have random fiber orientation and therefore, behave isotropic. During the fabrication, either by injection molding or by compression molding, short fibers do develop some orientation and impart some directionality to the specimens. In case of injection molding process the melt mix of thermoplastic and fibers flows through the channels of mold and narrow gate opening. Fibers confluence in the thermoplastic melt during the flow tends to develop orientation in the flow direction and adopt that orientation in the cooling stage thus imparting a specific directionality to the specific regions of the same specimen. In case of compression molding, since the manufacturing involve the physical mixing of thermoplastic pellets and fibers, the random orientation distribution of fibers is not guaranteed and fibers may sustain some directionality during fabrication. The goal was to determine these inherently developed orientations during both fabrication processes. A similar kind of anisotropy study of natural fiber filled thermoplastic composites had been done by Zampaloni et al [17,18]

A squeeze flow test as illustrated in the previous section was utilized to determine the fiber orientation of the wood fiber reinforced PHBV for injection and compression molding composites. An ideal isotropic short fiber composite disc deformed or compressed would result in a circular shape after the completion of compression process. Otherwise, a non circular shape or elliptical shape if obtained confirms the assumption of the directionality associated with the fiber orientations in the thermoplastic matrix. This is due to the flow velocity and strain rate within the matrix not being constant with respect to the fiber orientations described by angle "Θ". A polar coordinate system was used to assign the marking on the compressed discs with an increment of 20^0 starting with 0^0 marked initially, before the compression. The length of the lines from center to periphery of the compressed samples were recorded and plotted against the marked angles as shown in figure 4.1. For an ideal circularly deformed sample this plot must be a straight line. The squeeze flow test was performed on 20 wt% and 40 wt% wood fiber loaded injection molded composites and 30 wt% wood fiber loaded compression molding composite. Two different compositions were taken in case of injection molded process in order to show the significant effect of fiber loading on the inherently developed anisotropy of the composite.

Figures 4.7 and 4.8 shows the squeeze flow tests of 20 and 40 wt% wood fiber loaded PHBV injection molded composites. These plots are utilized to determine the preferred orientations of fibers by observing the trends of maxima and minima along the X axis i.e., angle. The test was performed on the three different sections of specimens as specified before. From the comparison of both the compositions it was

observed that the length change with respect to the angle in 20 wt% wood fiber samples is less variant

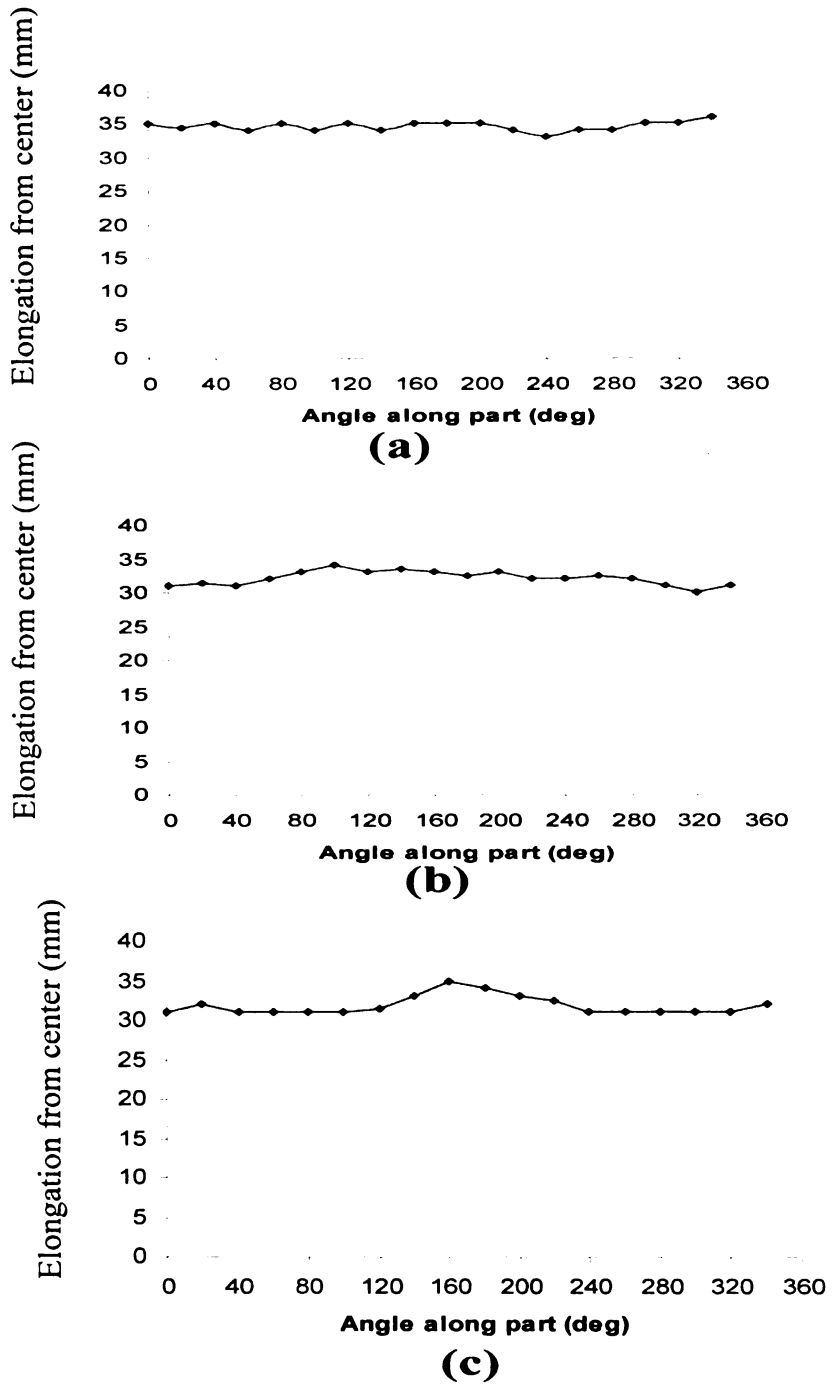

Figure 4.7 Squeeze flow test plots of 20 wt% fiber loaded injection molded composites (a) Gate section, (b) Center section, (c) Far off end section

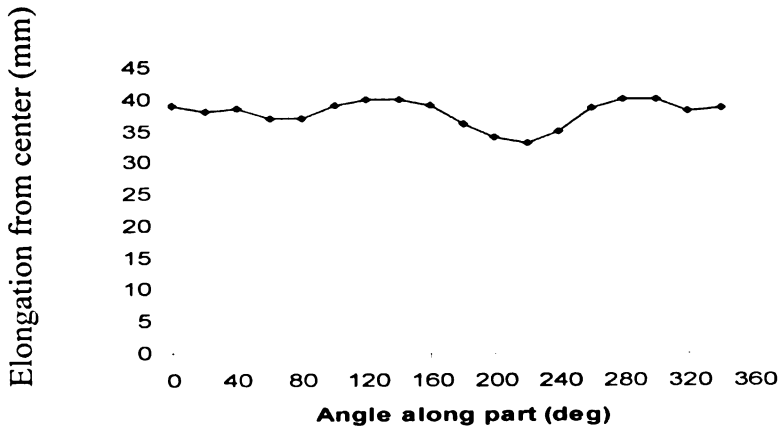

(a)

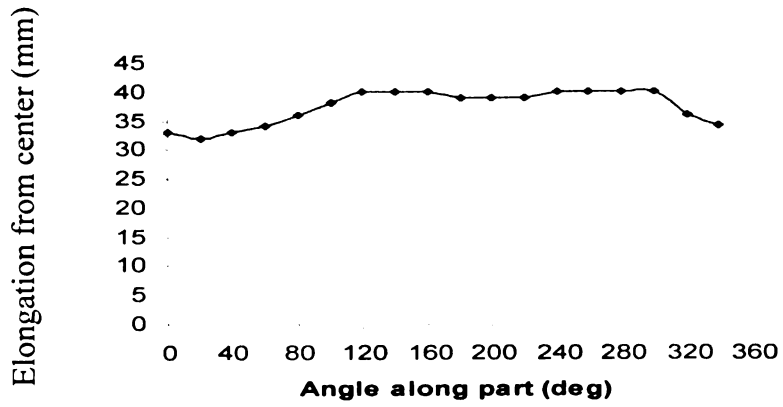

(b)

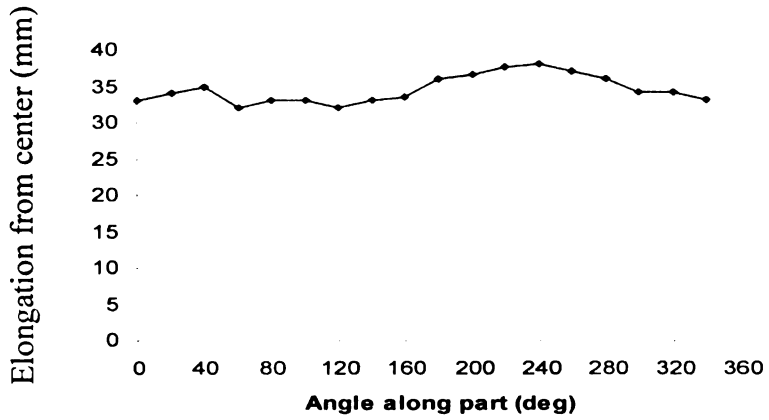

(c)

Figure 4.8 Squeeze flow test plots of 40 wt% fiber loaded injection molded composites (a) Gate section, (b) Center section, (c) Far off end section.

than in the 40 wt% at all the three sections of the specimen i.e., gate, middle and far off end. This was due to uneven resistance offered by fibers at higher concentration to the thermoplastic melt flow and this gives a quantified estimate of the directionally orientated distributions of fibers at certain angles. In other words, the certainty to obtain a complete randomly oriented distribution of fiber at higher concentration in a reinforced PHBV during injection molding was low. The squeeze flow tests at the three sections of the specimen of each composition independently, (Figure4.7 (a, b, c) and 4.8(a, b, c)) were performed in order to examine the uniform random distribution of fibers in the bulk of the specimen. The channeled flow of melt during the injection molding causes a set of fibers to directionally align differently in different sections of the same specimen. Investigating all the three sections (i.e., gate, center, far off) of the specimen, it was evident from the plots that the change in lengths with respect to angles differs from section to section. The trends of maxima and minima in any of the section were not similar to the either of the other two sections. Had the fiber orientation been similar through out the bulk of the specimen the plots of all the sections would be similar to one another or a straight line in case of the randomly distributed fibers. A close observation reveal an analogous underpinning trends in the maxima and minima's of the corresponding sections of the two compositions i.e., 20 wt% and 40 wt% fiber loading. This signifies that fibers take up similar orientations in the corresponding sections of both compositions irrespective of the concentration.

Figure 4.9 shows the squeeze flow test of compression molded specimens at 30 wt% fiber loading in PHBV. The plot of length change versus angle is linear to some extent, which concludes the absolute random distribution of fiber orientations in the

compression molded samples although the specimens were prepared by the physical mix-ups of fibers and pellets. From the analysis it was observed that the compression molded PHBV-wood fiber composite exhibit more isotropic characteristic than the injection molded.

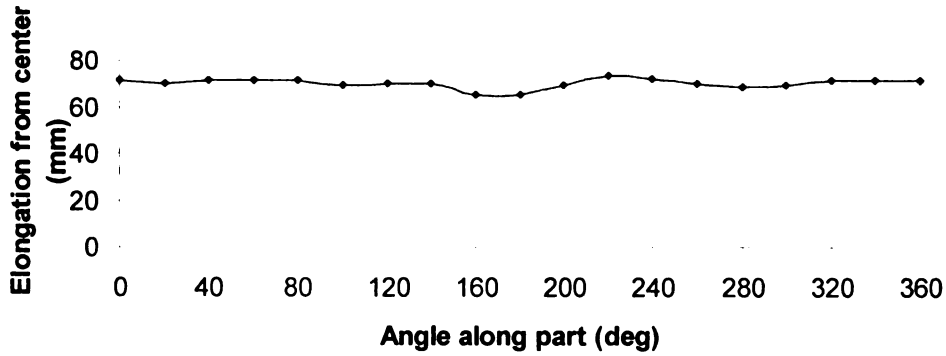

Figure 4.9 Squeeze flow test plots of 30 wt% fiber loaded compression molded composites

4.2.5 Morphology

Figure 4.10 and 4.11 are the SEM micrographs of 30 wt% wood fiber filled PHBV composites processed by compression and injection molding, respectively. Air channels developed due to air entrapment in the matrix during the processing were observed in the compression molded composite which were not evident in the injection molded specimens. At a higher magnification more inadequate interfacial contact between the fiber and the matrix was observed in case of compression molded than injection molded composite. Air entrapment and poor interfacial contact were primarily responsible for the lower tensile and flexural properties of compression molded composite.

4.3 Conclusion

Short wood fiber–PHBV composites were fabricated using two different molding processes i.e., injection molding and compression molding. These were characterized for the static and dynamic mechanical properties and isotropic characteristics. Injection molded composite had a better reinforcing effect from the wood fibers than compression molding. This was evident from the better tensile and flexural properties of injection molded composite which gave an improvement in young's modulus and flexural modulus by 104%. High elastic modulus and low dampening effect apparently suggested the same during dynamic mechanical analysis. Morphological observations carried out using SEM to study the fiber matrix interaction revealed poor adhesion and air entrapment in compression molded specimens. Anisotropy study carried out using squeeze flow test of both the molding processes

indicated the anisotropic behavior of injection molded specimens. Anisotropy varied with the sections of the specimens and composition of wood fiber in the composites.

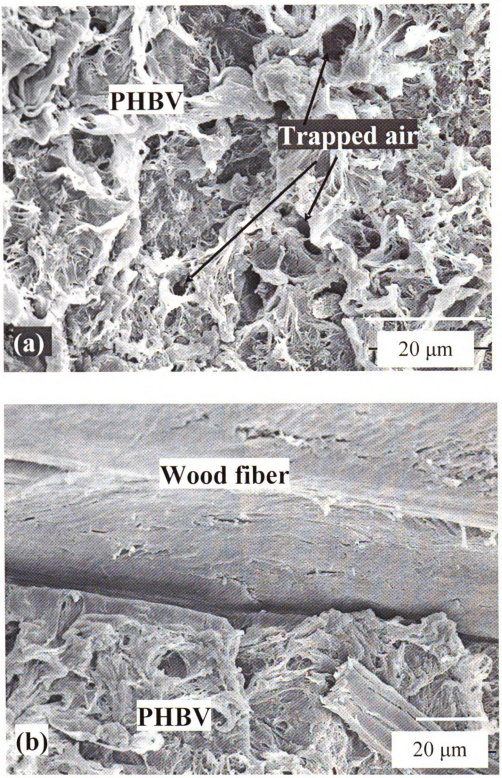

Figure 4.10: SEM micrographs of 30 wt% wood fiber loaded PHBV compression molded composite (a) 100X 20 μm (b) 1700X 20 μm

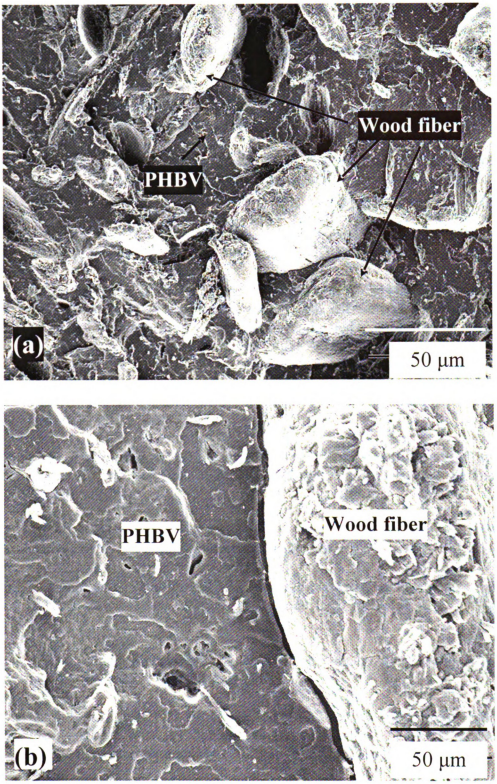

Figure 4.11: SEM micrographs of 30 wt% wood fiber loaded PHBV injection molded composite (a) 60X 500 µm (b) 500 X 50 µm

4.4 Reference

1. F.R. Cichocki Jr., J.L. Thomason, Thermoelastic anisotropy of a natural fiber, Composites Science and Technology 62 (2002) 669–678

2. Chao-Ming lin and Cheng-I Weng, Anisotropy in Sheet Molding Compounds During Compression Molding polymer composites, October 1997, 18, 5.

3. Ming Tian, Lijun Cheng, Wenli Liang, Liqun Zhang The Anisotropy of Fibrillar Silicate/Rubber Nanocomposites Macromol. Mater. Eng. 2005, 290, 681–687.

4. Bernd Lauke, Shao-Yun Fu, Strength anisotropy of misaligned short-fibre-reinforced polymers, , Composites Science and Technology 59 (1999) 699±708.

5. A. Tounsi, E. A. Adda Bedia and A. Benachour, A New Computational Method for Prediction of Transient Hygroscopicwith Different Degrees of Anisotropy Stresses during Moisture Desorption in Laminated Composite Plates, *Journal of Thermoplastic Composite Materials* 2005; 18; 37.

6. Ning Pan, Analytical characterization of the anisotropy and local hetrogenity of short fiber composites: Fiber Fraction as variable, Journal of composite Materials, 28,16, 1994.

7. P. S. Theocari & C. B. Demakod' The effective anisotropy of short-fiber composites due to fiber ellipticity, *Composites Science and Technology 57 (1997)*, 677-685.

8. M. H. Santarecomposites, Anisotropic effective moduli of cracked short-fiber reinforced R. S. Feltman, Journal of Applied Mechanics, 1999, Vol. 66, 709.

9. E. Kontou *, A. Kallimanis Thermo-visco-plastic behaviour of fibre-reinforced polymer composites, Composites Science and Technology 66 (2006) 1588–1596.

10. J.Beten, Creep damage and life analysis of anisotropic materials, Archives of applied mechanics 71, 2001, 78-88

11. G. V. Kozlov,1 A. I. Burya,2 G. E. Zaikov1,Anisotropy of a Fiber Structure and the Frictional Wear of Composites on the Basis of Polyarylate, Journal of Applied Polymer Science, Vol. 100, 2821–2823 (2006)

12. Yuanxin Zhou, P.K. Mallick Fatigue Performance of an Injection-Molded Short E-Glass Fiber-Reinforced Polyamide 6,6. I. Effects of Orientation, Holes, and Weld Line, POLYMER COMPOSITES—2006

13. Xin-Xing Zhang, Can-Hui Lu, Mei Liang, Preparation of Rubber Composites from Ground Tire Rubber Reinforced with Waste-Tire Fiber Through Mechanical Milling Journal of Applied Polymer Science, Vol. 103, 4087–4094 (2007)

14. A. Godara, D. Raabe Influence of fiber orientation on global mechanical behavior and mesoscale strain localization in a short glass-fiber-reinforced epoxy polymer composite during tensile deformation investigated using digital image correlation Composites Science and Technology 67 (2007) 2417–2427

15. Marie-Laure Dano, Guy Gendron, François Maillette and Benoît Bissonnette Experimental Characterization of Damage in Random Short Glass Fiber Reinforced Composites, *Journal of Thermoplastic Composite Materials* 2006; 19; 79

16. Wanjun Liu, L. T. Drzal, A. K. Mohanty, M. Misra, Influence of processing methods and fiber length on physicalproperties of kenaf fiber reinforced soy based biocomposites, Composites: Part B 38 (2007) 352–359

17. M. Zampaloni, F.Pourboghart, Kenaf natural fiber reinforced polypropylene composite: A discussion o manufacturing problems and solutions, Composites :Part A 38, 2007, 1569-1580.

18. M. Zampaloni, A multiple fiber orientation constitutive model for fiber mat reinforced thermoplastics with a random orientation applied to the stamp thermo-hydroforming prcess. PhD Dissertation , Michigan State University, 2003.

Chapter 5

Hybrid Green Composite from Talc, Wood Fiber and Bioplastic: Fabrication and Characterization

5.0 Introduction

As discussed in previous chapters, certain limitations of PHBV like, its narrow processing temperature range, thermal degradability, low toughness, and post crystallization phenomena does not allow to render its capability to perform as a material for the desired applications in structural, packaging, automotive and other sectors. Natural or wood fiber reinforcement of PHBV matrix was a step forward in the direction to improve its performance, while retaining biodegradability of the material. The abundance, economical, renewable, environment friendliness, and easy assimilation to the processing techniques make these as a sustainable reinforcing agent in the plastics. Inorganic particulate (clay, talc, $CaCO_3$) reinforcement in plastics is a common practice to improve the mechanical properties of plastic in a composite industry. Talc is a 2:1 layer phyllosilicate mineral with $Mg_3(Si_4O_{10})$-$(OH)_2$ as the unit structure. Talc alone or in combination with other particulate filler has been used as reinforcement in certain thermoplastics like polypropylene, nylon to improve upon their stiffness, tensile strength, creep resistance, and deformation temperature. In addition to these, talc reduces shrinkage, enhances scratch hardness and surface quality of the final product [1-7]. Its low cost and ease of use during processing makes it a profitable material to the processing industry. The major drawback of talc is that it limits the

ductility and eventually reduces the toughness of the thermoplastic. Its high density (~ 2.5-2.7 gm/cm^3) increases the weight to volume ratio of its composite, when used in a significant amount as a second constituent. In composites, surface wettability is the crucial parameter responsible for the interaction between talc particles and the polymer matrix. Gillian et al. reports the water contact angle of talc as 90^0 , and some other researchers within a range of 60 to 90^0 , thus, characterizing it as a hydrophobic material [8].

The objectivity of this research focuses to develop a completely biodegradable hybrid biocomposite consisting of talc and wood fibers in PHBV. Talc and PHBV have similar water contact angles; therefore both have similar hydrophobic surface nature. High surface energy of talc surface allows the wettability of PHBV and its miscibility leading to subsequent reinforcement of talc platelets in PHBV matrix. The talc reinforcement provides an additional benefit of cost, as the low cost talc replaces PHBV in the system. The increased density of the talc and PHBV system can be counter balanced by surrogating the certain proportion of talc with wood fiber, thereby, leveling the density of the composite to certain extent. This hybrid system of mineral and wood fiber, when reinforced in a bioplastic, i.e. PHBV, is expected to be completely biodegradable as all the components of the composite system are sourced naturally and are independently, biodegradable.

5.1 Experimental section

5.1.1 Materials

Polyhydroxybutyrate-co-valerate (PHBV) was obtained from Biomer, Germany with the trade name Biopol (Zeneca Bio Products). Micro sized talc was supplied by Luzenac America under the trade name of Jetfill 700C. The particulate dimensions of the talc range from 2 to 10 μm. Wood fibers used were the maple wood fiber from the American Wood fiber Schofield, WI with the trade name, 2010 MAPLE.

5.1.2 Fabrication of composites

Hybrid biocomposite specimens were fabricated using micro-compounder (manufactured and designed by DSM Research, Netherlands with a barrel volume of 15 cc) and a mini injection molder. It was equipped with co-rotating twin-screws of the length 150 mm and L/D (length to diameter ratio) 18, and has three consecutive heating zones. The wood fiber and PHBV were dried at a 110 ^{o}C and 80 ^{o}C under vacuum for 2 and 4 hours, respectively, to devoid of any moisture during processing. The hybrid composite fabrication was carried out as two step process, and that of the PHBV and wood fiber composite in a single step. The different compositions and processing parameters used during composite fabrication are listed in the Table 5.1. For the hybrid composite, PHBV pellets and wood fiber in fixed compositions as listed in Table 5.1 were physically mixed and fed to the micro-extruder. PHBV pellets and wood fibers were allowed to melt mix in the extruder for 4 minutes, and latter talc, as per the composition, was added to the melt mix of PHBV and wood fiber. Finally, all the three components were mixed for additional 4 minutes in the micro-extruder to attain an

appropriate dispersion of the talc and wood fibers in the melt. The processing temperatures of the three consecutive zones were 165, 160 and 155 ^{o}C. The melt from the extruder was collected in a pre heated mini injection (at a temperature of 155 ^{o}C), and was transferred to molding machine for specimen fabrication. The optimized injection pressure of 551.5 KPa was used to extricate the melt from the injection cylinder and thrust to the mold located in the mini molding machine. Finally, the specimen was removed from the mold and conditioned for 48 hours before testing.

Table 5.1: Processing parameters of the composites

PHBV (wt%)	Wood fiber (wt%)	Talc (wt%)	Processing Temperature (^{o}C)	Retention time (min.)
100	-	-	160	3
60	40		160	7
70	30	10	160	8 (4+4)
80	20	20	160	8 (4+4)
90	10	30	160	8(4+4)

5.1.3 *Testing and characterization*

5.1.3.1 Mechanical properties

Tensile and flexural properties of specimens were tested using a United Calibration Corp. SFM 20 testing machine as per ASTM D638 and ASTM D790 standards, respectively. The system controls and data analysis were performed using Datum software. The notch Izod impact testing was carried out on a Testing Machine Inc. (TMI) 43-02-01 as per ASTM D256 with the pendulum of impact energy 1.35 J.

5.1.3.2 Dynamic mechanical analysis (DMA).

The storage modulus, loss modulus and tan delta of the test specimens were evaluated using DMAQ800 supplied by TA Instruments. The specimens were heated from -30 to 125 ^{o}C with a heating rate of 2 ^{o}C/min. Single cantilever mode was used to test the specimens at an oscillating amplitude of 15 μm, and a frequency of 1 Hz.

5.1.3.3 Coefficient of linear thermal expansion (CLTE)

CLTE of the test specimens was determined using TMA 2940, equipped with an expansion probe. Heating rate was 3 ^{o}C/min with a constant applied load of 0.15 N. Temperature range of the reported results is from 30 to 90 ^{o}C.

5.1.3.4 Heat deflection temperature (HDT):

DMA Q800, TA instruments was used to find the HDT of various specimens as per ASTM D648 standards. The rectangular bars, 1.99 ×12 × 58 mm in three-point bending mode with an applying load of 66 psi were used for testing. Samples were heated at the rate of 2°C/ min from room temperature to the required temperature.

5.1.3.5 Differential scanning calorimetry (DSC)

DSC of specimens was performed using a model Q100 DSC, TA Instruments. The data was collected using heat and cool method. Specimens were heated up to 190 ^{o}C at a ramp rate of 10 ^{o}C/min and cooled under the similar ramp rate. The melting points and heat of crystallization reported are from the heating cycle. The crystallization temperature and heat of fusion are from the cooling cycle.

Data analyses of DMA, CLTE and DSC results were carried out on software "Universal Analysis" and three replications of each examination were performed.

5.1.3.5 Morphological studies

Morphological studies were conducted using a JEOL scanning electron microscope (model JSM-6400). Specimens were sputter-coated with gold to a thickness of ~10 nm in order to prevent charging during the examination. The SEM used was equipped with a lanthanum hexaboride (LaB_6) crystal as a source of electrons. An accelerating voltage of 13 KV was used to collect the SEM images.

5.2 Results and Discussion

5.2.1 Tensile Properties

Wood fiber and talc each added either alone or both in certain proportion enhances the Young's modulus of PHBV. Figure 5.1, provides the details of the tensile strength and modulus of PHBV and its composites with various compositions of wood fiber and talc. Though, there is increase in the Young's modulus of the PHBV with the loading of wood fiber at 40 wt% but the strength of the composites reduces, thereby not giving significant reinforcing effect of wood fibers in the matrices. Where as, the addition of 40 wt% talc not only increases the Young's modulus by ~ 260 %, but the strength as well by ~ 9 %, thus realizing the full potential of talc as reinforcement in PHBV. Substituting the wood fiber with the talc in subsequent stages lowers the strength of the hybrid composite a little but ratchet up the modulus by 9 and 5 % at 10 and 20 wt % wood fibers, respectively. Plummeted strength of the composite with the wood fibers is due to the insufficient interfacial interaction of the PHBV matrix and the fibers, which is visible in the SEM images of the impact fractured surfaces. Enhanced strength of the PHBV due to the talc reinforcement provides an edge over the PHBV-wood fiber composite, which has a lower strength than the hybrid composite. Hybrid composite has a higher modulus than PHBV by 280% at 20 wt% of talc and wood fiber each. Similar enhancement of 290% in the modulus of PHBV was observed at 30 wt% talc and 10 wt% wood fibers loadings. High density of talc enhances the density of the subsequent hybrid composite, therefore, at 20 wt% of talc and wood fiber, each, in PHBV gives the optimum weight to strength ratio.

The density of hybrid composite at 20 wt% talc and wood fiber each, as measured was 1.39 ± 0.03 gm/cm^3, and table 5.2 lists the density of PHBV and its composites with wood fiber and talc alone. The density was determined by using the buoyancy method i.e., weighing the specimens, when fully immersed in water, and compared to the determination form X-ray densometer. The results were comparable.

Table 5.2 : Density of the PHBV and its composites

	PHBV (neat)	Wood / PHBV (40/60)	Talc / PHBV (40/60)	Hybrid composite talc/wood/PHBV 20/20/60
Density (gm/cm^3)	1.25±0.01	1.31±0.02	1.54±0.02	1.39±0.03

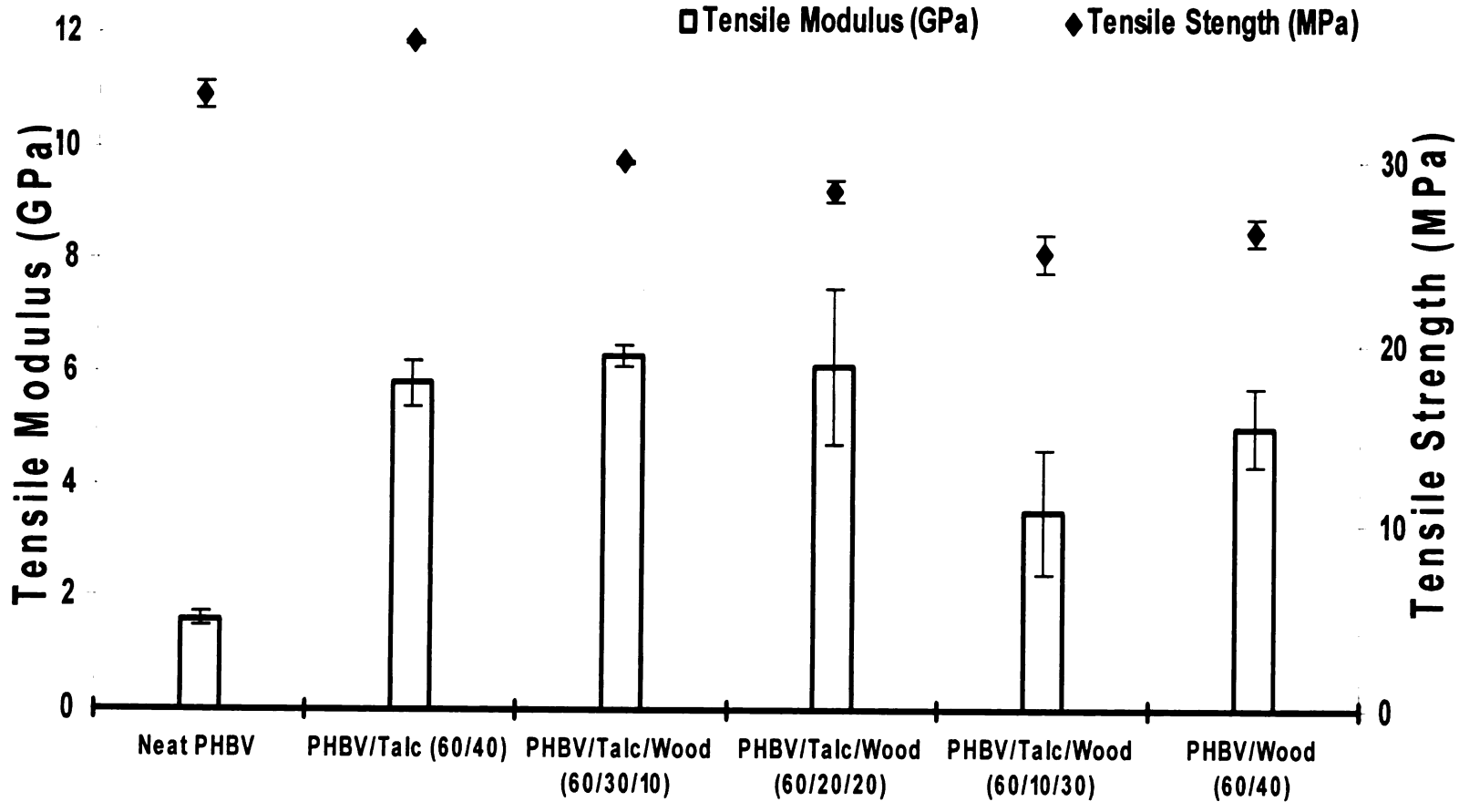

Figure 5.1: Tensile Properties of PHBV and its Composites

5.2.2 Flexural Properties

Figure 5.2 enumerate the flexural properties of PHBV and it composites in various proportion of talc and wood fiber. Trends of flexural strength and modulus are moderately identical to those of tensile. A leap of 270 % in modulus and 22 % in strength was observed with the 40 wt% talc in PHBV. Modulus of the hybrid composites plummeted while replacing the talc with wood fiber in each subsequent step of 10 wt% substitution. There was no difference in strength and modulus between the final two compositions (10/30/60 wt% talc/ wood fiber/ PHBV and 40/60 wt% wood fiber/PHBV) of composites. The modulus and strength of the composition at 20 wt% of talc and 20 wt% wood fiber was higher by 200% and 8%, respectively, from that of neat PHBV and by 17 % and 8 % from that of 40 wt% wood fiber in PHBV. Meager difference in the trends of flexural properties to that of tensile was due to different directional stresses induced to the specimen during the testing. During the tensile testing the specimen was induced to the uniaxial tensile stress while in the flexural testing the specimen was induced to uniaxial compression as well as tensile stress acting simultaneously in the opposite directions.

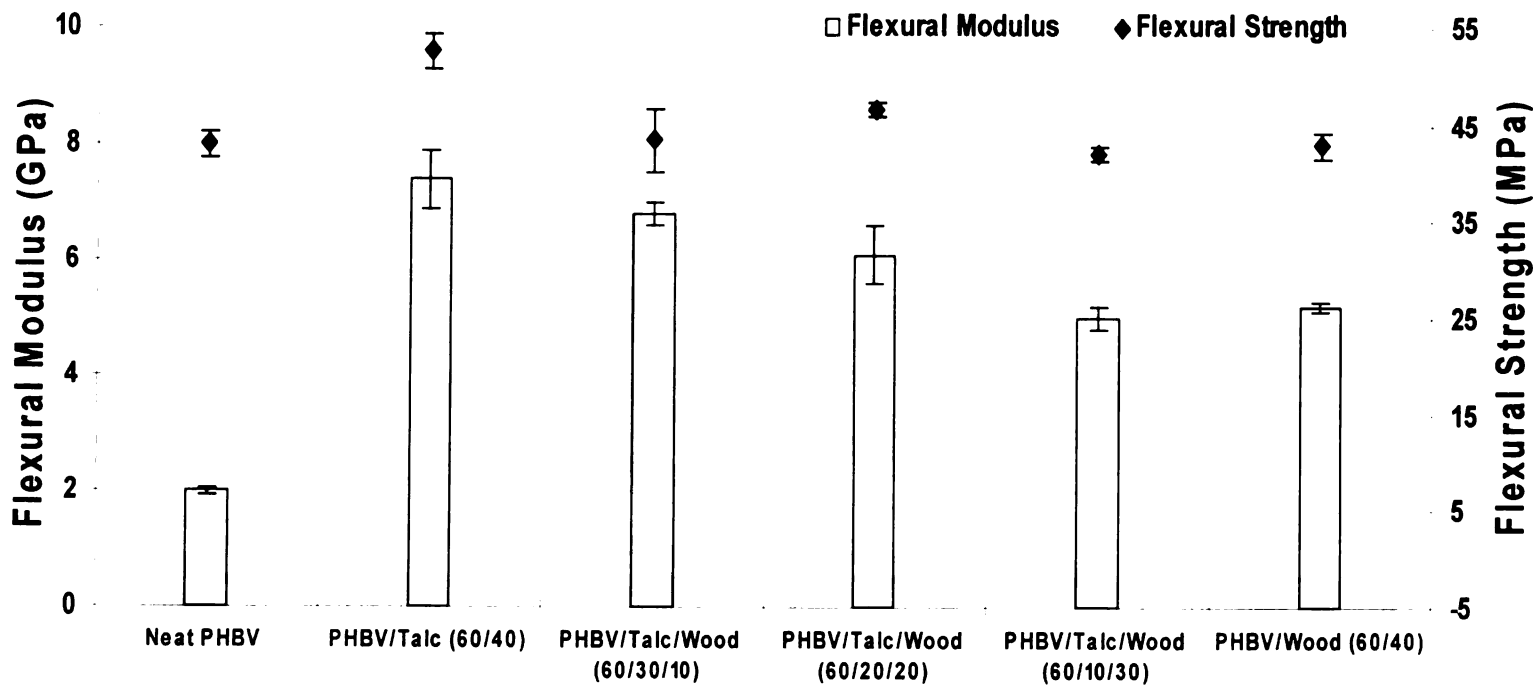

Figure 5.2: Flexural Properties of PHBV and its Composites

Theory

The surface energy of material is a crucial property in determining the wetting of the surface, which, in fact, governs the interface characteristics of the two adhering surfaces. In composites, the strength of the interface between reinforcing agent and the matrix plays an important role in deciding the efficiency of stress transferred from matrix to the reinforcing agent. The strength of the interface in turn governs the overall strength and modulus of the composite. Complete wetting of the matrix to the fiber or particulate surface provides an opportunity to have intimate contact and thus adhesion between the two. Wetting is an interfacial phenomenon that is governed by the surface energy or tension of the two interacting phases, in this case matrix (PHBV) and fiber (wood fiber) or inorganic particulate (talc).

Surface energy of the material is defined as sum of the two main components that are based on the molecular interactions. Hitherto, these were based on polar (γ^{P}) and nonpolar/disperse (γ^{d}) interaction energy components. More lately, these are referred as Liftshitz-van der Waals (γ^{LW}) and Lewis acid-base (γ^{AB}) interactions refined by Good, Van Oss and Chaudhary (GVOC). γ^{AB} is further refined in to the acid ($\gamma^{\oplus}$) and base (γ^{Θ}) components and calculated from their geometric mean as. [9-11]

$$\gamma^{AB} = 2\sqrt{\gamma^{\oplus}} \times \sqrt{\gamma^{\Theta}}$$

Total/net surface energy (γ) is the sum of the γ^{LW} and γ^{AB}, mathematically calculated as

$$\gamma = \gamma^{LW} + \gamma^{AB}$$

The surface energy of PHBV, maple wood fiber and talc are listed in table 5.3. These values have been taken from the various reference sources [10, 12-19].

Interfacial strength of the reinforcement and matrix can be well correlated with the interfacial energy/interfacial tension [20]. A generalized expression for an estimation of the interfacial tension between the two condensed interfaces is given by Giese and Van Oss [11, 21, 22].

$$\gamma_{xy} = \left(\sqrt{\gamma_x^{LW}} - \sqrt{\gamma_y^{LW}}\right)^2 +$$

$$2\left(\sqrt{\gamma_x^{\oplus}\gamma_x^{\ominus}} + \sqrt{\gamma_y^{\oplus}\gamma_y^{\ominus}} - \sqrt{\gamma_x^{\oplus}\gamma_y^{\ominus}} - \sqrt{\gamma_y^{\oplus}\gamma_x^{\ominus}}\right)$$

Here, LW are the Liftshitz-van der Waals interactions $\oplus, \ominus$ are the polar interactions and x, y are the interacting phases.

The interfacial strength can also be quantified from the thermodynamical work of adhesion (W_A) between the two interacting phases. W_A was related to surface tension components of the two interacting phases by Owens and Wendt [8, 11, 23]. W_A is taken as the geometric mean of the polar and the non polar interactions given by the following equation.

$$W_A = 2\sqrt{\gamma_x^{LW} \times \gamma_y^{LW}} + 2\sqrt{\gamma_x^{AB} \times \gamma_y^{AB}}$$

Table 5.3: Surface energy parameters of PHBV Maple wood

	γ (mJ/m^2)	γ^{LW} (mJ/m^2)	$\gamma\oplus$ (mJ/m^2)	$\gamma\ominus$ (mJ/m^2)	γ^{AB} (mJ/m^2)
PHBV	40.9[@]	~32.0[@]	-	-	~8.9[@]
Maple Wood fiber	47.7-53.3[β]	45.5[β]	0.02[β]	57.01[β]	2.14[β]
Talc	140-440[κ]	61[κ]	159[κ]	11[κ]	83.64[κ]

Data taken from references @ β κ

Table 5.4, provides the interfacial tension and thermodynamical work of adhesion between the PHBV-talc and PHBV-wood fiber interfaces calculated using the above equations. The theoretical values of the interfacial surface energy and W_A of PHBV-talc interface are higher than that of the PHBV-Wood fiber interface. This suggests positive and better interfacial interactions of PHBV with talc than with the wood fiber. Higher the interfacial energy or work of adhesion stronger the interface between the two phases. This was reflected in the improved tensile and flexural strength of the PHBV with the talc addition, and is verifiable from the SEM micrographs of the fractured specimens of the hybrid composite. Relatively, higher γ of the talc provides an opportunity for the lower γ PHBV matrix to completely wet its surface and have intimate interactions of the two surfaces. At higher temperature (melt temperature) γ of the polymeric materials further reduces [24] thus enhancing the wettability of PHBV in the melt state. The interfacial interaction between the PHBV and talc surface are possible due to the contributions of high acidic surface energy ($\gamma^{\oplus}$) component of talc which descend from the hydroxyl groups present on the lateral faces of talc lamella and the basic tendency of carbonyl group in the PHBV polyester. For the purpose of theoretical evaluation, the surface energy values of all the materials have been adapted from the different sources in literature. Though, there are numerous variation in the surface energy values of talc in various different available literature sources, but most of the values are at the higher end, and therefore, we adapted the theoretical value of 144 mJ/m^2 for our calculations. The marked variation in the γ of

talc is also due to its dependence on the type of processing (grinding/milling), geographical location of resource, size of particle, ratio of exposed faces (basal/lateral, lateral faces contribute to the γ^{AB} and basal to γ^{LW}) and methods of evaluation (

Table 5.4: Calculated Interfacial energy and Termodynamical Work of Adhesion

Interface type	γ_{xy} *(mJ/m²)*	W_A *(mJ/m²)*
PHBV-Wood fiber	**-20.2**	**85.0**
PHBV-Talc	**29.9**	**142.9**

experimental as well as theoretical). Another approximation taken for the γ_{xy} and W_A calculations was the assumption of equal contribution of $\gamma^{\oplus}$ and $\gamma^{\ominus}$ ($\gamma^{\oplus} = \gamma^{\ominus}$) to the γ of PHBV.

5.2.3 Dynamic Mechanical Analysis

Storage Modulus Figure 5.3, illustrates the storage modulus of the PHBV and its reinforced composites. As observed E′, the elastic component of the complex quantity, increased by ~ 75% at 20 wt.% talc loading, and further increased by 120% with the additional 20 wt% wood fiber loading, before the glass transition temperature (T_g), and the increase was 103 and 208%, respectively after the T_g i.e., in the rubbery stage. This

suggested that the fillers were posing restriction to the free rotation of the molecular chains above T_g. The relative increment of E′ in rubbery stage was higher than that in the glassy stage for the reason that Poisson's ratio in glassy polymer is less than 0.5 and the thermal stress induced due to the mismatch of the coefficient of linear thermal expansion of filler and matrix reduces the modulus of polymer near the filler particles[25]. The platelet shape of the talc also played a role in increasing the modulus, when compared to the increase in the rod like shape of wood fiber filler[25].

The loss Modulus E″ accounts for the viscous component of the complex modulus or the out of phase component with the applied strain, which generally increases with the addition of filler. 20 wt% of talc in PHBV increase its T_g by ~ 8^oC as observed from the shift of the E″ peak (Figure 5.4). Appearance of two distinct peaks in case of hybrid composite at 20 wt% of talc and wood fiber, each loaded in PHBV, have resulted due to two distinct phases of wood fiber and PHBV. The weak interface of wood fiber and PHBV which is not observed in case of the interface between talc and PHBV may have contributed to these.

The tan δ which is associated with the dampening effect or energy lost as a heat due interfacial interactions. The theoretical decrease in the Tan δ of talc filled and hybrid composite should be the same as percentage of loading in the composite as the energy loss is mainly associated to the dampening from the viscous component of the thermoplastic and not from the rigid filler particles. (Figure 5.5) Tan δ decreases, in case of a hybrid composite, by ~ 44%, but in case of only talc filled PHBV no decrement in its value was observed. The increase in the T_g of talc filled composite was

confirmed by the shift of the Tan δ peak towards the higher temperature. This specifies the restrictions imposed by the surface of talc particles to the freedom of rotation of the chain segment in the amorphous phase of matrix as a result of interfacial interaction between the talc and PHBV. The additional dampening effect can be due to the agglomerated talc particle-particle slippages or friction. The interfacial interactionbetween the PHBV molecules and the talc surface may have lead to higher energy losses due to the increased polymer particle friction, thus resulting in increased dampening effect. Lower dampening in case of hybrid particle was due to the additional stiffer wood fibers than the matrix.It has been reported that talc in polypropylene reduces its T_g due to the fact that talc act as nucleating agent which speeds up the crystallization causing an amorphous phase with higher mobility in PP-talc composites. This was observed in this case of these composites as well, suggesting that talc did effect the crystallization of PHBV which speeded up the cold crystallization as observed from the DSC results discussed next. Carboxylic groups (present at the chain ends of PHBV) reaction with the hydroxyl group on the lateral faces of the talc cleaved platelets can not be ruled out and those sites may have acted as additional nucleating sites for the crystallization [26].The another possibility can be of the hydrogen bonding between the carbonyl groups (present in the molecular chain of PHBV) and the hydroxyl groups of talc. Although, this can not be the predominant phenomena because the ratio of the lateral to basal cleavages is of the low order[8].

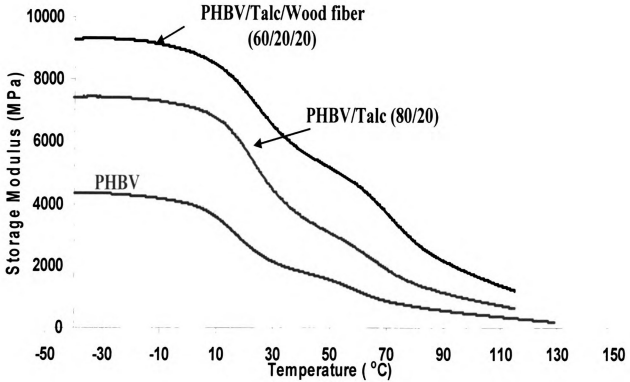

Figure 5.3: Storage Modulus of PHBV and its filled composite

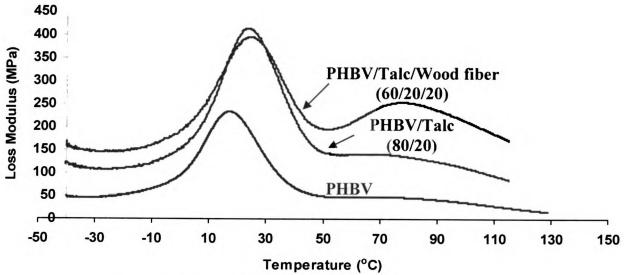

Figure 5.4: Loss Modulus of PHBV and its filled composite

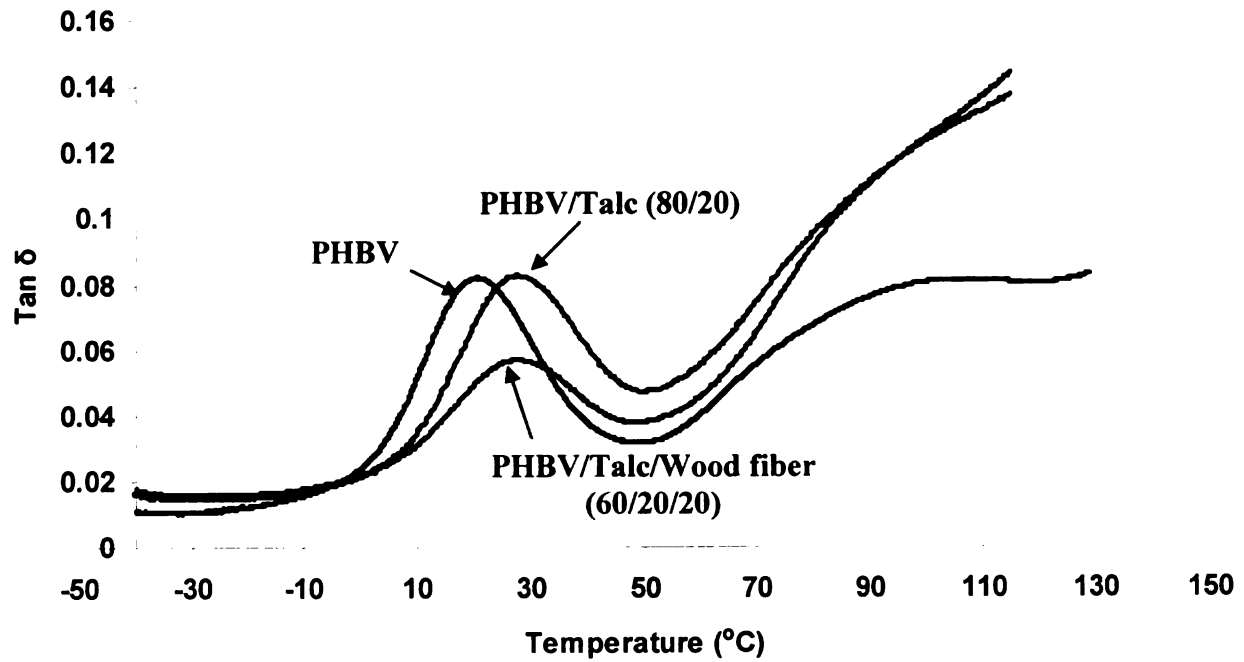

Figure 5.5: Tan δ of PHBV and its composite

5.2.4 Differential Scanning Calorimetry

A non isothermal DSC of PHBV and its composites with talc and wood fiber was carried out. Figure 5.6 illustrate the thermograms of PHBV, PHBV/talc (60/40 wt%) composite and its hybrid composites with 20 wt% talc and wood fiber each. Further details of the melting temperature (T_m) , melt crystallization temperature (T_c),

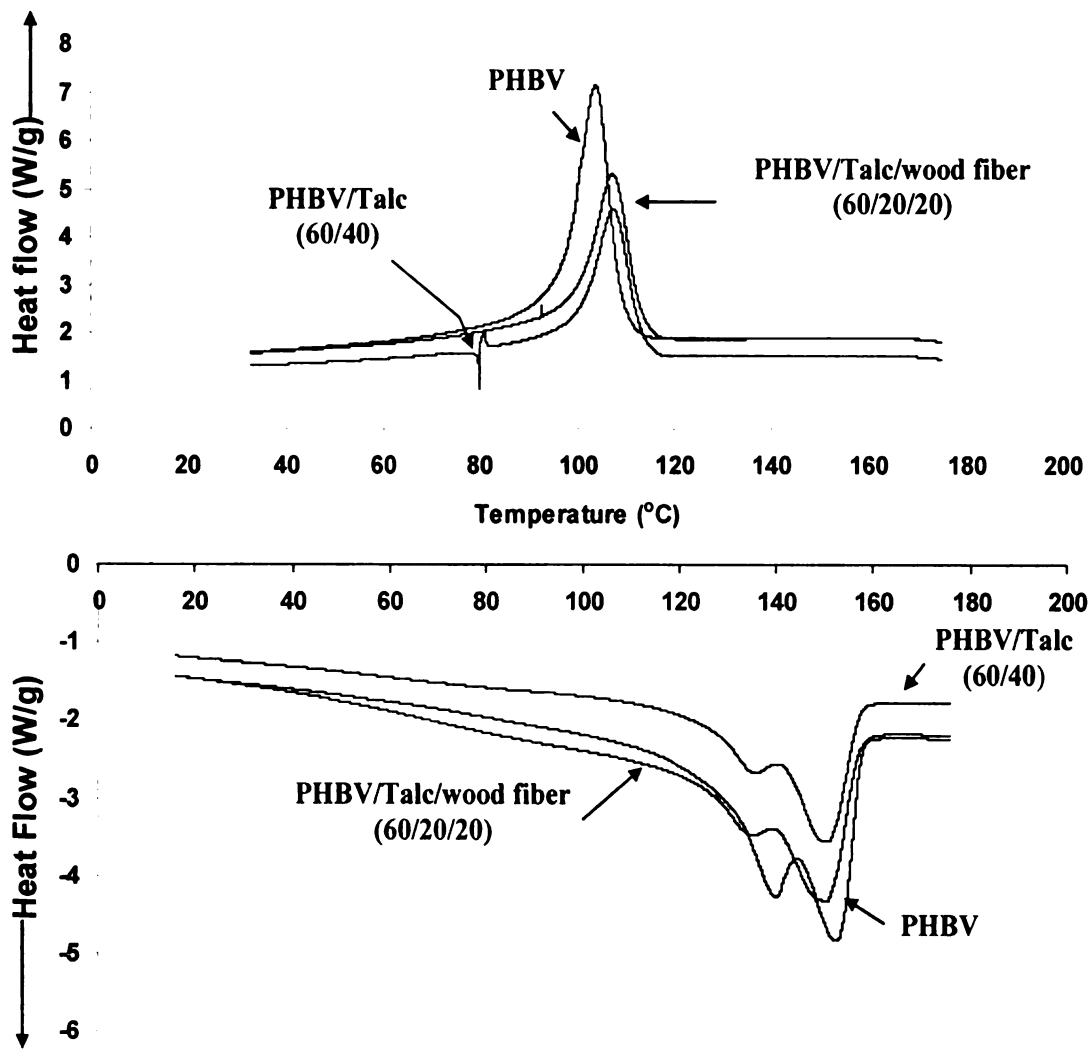

Figure 5.6: DSC curves of PHBV and its composites

cold crystallization enthalpy (ΔH_c), enthalpy of melting or crystallization (ΔH_f) and degree crystallinity (X_c) are provided in the Table 5.5. The melting point of PHBV decreases a little by 2 ^{o}C in presence of talc, but there is no significant change in the enthalpy of crystallization (ΔH_f) or degree of crystallinity (X_c) value.

Table 5.5: Details of DSC of PHBV and its composites

	T_m (^{o}C)	ΔH_f (J/g)	T_c (^{o}C)	ΔH_c (J/g)	X_c (%)
PHBV	152.6	39.5	103.8	36.5	36.2
PHBV/Talc (60/40)	149.8	22.0	107.6	20.9	33.6
PHBV/Talc/Wood fiber (60/20/20)	150.1	21.9	107.5	22.2	33.5

The biomodal endothermic peaks observed in case of PHBV melting region due to heterogeneous crystal morphology headed towards the homogenization of the spherullite growth in the presence of talc, which resulted in the slight drop of T_m. ΔH_c and ΔH_f of PHBV did not change in presence of either of the filler, thus not giving an indication of any change in net crystallization. T_c increased to 107 ^{o}C from 103 ^{o}C in

presence of talc, thereby indicating the increase in crystallization rate of PHBV during the cooling stage. The surface of talc acted as nucleating sites that allowed the PHBV nucleation growth at a higher temperature than the neat PHBV. The increased crystallinity rate is another indication of the interfacial interaction between the talc surface and PHBV molecular chains. X_C was not effected by any significant factor on the addition of either talc or both wood fiber and talc. X_c was calculated using, $X_c(\%) = \frac{\Delta H_f}{\Delta H_{f^o} \times w} \times 100$. ΔH_f was enthalpy of crystallization of PHBV and ΔH_{f^o} was enthalpy of crystallization at 100 % crystallinity of PHBV (109 J/g) [27, 28]. w, the weight fraction of PHBV in composite.

5.2.5 Impact Strength

Figure 5.7, illustrates the impact strength of PHBV and its hybrid composite. The impact strength of PHBV decreased from 25 J/mt to 19 J/mt on addition of 20 wt% talc and wood fiber each. In the previous chapter, it is described that the impact strength of PHBV decreases by 29% on addition of 40wt% wood or bamboo fiber. The decrease in this case was 24%, i.e. 5% lesser than only wood fiber reinforced composites, suggesting that talc does not lead to any additional drop in the impact strength of the hybrid composite, but rather it is a common phenomenon due to the addition of fillers. More over the decrease was due to the reduced interfacial interaction between the wood fiber and PHBV in presence of talc, which was visible in SEM micrographs.

Due to the low fiber-matrix interfacial interaction, fibers pull out used less energy that resulted in lower impact strength.

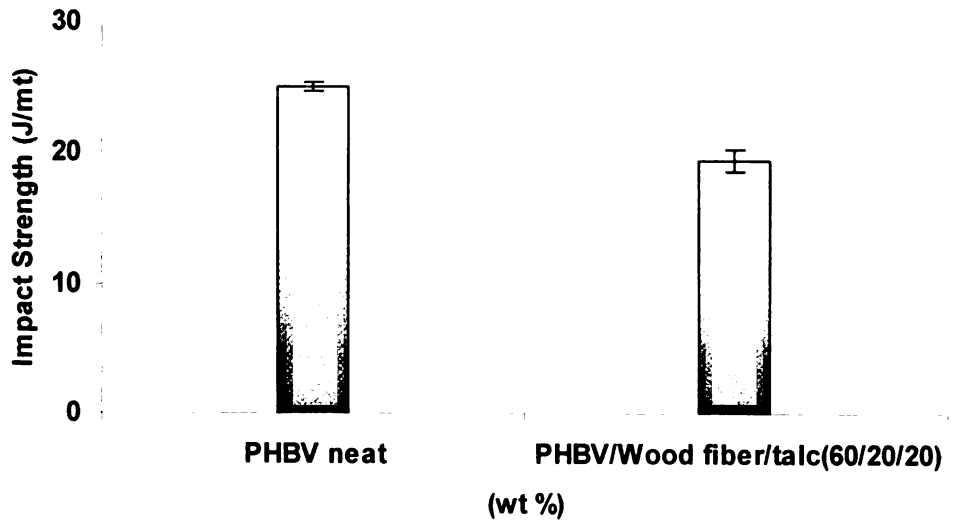

Figure 5.7: Impact strength of PHBV and its hybrid composite.

5.2.6 Morphology

Figure 5.8 and 5.9, shows the SEM photomicrographs of the impact fractured surface of hybrid composite Figure 5.8(a) and (b) are low and high magnification micrographs, respectively, showing the uniform distribution of talc particles in PHBV matrix. From the SEM images, it was observed that the major failure occurred due the fiber pull out from the matrix. The interfacial interactions between the wood fiber and matrix were not strong enough to resist the fiber pull out during the impact as a result the energy consumed was small in magnitude. A poor interface between the wood fiber and matrix is visible in the figure 5.8(b) at larger magnification. A poor interface between wood fiber and PHBV was also due to the presence of talc particles within the two surfaces that did not allow much of the interaction among the two and made the fiber slippage easy during the pull out. This is visible in the image in figure 5.9(a) that was obtained from the interface, where the fiber was pulled out. Figure 5.9(b) is a high magnification image to reveal the talc and PHBV interface. It shows a good dispersion and embedment of talc in PHBV matrix, suggesting a good interface between the two.

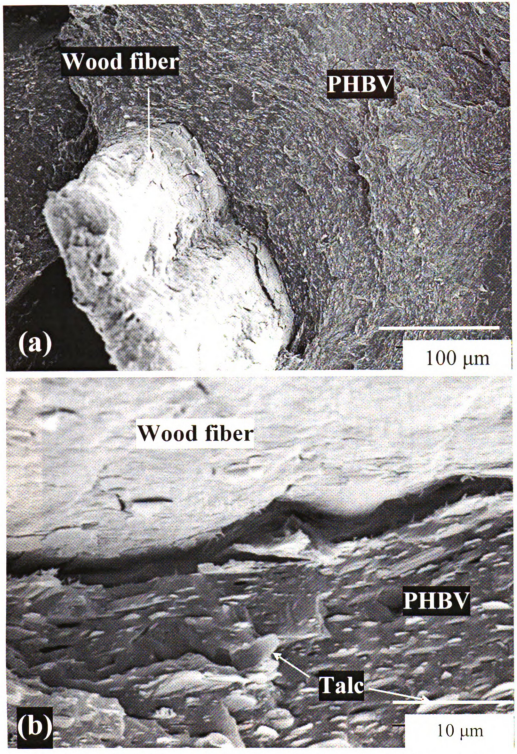

Figure 5.8: SEM Photomicrographs of fractured hybrid composite surface (a) Low magnification 270×, 100μm (b) High magnification 3000×, 10μm.

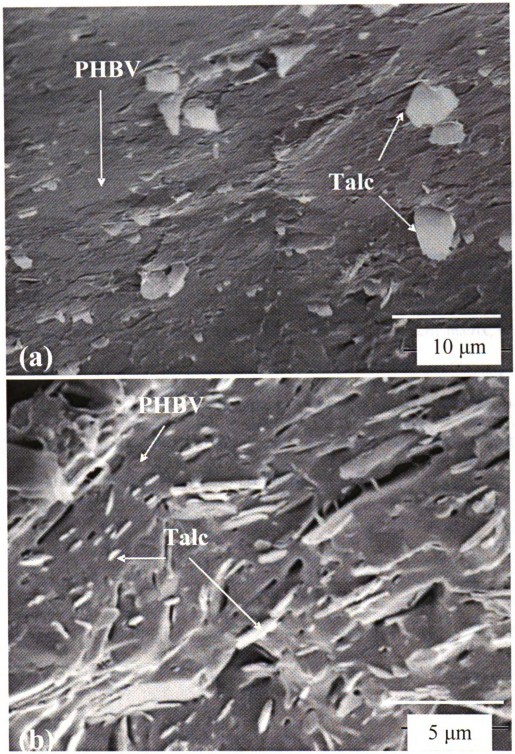

Figure 5.9: SEM Photomicrographs of Hybrid composite (a) Wood fiber pulled out interface with PHBV matrix, 2700×, 10μm (b) High magnification fractured surface of composite, 5500×, 5μm.

5.2.7 Ther

Fig

the hybri

properties

The reduc

previously

little. Bha

equal pro

biocompo

was more

was more

fiber was

of stiffne

5.2.7 Thermomechanical Properties

Figures 5.10, illustrate the CLTE and HDT of the neat PHBV in comparison to the hybrid biocomposite, and reflected the beneficial improvement in both the properties of the hybrid biocomposite. CLTE was reduced by 36% and HDT by $9^{o}C$. The reduction in CLTE was more due to the effect of talc than wood fiber, as reported previously [29], the wood fiber loading in PHBV affected the CLTE of PHBV only a little. Bhardwaj et al.[30] reported the reduction in CLTE of PHBV, approximately in equal proportion, with the addition of talc. The decrement on CLTE of hybrid biocomposite was due to the rigid and low CLTE filler in the polymeric matrix, which was more pronounced due to the presence of talc. The HDT of the hybrid biocomposite was more affected by the wood fiber than the talc. The HDT reduced, when the wood fiber was replaced by the 20 wt% of talc. The increase in HDT was due to the increase of stiffness at higher temperature of the fiber filled polymers.

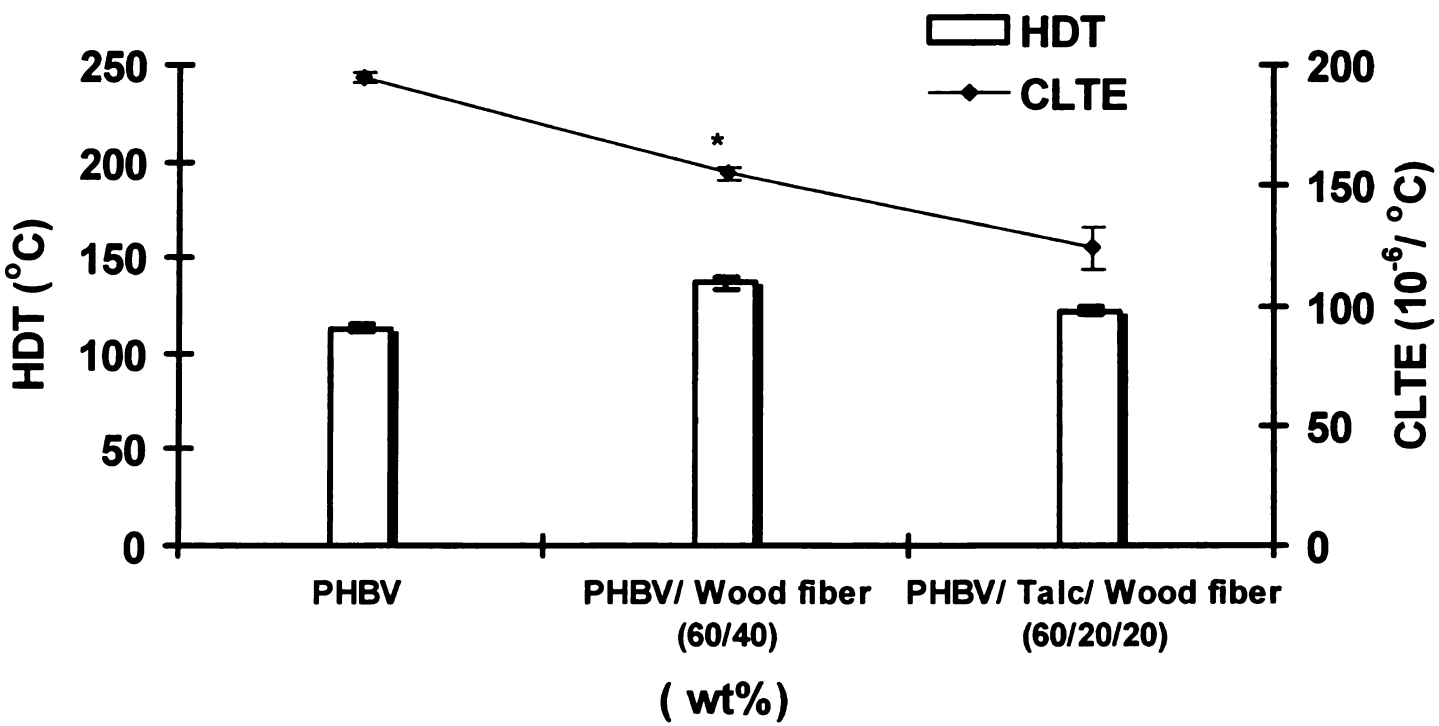

Figure 5.10: Coefficient of linear thermal expansion and Heat distortion temperature of PHBV and its hybrid composite
*** Value adapted from previous journal publication reference [29]**

5.3 Conclusion

The hybrid composites from wood fiber, talc and a bioplastic PHBV using the extrusion-injection molding technique were successfully fabricated. The composition at 20 wt% of wood fiber and talc in PHBV gave a leap of ~200% improvement in the Young's and flexural modulus. The dynamic-mechanical analysis supports the tensile and flexural results as well as explains the talc-PHBV and wood fiber-PHBV interfacial interactions. The high surface energy of talc particulates due to its high acidic character provides an opportunity for talc-PHBV interfacial interactions. The DSC analysis does not depict any additional crystallization of PHBV with the addition of talc in it. The impact strength of the PHBV reduced with addition of fillers. The Morphological analysis of the hybrid composite using SEM reveals the better interfacial interaction and dispersion of talc with PHBV than wood fiber.

5.4 References

1. Unal H., Mimaroglu A., and Alkan M., "Mechanical properties and morphology of nylon-6 hybrid composites". *Polym Int.*, 2004.53: p. 56-60.

2. Huneault M. A., Godfroy P.G., and Lafleur P.G., "Performance of TalcEthylene-Octene Copolymer/Polypropylene Blends". *Polymer Engineering and Science*, JUNE 1999.39(6): p. 1130-1138.

3. Ersoy O. G. and Nugay N., "Effect of Inorganic Filler Phase on Mechanical and Morphological Properties of Binary Immiscible Polymer Blends". *Polymer Bulletin Springer-Verlag* 2003(49): p. 465-472.

4. Browning R., Lim G. T., MoyseA., Sun L., and Hung-Jue Sue, "Effects of Slip Agent and Talc Surface-Treatment on the Scratch Behavior of Thermoplastic Olefins". *Polymer Engineering and Science @2006 Society of Plastics Engineers*, 2006.46: p. 601-608.

5. Dı´ez-Gutie´rreza S., Rodrı´guez-Pe´reza M.A., De Sajaa J.A., and Velascob J.I., "Dynamic mechanical analysis of injection-moulded discs of polypropylene and untreated and silane-treated talc-filled polypropylene composites". *Polymer* 1999.40: p. 5345-5353.

6. McInerney L. F., Kao N., and Bhaitacharya N., "Melt Strength and Extensibility of Talc-Filled Polypropylene". *Polymer Engineering and Science*, 2003.43(12): p. 1821-8129.

7. H. Unal, "Morphology and mechanical properties of composites based on polyamide 6 and mineral additives". *Materials and Design* 2004.25: p. 483-487.

8. Kaggwa G. B., Huynh L., Ralston J., and Bremmell K., "The Influence of Polymer Structure and Morphology on Talc Wettability". *Langmuir* 2006.22: p. 3221-3227.

9. Leeden M.C.V. and Gert Frens, "Surface Properties of Plastic Materials in Relation to their Adhering Performance (Review)". *Advance Engineering materials*, 2002.4(5): p. 280-289.

10. Meijer M. de, Haemers S., Cobben W., and Militz H., "Surface Energy Determinations of Wood: Comparison of Methods and Wood Species". *Langmuir* 2000.16: p. 9352-9359.

11. Lewin M., Mey-Marom A., and Frank R., "Surface free energies of polymeric materials, additives and minerals". *Polym. Adv. Technol.*, 2005.16: p. 429-441.

12. Douillard J.M., Salles F., Henry M., Malandrini H., and Clauss F., "Surface energy of talc and chlorite: Comparison between electronegativity calculation and immersion results". *Journal of Colloid and Interface Science*, 2007.305 p. 352-360.

13. Tarasevich Y. I., "The Surface Energy of Hydrophilic and Hydrophobic Adsorbents". *Colloid Journal*, 2007.69(2): p. 212-220.

14. Guerrouani N., Baldo A., Maarouf T., Belu A.M., Kassis C.M., and Andre' M., "Fluorinated-plasma coating on polyhydroxyalcanoate PHBV Effect on the biodegradation". *Journal of Fluorine Chemistry*, 2007.128: p. 925-930.

15. Terada K. and Yonemochi E., "Physicochemical properties and surface free energy of ground talc". *Solid State Ionics* 2004.172: p. 459-462.

16. Comarda M.P., CalvetR., Balard H., and DoddsaJ.A., "Influence of the geological history, particle size and carbonate content on the surface properties of talc as determined by inverse gas chromatography at infinite dilution". *Colloids and Surfaces A: Physicochem. Eng. Aspects*, 2004.238: p. 37-42.

17. Yekelera M., Ulusoya U., and Hicyılmazb C., "Effect of particle shape and roughness of talc mineral ground by different mills on the wettability and floatability". *Powder Technology* 2004.140: p. 68- 78.

18. Malandrini H., Clauss F., Partyka S., and Douillard J. M., "Interactions between Talc Particles and Water and Organic Solvents". *JOURNAL OF COLLOID AND INTERFACE SCIENCE*, 1997.194: p. 183-193.

19. M.Gindl and S.Tschegg, "Significance of the Acidity of Wood to the Surface Free Energy Components of Different Wood Species". *Langmuir*, 2002 18: p. 3209-3212.

20. Tu L., Kruger D., Wagener J.B., and Carstens P.A.B., "Wettability of Surface Oxyfluorinated Polypropylene Fibers and its Effect on Interfacial Bonding with Cementitious Matrix". *Journal of Adhesion*, 1997.62: p. 187-211.

21. Giese R.F and van Oss C.J, *"Colloid and surface properties of clays and related minerals"*. Surfactant Science, ed. H. A.T. 2002, New York: Marcel Dekker.

22. Li Z., Giese R.F., Van OssC.J., Yvon J., and Cases J., "The Surface Thermodynaic Properties of Talc Treated with Octadecylamine". *Journal of Colloid and Interface Science*, 1993.156: p. 279-284.

23. Owens D.K and Wendt R.C, *Journal of Applied Polymer Science*, 1969.13: p. 1741.

24. WOK D.Y., CHEUNG L.K., PARK C.B., and NEUMA A.W., "Study on the Surface Tensions of Polymer Melts Using Axisymmetric Drop Shape Analysis". *Polymer Engineering and Science*, 1998 38(5): p. 757-764.

25. Nielsen L.E, "Dynamic Mechanical Properties of Filled Polymers". *Applied Polymer Symposia*, 1969(12): p. 249-265.

26. Weihua K., He Y., and Inoue Y., "Fast Crystallization of poly(3-hydroxybutyrate) and poly(3-hydroxybutyrate-co-valerate) with talc and boron nitride as nucleating agents". *Polymer International*, 2005.54: p. 780-789.

27. Buzarovska A, Bogoeva-Gaceva G, Grozdanov A, Avella M, Gentile G, and Errico M, "Potential use of rice straw as filler in eco-composite materials". *Australian Journal of Crop Science*, 2008.1(2): p. 37-42

28. Scandola M, Focarete M L, Adamus G, Sikorska W, Baranowska I, Swierczek G M, Kowalczuk M, and Jedlinski Z, "Polymer blends of natural poly(3-hydroxybutyrate- co-3-hydroxyvalerate) and a synthetic atactic poly(3-hydroxybutyrate)Characterization and biodegradation studies". *Macromolecules*, 1997.30: p. 2568-2574.

29. Singh S. and Mohanty A.K., "Wood fiber reinforced bacterial bioplastic composites: Fabrication and performance evaluation". *Composite Science and Technoogy*, 2007.67(9): p. 1753-63.

30. Whaling A., Bhardwaj R., and Mohanty A. K., "Novel Talc-Filled Biodegradable Bacterial Polyester Composites". *Ind. Eng. Chem. Res.* , 2006.45: p. 7497-7503.

Chapter 6

Conclusion

The objective, in entirety, of this research was to shift W/NPCs from conventional olefin plastic to a fully green biocomposites from renewable source based and biodegradable bioplastic, i.e., PHBV. During the course of changeover from partially to fully green biocomposites, the issues pertaining to biopolymers are addressed. This thesis also discusses the other emerging issues, during the processing, of biopolymer based W/NPCs like cost, processablity, performance in comparison to the conventional WPCs, compatibility of reinforcing agent and matrix, availability, and anisotropy. The development of all green hybrid biocomposite from PHBV, wood fiber and talc was attained in four sequential phases as follows.

In the first phase, biodegradable biocomposite from PHBV and maple wood fiber were fabricated using extrusion followed by injection molding. The loading level of wood fiber in biocomposites was varied from 10 to 40 wt%. It was noted that the tensile and flexural modulus at 40 wt% of wood fiber were enhanced by ~167%, when compared with neat PHBV. The theoretical Young's modulus values of biocomposites obtained from Halpin-Tsai and Tsai-Pagano equations were consistent with the experimental values. The effectiveness of fibers on the storage modulus of the composite was evaluated by the coefficient factor, C. The heat deflection temperature was increased by 21%, and the coefficient of linear thermal expansion reduced by 18 % at 40 wt% of wood fiber. The toughness of the biocomposites decreased with the fiber loading. SEM photomicrographs exhibited the good dispersion at 30 wt% wood fiber but fiber aggregation at 40 wt%.

In the second phase, the biocomposites from a bamboo fiber and PHBV were fabricated with the similar process, i.e., extrusion followed by injection molding, as PHBV-Wood fiber biocomposite in stage one. The need for the bamboo fiber in substitution to wood fiber was emphasized. Comparative analysis of the two different kind of lignocellulosic fiber (wood and bamboo) at 30 and 40 wt.% fiber loading were carried out with respect to their mechanical, thermomechanical, thermal, FTIR and morphological aspects. Both the fibers, embedded in the PHBV matrix, gave similar tensile and flexural modulus, though they had different aspect ratios. Statistically, no appreciable difference among the mechanical properties of two biocomposites, obtained from two different types of lignocellulosic fibers, was noted. A difference between the net crystallinity of the biocomposites was observed in DSC and FTIR. Notch impact strength of PHBV decreased with the fiber addition and the reduction was greater in case of bamboo fiber composites. The effect of the fiber type on the thermal stability of composites was not observed, but incorporation of wood fiber gave a higher heat deflection temperature (HDT) versus the bamboo fiber. Scanning electron microscopy (SEM) photomicrographs demonstrated the existence of similar kinds of interfacial interaction between the two types of fibers and PHBV

In the third phase, the research was focused on the processing of the PHBV-wood fiber biocomposite. These were fabricated using two different molding processes i.e., injection molding and compression molding, and characterized for the static and dynamic mechanical properties, and isotropic characteristics. Injection molded composite performed better than compression molding, which was apparent from the better tensile and flexural properties of injection molded composite that gave an

improvement in Young's modulus and flexural modulus by 104%. High elastic modulus and low dampening effect apparently suggested the same during dynamic mechanical analysis. Morphological observations revealed poor adhesion and air entrapment in compression molded specimens. Study of anisotropy was performed using squeeze flow test of both the processes, and it indicated the anisotropic behavior of injection molded specimens. Anisotropy varied;(a) along the sections of injection molded specimens, and (b) composition of wood fiber in the biocomposites.

In the final stage "all green hybrid bioplastic composites" with the dual reinforcements of talc and wood fiber were designed, fabricated and characterized. The composition at 20 wt% of wood fiber and talc, each in PHBV, gave a leap of ~200% improvement in the Young's and flexural modulus. The analysis of the dynamic-mechanical is in unison with the tensile and flexural analysis as well as explains the talc-PHBV and wood fiber-PHBV interfacial interactions. The high surface energy of talc particulates due to their high acidic nature provides better talc-PHBV interfacial interactions than wood fiber-PHBV interface. The calorimetric analysis was carried out, and no additional crystallization of PHBV in the presence of talc was observed. The impact strength of the PHBV plummeted with addition of fillers. The Morphological analysis reveals the better interfacial interaction and dispersion of talc, in PHBV, than wood fiber.

The future scope of this research can be protracted with the realization of the reinforcing effect of nano sized talc in the PHBV matrix. The nano size talc may reduce the amount of talc with a substantial increase in mechanical properties of the matrix, thus reducing the specific density of the biocomposite and providing the opportunity to

load the matrix with higher fiber content. This would also reduce cost of the biocomposites. The toughness improvement of the biocomposite still remains a challenge that lays in the future scope of research. Toughness of these biocomposite can be attained by modifying the surface functionality on surface of the wood fiber. This would lead to either a chemically bonded interface between the wood fiber and PHBV or high surface energy wood fiber that allows the complete wetting of the matrix on the fiber surface. The second approach to enhance upon the toughness is to enhance the toughness of the matrix by blending or nanostructured reinforcement.